**(12) STANDARD PATENT APPLICATION** (11) Application No. **AU 2026201434 A1**
**(19) AUSTRALIAN PATENT OFFICE**

(54) Title
**Engineered adeno-associated (AAV) vectors for transgene expression**

(51) International Patent Classification(s)
***C07K 14/015*** (2006.01) ***C12N 15/86*** (2006.01)

(21) Application No: **2026201434** (22) Date of Filing: **2026.02.26**

(43) Publication Date: **2026.03.19**
(43) Publication Journal Date: **2026.03.19**

(62) Divisional of:
**2020248116**

(71) Applicant(s)
**President and Fellows of Harvard College;The General Hospital Corporation**

(72) Inventor(s)
**MAGUIRE, Casey A.;HUDRY, Eloise Marie;HANLON, Killian S.**

(74) Agent / Attorney
**RnB IP Pty Ltd, PO Box 9530, DEAKIN, ACT, 2600, AU**

# Abstract

Engineered AAV vectors for transgene expression, e.g., in the CNS, PNS, inner ear, heart, or retina, and methods of use thereof. Also provided are methods for discovering new engineered AAV vectors that mediate transgene expression in desired cell types.

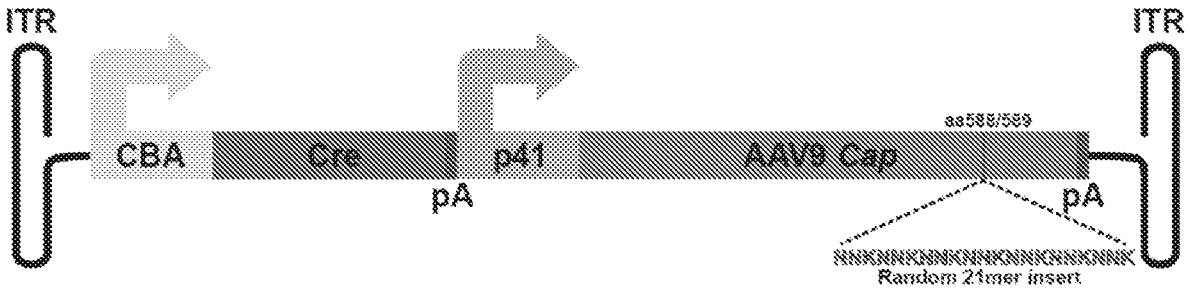


FIG. 1A

# Engineered Adeno-Associated (AAV) Vectors for Transgene Expression

## CLAIM OF PRIORITY

This application claims the benefit of U.S. Provisional Application Serial No. 62/825,703, filed on March 28, 2019. The entire contents of the foregoing are incorporated herein by reference.

## FEDERALLY SPONSORED RESEARCH OR DEVELOPMENT

This invention was made with Government support under Grant Nos. AG047336 and DC017117 awarded by the National Institutes of Health. The Government has certain rights in the invention.

## TECHNICAL FIELD

Described herein are engineered AAV vectors for transgene expression, e.g., in the CNS, PNS, inner ear, heart, or retina, and methods of use thereof. Also provided are methods for discovering new engineered AAV vectors that mediate transgene expression in desired cell types.

## BACKGROUND

While AAV9 vectors have shown remarkable potential for delivery to the CNS after systemic delivery, resulting in clinical success in pediatric patients with spinal muscular atrophy[1], systemic injection of high doses of AAV vectors can lead to induction of a T-cell response that can eliminate transduced cells[2]. In monkeys, there is one report in which high systemic doses of an AAV9-like vector resulted in toxicity and death of the animal which was attributed to systemic inflammation[3]. A recent phase I clinical trial using high dose AAV9 to treat muscular dystrophy was placed on hold by the FDA due to an immune reaction after vector infusion in one patient. The reason high doses are required is due to the relatively low efficiency of AAV on a per-vector genome copy basis to provide adequate transgene expression in a substantial number of target cells. Thus, developing new AAV capsids which allow more efficient transduction at lower doses

should result in better therapeutic efficacy while lowering safety issues, such as immunotoxicity.

## SUMMARY

Described herein are methods that use an adeno-associated virus (AAV) vector genome with a two-part expression cassette to identify novel virus clones. The first is a Cre-recombinase cassette under a promoter of interest. The second part is an AAV promoter to drive expression of an engineered capsid gene, cloned "in cis" to the first section of the viral genome. Virus vectors are selected for transgene expression (highly sensitive Cre expression) using cells that express a reporter gene (e.g., green fluorescent protein) with an upstream loxP/stop site, thus preventing reporter expression until AAV vector-delivered Cre removes the stop site. Reporter gene positive cells can be isolated and recovered AAV capsid sequences will have a higher likelihood of mediating efficient transgene expression. Also described herein are engineered viral sequences that drive efficient expression in the central nervous system (CNS) and peripheral nervous system (PNS), heart, liver, and inner ear.

Thus, provided herein are AAV capsid proteins comprising an amino acid sequence that comprises at least four contiguous amino acids from the sequence STTLYSP (SEQ ID NO:1) or FVVGQSY (SEQ ID NO:2). In some embodiments, the AAV capsid proteins comprise an amino acid sequence that comprises at least five contiguous amino acids from the sequence STTLYSP (SEQ ID NO:1) or FVVGQSY (SEQ ID NO:2). In some embodiments, the AAV capsid proteins comprise an amino acid sequence that comprises at least six contiguous amino acids from the sequence STTLYSP (SEQ ID NO:1) or FVVGQSY (SEQ ID NO:2). Alternatively, the AAV capsid proteins comprise an amino acid sequence that comprises at least four, five, or six contiguous amino acids from the sequences shown in FIGs. 2A or 7C (SEQ ID NOs:17-150).

In some embodiments, the AAV is AAV9.

In some embodiments, the AAV capsid proteins comprises AAV9 VP1.

In some embodiments, the sequence is inserted into the capsid at a position corresponding to amino acids 588 and 589 of SEQ ID NO:6, at the VP1/VP2 interface (amino acid 138) or any site between 583-590.

Also provided herein are nucleic acids encoding an AAV capsid protein as described herein.

Additionally, provided herein are AAVs comprising the capsid proteins described herein, and preferably not comprising a wild type VP1, VP2, or VP3 capsid protein. In some embodiments, the AAVs further comprising a transgene, preferably a therapeutic transgene.

Further provided are methods of delivering a transgene to a cell, e.g., a cell in vivo or ex vivo/in vitro. The methods include contacting the cell with an AAV as described herein. In some embodiments, the cell is a neuron (optionally a dorsal root ganglion neuron or spiral ganglion neuron), astrocyte, cardiomyocyte, or myocyte, astrocyte, glial cell, inner hair cell, outer hair cell, supporting cell, fibrocyte of the inner ear, photoreceptors, interneurons, retinal ganglion, or retinal pigment epithelium.

In some embodiments, the cell is in a living subject, e.g., a mammalian subject, preferably a human. In some embodiments, the cell is in a tissue selected from the brain, spinal cord, dorsal root ganglion, heart, inner ear, eye, or muscle, and a combination thereof. In some embodiments, the subject has Alzheimer's Disease; Parkinson's Disease; X-linked Adrenoleukodystrophy; Canavan's ; Niemann Pick; Spinal muscular atrophy; Huntington's Disease; Connexin-26; Usher Type 3A; Usher Type 2D; Hair cell-related hearing loss; Hair cell-related hearing loss (DFNB7/11); Inner hair cell-related hearing loss (DFNB9); Usher Type 1F; Usher Type 1B; Retinitis pigmentosa (RP; non-syndromic); Leber congenital amaurosis; Leber Hereditary Optic Neuropathy; Usher Syndrome (RP; syndromic with deafness); Duchenne Muscular Dystrophy; Allograft vasculopathy; or Hemophilia A and B. The methods and compositions described herein can be used to treat these conditions, by administration of a therapeutically effective amount of an AAV carrying a therapeutic transgene, sufficient to ameliorate, reduce risk of, or delay onset of one or more symptoms of the condition.

In some embodiments, the cell is in the brain of the subject, and the AAV is administered by parenteral delivery; intracerebral; or intrathecal delivery.

In some embodiments, the intrathecal delivery is via lumbar injection, cisternal magna injection, or intraparenchymal injection.

In some embodiments, the AAV is delivered by parenteral delivery, preferably via intravenous, intraarterial, subcutaneous, intraperitoneal, or intramuscular delivery.

In some embodiments, the cell is in the eye of the subject, and the AAV is administered by subretinal or intravireal injection.

In some embodiments, the cell is in the inner ear of the subject, and the AAV is administered to the cochlea through application over or through the round window membrane, through a surgically drilled cochleostomy adjacent to the round window, a fenestra in the bony oval window, or a semicircular canal.

Also provided herein are library construct AAVs comprising:

(i) a sequence encoding a Cre recombinase driven by a promoter;

(ii) a sequence encoding an AAV9 capsid protein with a peptide as described herein, e.g., a heptamer peptide, inserted between the sequences encoding amino acids (aa) 588-589 of the capsid, driven by a promoter, downstream of the Cre cassette. In some embodiments, the peptide comprises a random peptide sequence or a pre-selected peptide sequence.

Further provided are libraries comprising a plurality of the library constructs as described herein. In some embodiments, wherein the peptide sequences are random, the library comprises library constructs having sequences encoding all possible variants of the heptamer.

Additional provided herein are methods for identifying an engineered capsid that mediates transgene expression in a pre-selected cell type. The methods include: (a) administering the library of claims 23 or 24 to a non-human model animal, preferably a mammal, wherein the cells of the model animal express a loxP-flanked STOP cassette upstream of a reporter sequence; (b) isolating cells of the pre-selected cell type; (c) selecting cells in which the reporter sequence is expressed; (d) isolating at least part of the library construct, preferably a part comprising the heptamer, from the selected cells in which the reporter sequence is expressed from step (c); and (e) determining identity of the heptamers in the library constructs isolated in step (d), wherein the heptamers that are isolated can mediate transgene expression in the pre-selected cell type.

In some embodiments, the reporter sequence encodes a fluorescent reporter protein.

In some embodiments, the model animal is transgenic for the loxP-flanked STOP cassette upstream of a reporter sequence, or wherein the loxP-flanked STOP cassette upstream of a reporter sequence can be expressed from a second construct.

In some embodiments, determining identity of the heptamers in the library constructs comprises using DNA sequencing analysis.

In some embodiments, the methods also include before and/or after step (e): using PCR to amplify sequences comprising the heptamer sequences, optionally comprising full capsid sequences, from the library constructs isolated in step (d); cloning the amplified sequences back to a second set of library vectors; repackaging the second set of library vectors; and performing steps (a)-(d) or (a)-(e) on the second set of library vectors.

Unless otherwise defined, all technical and scientific terms used herein have the same meaning as commonly understood by one of ordinary skill in the art to which this invention belongs. Methods and materials are described herein for use in the present invention; other, suitable methods and materials known in the art can also be used. The materials, methods, and examples are illustrative only and not intended to be limiting. All publications, patent applications, patents, sequences, database entries, and other references mentioned herein are incorporated by reference in their entirety. In case of conflict, the present specification, including definitions, will control.

Other features and advantages of the invention will be apparent from the following detailed description and Figures, and from the claims.

## DESCRIPTION OF DRAWINGS

**FIGs. 1A-B. iTransduce library for selection of novel AAV capsids capable of efficient transgene expression in target tissue. a.** Two-component system of the library construct. 1. Cre recombinase is driven by a minimal chicken beta actin (CBA) promoter. 2. p41 promoter driven AAV9 capsid with random heptamer peptide inserted between aa 588-589, cloned downstream of the Cre cassette. **b.** Selection strategy. i. The iTransduce library comprised of different peptide inserts expressed on the capsid (represented by different colors), are injected i.v. into Ai9 transgenic mouse with a loxP-flanked STOP cassette upsteam of the tdTomato reporter gene, inserted into the Gt(ROSA)26Sor locus.

AAV capsids able to enter the cell of interest but do not functionally transduce the cell (no Cre expression) do not turn on tdTomato expression. Capsids that can mediate functional transduction (express Cre) will turn on tdTomato expression. ii. Cells are isolated from the organ of interest (e.g. brain), and transduced cells are sorted for tdTomato expression and optionally cell markers. iii. Capsid DNA is PCR-amplified from the sorted cells, cloned back to the library vector and repackaged for another round of selection. DNA sequencing analysis is utilized after each round to monitor selection process.

**FIGs. 2A-B. Identification of AAV-S and AAV-F after two rounds of in vivo selection for brain transduction after systemic injection.** Donut charts indicate the frequency of particular peptide inserts determined by next-generation sequencing**.** **a.** Table of Round 2 vector sequences after production but before injection (SEQ ID NOS:17-86). **b.** Donut chart of peptide frequency appearing in iTransduce isolation after Round 2 injection (SEQ ID NOs.1-3). "Others" indicates sequence variants appearing as less than 1% of the total pool (in (a), variants isolated after Round 2 screen are also highlighted, appearing at less than 1%). * indicates a stop codon.

**FIGs. 3A-F. AAV-F efficiently transduces the brain of mice after systemic injection. a.** Single-stranded AAV-GFP expression cassette used to compare capsids' transduction potential. ITR, inverted terminal repeats; CBA, hybrid CMV enhancer/chicken beta actin promoter; WPRE, woodchuck hepatitis virus post transcriptional regulatory element; pA, poly A signals (both SV40 and bovine growth hormone derived). **b**. Representative low magnification images of whole brain sagittal sections from C57BL/6 mice (males) transduced with $1x10^{11}$ vg (low dose) of AAV9, AAV9-PHP.B, AAV-S, or AAV-F. **c.** Representative images of sagittal section of brains after injection of $8x10^{11}$ vg (high dose) of each vector in C57BL/6 males. **d.** Example sections of spinal cords transduced by each of the four vectors administered intravenously at the higher dose ($8x10^{11}$ vg/mouse). **e.** Quantitation of native GFP expression from each vector by the percentage of sections covered by fluorescence at low (left panel) and high (right panel) doses. **f.** Multiregional comparison of transduction in the brain at the higher dose. ***, $p< 0.001$; ****, $p < 0.0001$ after one-way ANOVA with Tukey's multiple comparison test (n=3 each group).

**FIGs. 4A-E. AAV vector comparison of neuron and astrocyte transduction and biodistribution.** High magnification images of AAV9, AAV-PHP.B, AAV-S and AAV-F transduced cells (GFP positive) after co-immunostaining with markers for **a.** neurons (NeuN) and **b.** astrocytes (glutamine synthetase, GS), Merged cells also include nuclear staining by DAPI. **c.** Stereological evaluation of the percentage of transduced cortical astrocytes and neurons after i.v. delivery of $1x10^{11}$ vg of each vector. $P < 0.0001$ one-way ANOVA. (*) and (**) represent the significant differences between each vector group after Tukey's multiple comparisons test (n=3 mice/group). **d.** Biodistribution of vectors in the brain and liver as measured by qPCR of vector genomes, normalized by GAPDH genomic DNA levels (input DNA). **e.** Transduction of AAV9, AAV9-PHP.B, AAV-S, and AAV-F in peripheral organs following intravenous administration at $8x10^{11}$ vg in C57BL/6 males. Retinal images: RPE, retinal pigment epithelium; ONL; outer nuclear layer; OPL, outer plexiform layer; INL, inner nuclear layer; IPL, inner plexiform layer; GCL, ganglion cell layer. ****, $p < 0.0001$ (n=3 mice/group, one-way ANOVA with Tukey's multiple comparisons test).

**FIGs. 5A-C. AAV-F mediates high transduction efficiency in male and female C57BL/6 mice and also in BALB/c mice. a.** Representative images of GFP signal across sagittal brain sections in male and female mice (n=3) transduced by AAV-F at $1x10^{11}$ vg/mouse. **b.** Sagittal brain sections of male BALB/c mice injected with AAV-F (left) or AAV9-PHP.B (right) at $1x10^{11}$ vg/ mouse. DAPI was provided as a counterstain along-side GFP to visualize PHP.B-treated brain sections. **c.** Quantitation of endogenous GFP expression from each vector by the percentage of sections covered by fluorescence. **, $p < 0.01$. Unpaired t-test (n=3 mice/group).

**FIGs. 6A-B. AAV-F mediates higher transduction efficiency than AAV9 in human cortical neurons. a.** GFP expression in fetal-derived primary human neurons, transduced by AAV-F. Neurons were co-labelled with an antibody to β-Tubulin to quantify transduction. **b.** Quantitation of transduction efficiency of human neurons by AAV9, AAV-S and AAV-F. *, $p < 0.05$.

**FIGs. 7A-C. iTransduce library functionally elicits Cre recombination and PCR amplification of 7-mer peptide-encoding inserts in cap gene can be rescued from tissue. a.** Examples of tdTomato DAB staining in tissues after transduction with the

unselected iTransduce library in an Ai9 floxed/STOP tdTomato transgenic mouse (right panels). PBS was as injected as control (left panels). Red arrows indicate examples of transduced cells. **b.** Examples of PCRs rescuing the insert-containing region of the Cap gene from various tissues, including brain, compared to wild-type and transgenic untransduced mice. **c.** Table illustrating the spectrum of variants seen after the first round of selection, with the most frequent variants highlighted (SEQ ID NOs:87-150). "Others" indicates grouped sequence variants, each of which appears as less than 1% of the total pool. * indicates a stop codon.

**FIGs. 8A-B. Cre-based selection in Round 2 reveals transduction-competent AAVs. a.** Flow cytometry analysis of tdTomato-positive cells. Following dissociation of mouse brains, the cell suspension was analyzed and sorted for tdTomato positive cells, with gating drawn based on forward and side scatter (FSC, SSC) to exclude non-viable cells (Total events), to capture only single cells (Singlets), and finally for tdTomato expression (tdTomato +/- cells). To sort tdTomato-positive cells from the AAV library-transduced brains, gating was established based upon a negative control (PBS-injected Ai9) and a positive control (Ai9 mice transduced with AAV9-PHP.B carrying a hSyn-Cre neuron-specific cassette). **b.** Cre-dependent recombination events are detected after DAB immunostaining for tdTomato in the liver and brain after injection of the Round 2 library (compared to PBS or AAV9-PHP.B hSyn-Cre injections). Arrow indicates a positive cell (astrocyte) in the brain of the AAV library injected mouse.

**FIGs. 9A-B. Transduction of the brain by AAV-F and AAV-S after intravenous delivery of a low ($1x10^{11}$ vg) or high doses of vector ($8x10^{11}$ vg).** Transduction profile in the brain after transduction by AAV9, AAV9-PHP.B, AAV-S and AAV-F in n=3 mice, demonstrating endogenous (unstained) GFP fluorescence in sagittal sections. Mice were administered with either $1x10^{11}$ vg **(a)** or $8x10^{11}$ vg **(b)**. Each section in each group is taken from an individual mouse.

**FIGs. 10A-B. (a) AAV-F transduces multiple subtypes of neurons in the mouse brain.** GFP expression driven by AAV-F was detected in a broad range of neuronal subtypes across different regions of the brain and CNS. CamKII, excitatory neurons. GAD67, inhibitory neurons. Tyrosine hydroxolase (TH), Purkinje neurons. Choline acetyltransferase (ChAT), motor neurons (white arrows represent examples of

transduced neurons for each subtype). **(b) AAV-F mediates efficient transduction while AAV9 does not at $1x10^{11}$ vg/mouse.** Representative 10x images from mice from FIG. 3b show GFP expression in striatum, hippocampus, and cerebellum from mice injected with AAV-F and AAV9.

**FIG. 11. Biodistribution of AAV-F after systemic delivery.** AAV-F biodistribution as compared to AAV9 is shown in skeletal muscle, heart, and spinal cord tissue. Biodistribution was measured by qPCR of vector genomes, and samples were normalized against GAPDH genomic DNA for equal input. n.s, not significant. *, $p < 0.05$ (n=3 mice/group, each mouse sample run in triplicate, two-tailed t-test).

**FIGs. 12A-E. Quantification of empty capsids by transmission electron microscopy (TEM). a-d.** Representative image segments of electron micrographs of AAV9 and AAV-F preps. Two preps each of AAV9 (**a,b**) and AAV-F (**c,d**) were quantified, by counting full vs. empty capsids across five images for each prep (examples of empty capsids are indicated by arrows). **e.** Quantification of empty capsid percentages for AAV9 and AAV-F preps. n.s: not significant ($p = 0.54$, unpaired t-test).

**FIG. 13. Sustained neural transduction after direct intracranial injection of AAV-F and AAV-S.** Representative images of GFP fluorescence signal (and DAPI) across mouse brain sagittal sections after direct intracortical and intrahippocampal injections of AAV-F (upper panels) or AAV-S (lower panels) ($1.65x10^{10}$ and $5.6x10^{10}$ gc/injection site for AAV-F and AAV-S, respectively). Scale bar: 1000μm for the low-magnification images of full brain and 200 μm for Higher-magnification images of the cortex and hippocampus.

**FIGs. 14A-F. Widespread transduction of spinal cord and brain after lumbar intrathecal injection of AAV-F vector.** Ten microliters of AAV9 ($1.25x10^{11}$ vg) or AAV-F ($8.8x10^{10}$ vg) packaging a single stranded AAV-CBA-GFP expression cassette were injected intrathecally in the lumbar region of adult mice (n=2/vector). Three weeks later, mice were killed and spinal cord and brain analyzed for GFP expression after anti-GFP immunostaining. **(a) Top images:** Full coronal brain section scans showing robust transduction of brain with AAV-F but not AAV9. **Lower images:** Full section scans of spinal cord with AAV-F and AAV9. AAV-F injected mice showed very high GFP signal. AAV9 showed very low expression in both mice. All images were taken at an exposure

time of 33ms; an additional image at 4ms was taken for AAV-F to better resolve features. White outlines of section limits are included where section is dim. Where not listed, scale bars equal 250μm. **(b-d)** High magnification images of spinal cords from mice treated with AAV9 (b) and AAV-F (c,d). GFAP indicates astrocyte-specific staining and NeuN for neurons. The area of the spinal cord is indicated in the upper right of each image. Images in lower panels are higher magnification images of the boxed in area in the upper image. **(e, f)** High magnification images of AAV-F transduced brain after intrathecal injection. (e) depicts astrocytes (f) neurons transduced by AAV-F. AAV9 did not mediate detectable transduction of brain after intrathecal injection. SC, spinal cord; CC, corpus callosum, CP, caudate putamen.

**FIGs. 15A-D. GFP fluorescence following AAV-S-CBA-GFP administration to the inner ear. (a,b)**: Representative images of cochlear sensory epithelium transduced with AAV-S (63x magnification). **(c)**: Transduction in the spiral limbus. (**d**): Transduction in spiral ganglion region. Z and arrow indicates different layers of Z-stack. OHC: outer hair cells. IHC: inner hair cells.

**FIGs. 16A-B. Use of the iTransduce library in non-transgenic NHP to select AAV capsids that efficiently transduce inner-ear fibrocytes and spinal cord. (A) i**. Cynomolgus monkeys (or other non-human primates) are co-injected with the AAV capsid library along with an AAV9-PHP.B encoding a GJB2-driven floxed-Stop-tdTomato cassette. **ii**. AAV9-PHP.B will selectively express tdTomato in fibrocytes (indicating by shading) when an AAV library capsid expresses Cre. **iii**. the inner ear is dissociated and **iv**. tdTomato positive fibrocytes are flow-sorted. **v**. Potentially functional capsids are PCR-amplified from recovered DNA from the sorted cells, the library is repackaged and another round of selection is performed. Next generation DNA sequencing analysis is utilized after each round to monitor selection process. Abbreviations: TM, tectorial membrane; OC, organ of Corti; SL, spiral ligament. **(B)**. **i**. Cynomolgus monkeys (or other non-human primates) are co-injected with the AAV capsid library along with an AAV9- encoding a CBA-driven floxed-Stop-mPlum cassette. **ii**., **iii**. AAV9 will express mPlum in spinal cord (indicating by shading) when an AAV library capsid expresses Cre. The spinal cord is dissociated and mPlum positive cells are flow-sorted. **iv**. Potentially functional capsids are PCR-amplified from recovered DNA

from the sorted cells, the library is repackaged and another round of selection is performed. Next generation DNA sequencing analysis is utilized after each round to monitor selection process.

## DETAILED DESCRIPTION

A promising approach to efficient delivery of transgenes to target cells is via a process of submitting a pool, or library, of AAV vector capsids variants to an *in vivo* selection process – a veritable "survival of the fittest" approach[4-8]. AAV library approaches which use random oligomer nucleotides to insert short (6-9 amino acid) random peptides into an exposed region on the capsid surface have demonstrated success in identifying new AAV capsid variants with unique properties such as enhanced transduction of target tissues[9, 10]. One major limitation of AAV libraries is that the end readout of the selection process does not always differentiate capsids which mediate functional transgene expression from those which do not. AAV transduction is a process involving multiple steps, from cell receptor binding and entry to nuclear transport, second-strand synthesis and finally gene and protein expression[11]. A recent advance on the conventional AAV library approach, called CREATE, engineered a Cre-sensitive AAV genome which enabled selectively isolate capsids that have successfully trafficked to the nucleus in the context of a Cre-expressing transgenic animal[12]. Herein is described a capsid selection system, one example of which is called iTransduce, that utilizes the power of the *Cre/loxP* system. Instead of using Cre transgenic mice, the AAV was engineered to encode both the capsids with peptide inserts, along with a Cre-expression cassette. Selection was then performed in mice with a Cre-sensitive fluorescent reporter to enable selection of capsids which mediate the entire process of transduction including transgene expression. *In vivo* selection of the library resulted in the identification of an AAV capsid that mediates remarkable transduction efficiency of the CNS, and another capsid that mediates transduction in the inner ear.

Using the iTransduce system, we have isolated two new AAV capsids, referred to herein as AAV-F and AAV-S, which mediate highly efficient transgene expression in the murine CNS (two strains tested) and inner ear, respectively. The AAV-F capsid also mediated robust transduction of primary human neurons.

Interestingly, using expression-based selection, 3 peptide clones (STTLYSP (SEQ ID NO:1), FVVGQSY (SEQ ID NO:2), and FQPCP* (SEQ ID NO:3) were identified that represented 97% of NGS reads. Since FQPCP* had a stop codon, it was reasoned that this genome was cross-packaged in another capsid during production, a phenomenon noted to occur with AAV libraries[15]. This may also be the case for STTLYSP (SEQ ID NO:1, "AAV-S"), (**FIG. 2**). AAV-S was not a defective vector, as it mediated robust transduction of peripheral organs (**FIG. 4e**) and the inner ear (**FIG. 15**). Since it had such a high production efficiency (Table 4), AAV-S may have had a propensity to be cross-packaged. On the other hand, AAV-F (FVVGQSY (SEQ ID NO:2)) was extremely efficient at transduction and was one of only two prospective candidates from the NGS (**FIG. 2**). Both of these candidates were detectable at very low levels in the Round 2 library pool (**FIG. 2**) – as such, we could confirm that their enrichment was not due to a preexisting bias.

Since we performed a demonstration of the iTransduce system using an agnostic approach to cell type (whole brain), it is not surprising that AAV-F was highly tropic to astrocytes and neurons, cells that are transduced by AAV9. In future studies we will combine cell specific promoters to drive Cre expression from the AAV library vector as well as magnetic cell sorting to isolate capsids that can transduce cells that are refractory to conventional AAV vector transduction.

In addition to the potential of the iTransduce system to select clinical candidate AAV vectors, it can be used to identify vectors for use as research tools. The recently identified AAV-PHP.B capsid has served as an efficient vector to genetically modify the murine brain[12]. However, it does not transduce BALB/c or BALB/c related mouse lineages[13, 14 16]. Interestingly, robust transduction of BALB/c and C57BL/6 murine brain was observed after intravenous injection of AAV-F. This indicates that the mechanism of enhanced transduction over AAV9 differs between AAV-PHP.B and AAV-F. It also enables AAV-F to be utilized as an efficient tool for CNS research in the popular BALB/c strain (labome.com/method/Laboratory-Mice-and-Rats.html). Additionally, as shown herein AAV-F can also mediate robust transgene expression in the CNS after both direct and intrathecal bolus injection, and AAV-S can mediate transgene expression in the inner ear.

Future studies in larger animals can be carried out to further test AAV-F, e.g., in preclinical studies. Dose escalation studies can be performed to test for dose-related toxicity of AAV-F, as was observed with PHP.B in NHPs[14]. Iterative rounds of selection can be done in different species (e.g. mice then rats) to allow better cross-species translation of the transduction efficiency. For example, this could be done in mice followed by floxed STOP tdTomato transgenic rats[17]. Alternatively, direct selection of the iTransduce library can be performed in transgenic marmosets[18, 19] or even in other non-human non-transgenic primates (**FIGs. 16A and B**).

**Methods of identifying optimized capsid sequences**

"Virus vector libraries" are pooled variants of viruses, which under selective pressure (in vivo or in vitro) can drive isolation of clones of viruses specific for a target cell/tissue/organ of interest. One limitation of current library technologies is that many of the candidate virus clones do not mediate transgene expression (the required final function of the vector). The main reason for this limitation is that there has been no strategy devised to allow vector selection based on vector-mediated transgene expression. Described herein are methods that use an adeno-associated virus (AAV) vector genome with a two-part expression cassette. The first is a Cre-recombinase cassette under a promoter of interest. The second part is an AAV promoter to drive expression of the capsid gene, cloned “in cis” to the first section of the viral genome. Virus vectors can now be selected for transgene expression (highly sensitive Cre expression) using cells that express a reporter gene (e.g., green fluorescent protein) with an upstream loxP/stop site, thus preventing reporter expression until AAV vector-delivered Cre removes the stop site. Reporter gene positive cells can be isolated and recovered AAV capsid sequences will have a higher likelihood of mediating efficient transgene expression.

Thus provided herein are library construct AAVs comprising: (i) a Cre recombinase driven by a promoter, e.g., a minimal chicken beta actin (CBA) promoter; (ii) a promoter (e.g., p41 promoter)-driven AAV9 capsid sequence with a sequence encoding a peptide as described herein, e.g., a random heptamer peptide or selected heptamer peptide, inserted into a capsid protein, downstream of the Cre cassette. Preferably the peptide is inserted between the sequences encoding amino acids (aa) 588-

589 of the capsid, but it can also be inserted elsewhere as long as it doesn't interfere with function of the virus and maintains its activity in promoting infection of selected cells, e.g., at the VP1/VP2 interface (amino acid 138) or any site between 583-590. The CBA promoter is strong, active promoter to drive Cre in most cell types. The P41 promoter is an AAV specific natural promoter which drives Cap gene expression Other promoters that can be used include, but are not limited to, Synapsin promoter, GFAP promoter, CD68 promoter, F4/80 promoter, CX3CR1 promoter, CD3 or CD4 promoter, CMV promoter, liver specific promoter; other examples are listed below. The constructs can also include a stop codon at the end of the Cre cDNA and at the end of the cap DNA. There are poly A signals after the Cre cassette and the cap cassette. Cre recombinases are known in the art, see, e.g., Van Duyne, Microbiol Spectr. 2015 Feb;3(1):MDNA3-0014-2014. Fig. 1A provides an exemplary library construct.

Also provided herein are libraries (i.e., compositions comprising a plurality of the library constructs). Where random heptamer sequences are used, preferably the library comprises constructs with sequences encoding all or almost all possible variants of the heptamer).

The methods, illustrated in Fig. 1B(i), can include administering a library comprised of different peptide inserts expressed on the capsid (represented by different shades of gray) to a model animal, e.g., a mammal such as a mouse (e.g., an Ai9 transgenic mouse), rabbit, rat, or monkey. The model animal comprises a loxP-flanked STOP cassette upstream of a reporter sequence, e.g., a fluorescent reporter protein sequence, e.g., a tdTomato reporter gene, optionally inserted into a Gt(ROSA)26Sor locus. The model animal can be transgenic, or the loxP-flanked STOP cassette upstream of a reporter sequence can be expressed from a second construct, e.g., a second AAV administered to the animal model (e.g., administered before, after, or concurrently with the library constructs). Any AAV capsids that enter the cell of interest but do not functionally transduce the cell (no Cre expression) do not turn on expression of the reported. Capsids that can mediate functional transduction (express Cre) will turn on tdTomato expression. As shown in Fig. 1B(ii), cells are isolated from the organ of interest (e.g., brain, eye, ear, retina, heart, etc.), and then transduced cells can then be sorted for reporter gene expression and optionally cell markers. As shown in Fig. 1B(iii), capsid

DNA is obtained and analyzed, e.g., optionally by PCR-amplifying sequences from the sorted cells, cloning them back to the library vector and repackaged for another round of selection. DNA sequencing analysis can be utilized after each round to monitor selection process.

*Promoters*

The library constructs described herein include two promoters; one driving the Cre recombinase, and a second driving the AAV capsid sequence.

A number of promoter sequences are known in the art, including so-called "ubiquitous" promoters that drive expression in most cell types, e.g., cytomegalovirus (CMV) promoter (optionally with the CMV enhancer), chicken beta-actin (CBA) promoter, Rous sarcoma virus (RSV) LTR promoter (optionally with the RSV enhancer), SV40 promoter, dihydrofolate reductase promoter, phosphoglycerol kinase promoter, phosphoglycerol kinase (PGK) promoter, EF1alpha promoter, Ubiquitin C (UBC), B-glucuronidase (GUSB), and CMV immediate/early gene enhancer/CBA promoter.

Expression of the Cre-recombinase can also be driven by a tissue-specific promoter, e.g., a tissue-specific promoter for CNS, liver, heart cochlea, retina, or T cells, *inter alia*. In some embodiments, the tissue specific promoter for CNS includes neuronal, macrophage/microglial promoter and astrocyte promoters. A number of tissue specific promoters are known in the art, including synapsin promoter (neurons), neuron-specific enolase (NSE) (neurons), MeCP2 (methyl-CPG binding protein 2) (neurons), a glial fibrillary acidic protein (GFAP) (astrocytes), oligodendrocyte transcription factor 1 (Olig1) (oligodendrocytes), CNP (2',3'-Cyclic-nucleotide 3'-phosphodiesterase) (broad), or CBh (hybrid CBA or a MVM intron with CBA promoter)(broad). See, e.g., US20190032078. Macrophage/microglial promoters include, but are not limited to, a C-X3-C motif chemokine receptor 1 (CX3CR1) promoter, CD68 promoter, an ionized calcium binding adaptor molecule 1 (IBA1) promoter, a transmembrane protein 119 (TMEM119) promoter, a spalt like transcription factor 1 (SALL1) promoter, an adhesion G protein-coupled receptor E1 (F4/80) promoter, a myeloproliferative sarcoma virus enhancer, negative control region deleted, d1587rev primer-binding site substituted (MND) promoter; integrin subunit alpha M (ITGAM; CD11b- myeloid cells (neutrophils, monocytes, and macrophages)) promoter. For expression in the inner ear, the promoter

can be, e.g., a PKG, CAG, prestin, Atoh1, POU4F3, Lhx3, Myo6, α9AchR, α10AchR, oncomod, or myo7A promoter; see Ryan et al., Adv Otorhinolaryngol. 2009; 66: 99–115.

*Reporter Proteins*

A number of reporter proteins are known in the art, and include green fluorescent protein (GFP), variant of green fluorescent protein (GFP10), enhanced GFP (eGFP), TurboGFP, GFPS65T, TagGFP2, mUKGEmerald GFP, Superfolder GFP, GFPuv, destabilised EGFP (dEGFP), Azami Green, mWasabi, Clover, mClover3, mNeonGreen, NowGFP, Sapphire, T-Sapphire, mAmetrine, photoactivatable GFP (PA-GFP), Kaede, Kikume, mKikGR, tdEos, Dendra2, mEosFP2, Dronpa, blue fluorescent protein (BFP), eBFP2, azurite BFP, mTagBFP, mKalamal, mTagBFP2, shBFP, cyan fluorescent protein (CFP), eCFP, Cerulian CFP, SCFP3A, destabilised ECFP (dECFP), CyPet, mTurquoise, mTurquoise2, mTFPI, photoswitchable CFP2 (PS-CFP2), TagCFP, mTFP1, mMidoriishi-Cyan, aquamarine, mKeima, mBeRFP, LSS-mKate2, LSS-mKatel, LSS-mOrange, CyOFP1, Sandercyanin, red fluorescent protein (RFP), eRFP, mRaspberry, mRuby, mApple, mCardinal, mStable, mMaroonl, mGarnet2, tdTomato, mTangerine, mStrawberry, TagRFP, TagRFP657, TagRFP675, mKate2, HcRed, t-HcRed, HcRed-Tandem, mPlum, mNeptune, NirFP, Kindling, far red fluorescent protein, yellow fluorescent protein (YFP), eYFP, destabilised EYFP (dEYFP), TagYFP, Topaz, Venus, SYFP2, mCherry, PA-mCherry, Citrine, mCitrine, Ypet, IANRFP-AS83, mPapayal, mCyRFP1, mHoneydew, mBanana, mOrange, Kusabira Orange, Kusabira Orange 2, mKusabira Orange, mOrange 2, $mKO_K$, mKO2, mGrapel, mGrape2, zsYellow, eqFP611, Sirius, Sandercyanin, shBFP-N158S/L173I, near infrared proteins, iFP1.4, iRFP713, iRFP670, iRFP682, iRFP702, iRFP720, iFP2.0, mIFP, TDsmURFP, miRFP670, Brilliant Violet (BV) 421, BV 605, BV 510, BV 711, BV786, PerCP, PerCP/Cy5.5, DsRed, DsRed2, mRFPl, pocilloporin, Renilla GFP, Monster GFP, paGFP, or a Phycobiliprotein, or a biologically active variant or fragment of any one thereof.

*Kits*

Also provided herein are kits comprising one or more library construct AAVs as described herein, with or without the random heptamer sequences. The kits can also include a construct comprising a loxP-flanked STOP cassette upstream of a reporter sequence.

**Engineered AAV capsid proteins**

The present methods identified two peptide sequences that alter the ability of an AAV to mediate transgene expression in specified cells when inserted into the capsid of the AAV, e.g., AAV1, AAV2, AAV8, or AAV9. In some embodiments, the peptides comprise sequences of at least 7 amino acids. In some embodiments, the amino acid sequence comprises at least 4, e.g., 5, 6, or 7 contiguous amino acids of the sequences (STTLYSP (SEQ ID NO:1) or FVVGQSY (SEQ ID NO:2).

Peptides including reversed sequences can also be used, e.g., PSYLTTS (SEQ ID NO:4) and YSQGVVF (SEQ ID NO:5). Alternatively, the peptides can comprise at least four, five, or six contiguous amino acids from the sequences shown in FIGs. 2A or 7C (SEQ ID NOs:17-150).

***AAVs***

Viral vectors for use in the present methods, kits and compositions include recombinant retroviruses, adenovirus, adeno-associated virus, alphavirus, and lentivirus, preferably comprising a capsid peptide as described herein and optionally a transgene for expression in a target tissue.

A preferred viral vector system useful for delivery of nucleic acids in the present methods is the adeno-associated virus (AAV). AAV is a tiny non-enveloped virus having a 25 nm capsid. No disease is known or has been shown to be associated with the wild type virus. AAV has a single-stranded DNA (ssDNA) genome. AAV has been shown to exhibit long-term episomal transgene expression, and AAV has demonstrated excellent transgene expression in the brain, particularly in neurons. Space for exogenous DNA is limited to about 4.7 kb. An AAV vector such as that described in Tratschin et al., Mol. Cell. Biol. 5:3251-3260 (1985) can be used to introduce DNA into cells. A variety of nucleic acids have been introduced into different cell types using AAV vectors (see for example Hermonat et al., Proc. Natl. Acad. Sci. USA 81:6466-6470 (1984); Tratschin et al., Mol. Cell. Biol. 4:2072-2081 (1985); Wondisford et al., Mol. Endocrinol. 2:32-39 (1988); Tratschin et al., J. Virol. 51:611-619 (1984); and Flotte et al., J. Biol. Chem. 268:3781-3790 (1993). There are numerous alternative AAV variants (over 100 have been cloned), and AAV variants have been identified based on desirable characteristics.

In some embodiments, the AAV is AAV1, AAV2, AAV3, AAV4, AAV5, AAV6, AV6.2, AAV7, AAV8, rh.8, AAV9, rh.10, rh.39, rh.43 or CSp3; for CNS use, in some embodiments the AAV is AAV1, AAV2, AAV4, AAV5, AAV6, AAV8, or AAV9. As one example, AAV9 has been shown to somewhat efficiently cross the blood-brain barrier. Using the present methods, the AAV capsid can be genetically engineered to increase permeation across the BBB, or into a specific tissue, by insertion of a peptide sequence as described herein into the capsid protein, e.g., into the AAV9 capsid protein VP1 between amino acids 588 and 589.

An exemplary wild type AAV9 capsid protein VP1 (Q6JC40-1) sequence is as follows:

```
         10          20          30          40          50
MAADGYLPDW LEDNLSEGIR EWWALKPGAP QPKANQQHQD NARGLVLPGY
         60          70          80          90         100
KYLGPGNGLD KGEPVNAADA AALEHDKAYD QQLKAGDNPY LKYNHADAEF
        110         120         130         140         150
QERLKEDTSF GGNLGRAVFQ AKKRLLEPLG LVEEAAKTAP GKKRPVEQSP
        160         170         180         190         200
QEPDSSAGIG KSGAQPAKKR LNFGQTGDTE SVPDPQPIGE PPAAPSGVGS
        210         220         230         240         250
LTMASGGGAP VADNNEGADG VGSSSGNWHC DSQWLGDRVI TTSTRTWALP
        260         270         280         290         300
TYNNHLYKQI SNSTSGGSSN DNAYFGYSTP WGYFDFNRFH CHFSPRDWQR
        310         320         330         340         350
LINNNWGFRP KRLNFKLFNI QVKEVTDNNG VKTIANNLTS TVQVFTDSDY
        360         370         380         390         400
QLPYVLGSAH EGCLPPFPAD VFMIPQYGYL TLNDGSQAVG RSSFYCLEYF
        410         420         430         440         450
PSQMLRTGNN FQFSYEFENV PFHSSYAHSQ SLDRLMNPLI DQYLYYLSKT
        460         470         480         490         500
INGSGQNQQT LKFSVAGPSN MAVQGRNYIP GPSYRQQRVS TTVTQNNNSE
        510         520         530         540         550
FAWPGASSWA LNGRNSLMNP GPAMASHKEG EDRFFPLSGS LIFGKQGTGR
        560         570         580         590         600
DNVDADKVMI TNEEEIKTTN PVATESYGQV ATNHQSAQAQ AQTGWVQNQG
        610         620         630         640         650
ILPGMVWQDR DVYLQGPIWA KIPHTDGNFH PSPLMGGFGM KHPPPQILIK
        660         670         680         690         700
NTPVPADPPT AFNKDKLNSF ITQYSTGQVS VEIEWELQKE NSKRWNPEIQ
        710         720         730
YTSNYYKSNN VEFAVNTEGV YSEPRPIGTR YLTRNL     (SEQ ID NO:6)
```

Thus provided herein are AAV that include one or more of the peptide sequences described herein, e.g., an AAV comprising a capsid protein comprising a sequence described herein, e.g., a capsid protein comprising SEQ ID NO:1 or SEQ ID NO:2, wherein a peptide sequence has been inserted into the sequence, e.g., between amino acids 588 and 589.

Exemplary sequences of AAVs are provided below. The inserted peptide sequences are bold and double-underlined highlighted in the protein sequences, and bold and capitalized in the DNA sequences.

AAV-F capsid protein sequence

MAADGYLPDWLEDNLSEGIREWWALKPGAPQPKANQQHQDNARGLVLPGYKYLG
PGNGLDKGEPVNAADAAALEHDKAYDQQLKAGDNPYLKYNHADAEFQERLKEDTSFGGN
LGRAVFQAKKRLLEPLGLVEEAAKTAPGKKRPVEQSPQEPDSSAGIGKSGAQPAKKRLN
FGQTGDTESVPDPQPIGEPPAAPSGVGSLTMASGGGAPVADNNEGADGVGSSSGNWHCD
SQWLGDRVITTSTRTWALPTYNNHLYKQISNSTSGGSSNDNAYFGYSTPWGYFDFNRFH
CHFSPRDWQRLINNNWGFRPKRLNFKLFNIQVKEVTDNNGVKTIANNLTSTVQVFTDSD
YQLPYVLGSAHEGCLPPFPADVFMIPQYGYLTLNDGSQAVGRSSFYCLEYFPSQMLRTG
NNFQFSYEFENVPFHSSYAHSQSLDRLMNPLIDQYLYYLSKTINGSGQNQQTLKFSVAG
PSNMAVQGRNYIPGPSYRQQRVSTTVTQNNNSEFAWPGASSWALNGRNSLMNPGPAMAS
HKEGEDRFFPLSGSLIFGKQGTGRDNVDADKVMITNEEEIKTTNPVATESYGQVATNHQ
SAQ**<u>FVVGQSY</u>**AQAQTGWVQNQGILPGMVWQDRDVYLQGPIWAKIPHTDGNFHPSPLMGG
FGMKHPPPQILIKNTPVPADPPTAFNKDKLNSFITQYSTGQVSVEIEWELQKENSKRWN
PEIQYTSNYYKSNNVEFAVNTEGVYSEPRPIGTRYLTRNL(SEQ ID NO:7)

AAV-F capsid DNA sequence

atggctgccgatggttatcttccagattggctcgaggacaaccttagtgaagga
attcgcgagtggtgggctttgaaacctggagcccctcaacccaaggcaaatcaacaaca
tcaagacaacgctcgaggtcttgtgcttccgggttacaaataccttggacccggcaacg
gactcgacaaggggagccggtcaacgcagcagacgcggcggccctcgagcacgacaag
gcctacgaccagcagctcaaggccggagacaacccgtacctcaagtacaaccacgccga
cgccgagttccaggagcggctcaaagaagatacgtcttttgggggcaacctcgggcgag
cagtcttccaggccaaaaagaggcttcttgaacctcttggtctggttgaggaagcggct
aagacggctcctggaaagaagaggcctgtagagcagtctcctcaggaaccggactcctc

cgcgggtattggcaaatcgggtgcacagcccgctaaaaagagactcaatttcggtcaga
ctggcgacacagagtcagtcccagaccctcaaccaatcggagaacctcccgcagccccc
tcaggtgtgggatctcttacaatggcttcaggtggtggcgcaccagtggcagacaataa
cgaaggtgccgatggagtgggtagttcctcgggaaattggcattgcgattcccaatggc
tgggggacagagtcatcaccaccagcacccgaacctgggccctgcccacctacaacaat
cacctctacaagcaaatctccaacagcacatctggaggatcttcaaatgacaacgccta
cttcggctacagcacccccctgggggtattttgacttcaacagattccactgccacttct
caccacgtgactggcagcgactcatcaacaacaactggggattccggcctaagcgactc
aacttcaagctcttcaacattcaggtcaaagaggttacggacaacaatggagtcaagac
catcgccaataaccttaccagcacggtccaggtcttcacggactcagactatcagctcc
cgtacgtgctcgggtcggctcacgagggctgcctcccgccgttcccagcggacgttttc
atgattcctcagtacgggtatctgacgcttaatgatggaagccaggccgtgggtcgttc
gtccttttactgcctggaatatttcccgtcgcaaatgctaagaacgggtaacaacttcc
agttcagctacgagtttgagaacgtacctttccatagcagctacgctcacagccaaagc
ctggaccgactaatgaatccactcatcgaccaatacttgtactatctctcaaagactat
taacggttctggacagaatcaacaaacgctaaaattcagtgtggccggacccagcaaca
tggctgtccagggaagaaactacatacctggacccagctaccgacaacaacgtgtctca
accactgtgactcaaaacaacaacagcgaatttgcttggcctggagcttcttcttgggc
tctcaatggacgtaatagcttgatgaatcctggacctgctatggccagccacaaagaag
gagaggaccgtttctttcctttgtctggatctttaatttttggcaaacaaggaactgga
agagacaacgtggatgcggacaaagtcatgataaccaacgaagaagaaattaaaactac
taacccggtagcaacggagtcctatggacaagtggccacaaaccaccagagtgcccaa**T**
**TTGTTGTTGGTCAGAGTTAT**gcacaggcgcagaccggctgggttcaaaaccaaggaata
cttccgggtatggtttggcaggacagagatgtgtacctgcaaggacccatttgggccaa
aattcctcacacggacggcaactttcacccttctccgctgatgggagggtttggaatga
agcacccgcctcctcagatcctcatcaaaaacacacctgtacctgcggatcctccaacg
gccttcaacaaggacaagctgaactctttcatcacccagtattctactggccaagtcag
cgtggagatcgagtgggagctgcagaaggaaaacagcaagcgctggaacccggagatcc
agtacacttccaactattacaagtctaataatgttgaatttgctgttaatactgaaggt
gtatatagtgaaccccgccccattggcaccagatacctgactcgtaatctg (SEQ ID
NO:8)

AAV-S capsid protein sequence

MAADGYLPDWLEDNLSEGIREWWALKPGAPQPKANQQHQDNARGLVLPGYKYLG
PGNGLDKGEPVNAADAAALEHDKAYDQQLKAGDNPYLKYNHADAEFQERLKEDTSFGGN
LGRAVFQAKKRLLEPLGLVEEAAKTAPGKKRPVEQSPQEPDSSAGIGKSGAQPAKKRLN
FGQTGDTESVPDPQPIGEPPAAPSGVGSLTMASGGGAPVADNNEGADGVGSSSGNWHCD
SQWLGDRVITTSTRTWALPTYNNHLYKQISNSTSGGSSNDNAYFGYSTPWGYFDFNRFH
CHFSPRDWQRLINNNWGFRPKRLNFKLFNIQVKEVTDNNGVKTIANNLTSTVQVFTDSD
YQLPYVLGSAHEGCLPPFPADVFMIPQYGYLTLNDGSQAVGRSSFYCLEYFPSQMLRTG
NNFQFSYEFENVPFHSSYAHSQSLDRLMNPLIDQYLYYLSKTINGSGQNQQTLKFSVAG
PSNMAVQGRNYIPGPSYRQQRVSTTVTQNNNSEFAWPGASSWALNGRNSLMNPGPAMAS
HKEGEDRFFPLSGSLIFGKQGTGRDNVDADKVMITNEEEIKTTNPVATESYGQVATNHQ
SAQ**STTLYSP**AQAQTGWVQNQGILPGMVWQDRDVYLQGPIWAKIPHTDGNFHPSPLMGG
FGMKHPPPQILIKNTPVPADPPTAFNKDKLNSFITQYSTGQVSVEIEWELQKENSKRWN
PEIQYTSNYYKSNNVEFAVNTEGVYSEPRPIGTRYLTRNL (SEQ ID NO:9)

AAV-S capsid DNA sequence

atggctgccgatggttatcttccagattggctcgaggacaaccttagtgaagga
attcgcgagtggtgggctttgaaacctggagcccctcaacccaaggcaaatcaacaaca
tcaagacaacgctcgaggtcttgtgcttccgggttacaaataccttggacccggcaacg
gactcgacaaggggagccggtcaacgcagcagacgcggcggccctcgagcacgacaag
gcctacgaccagcagctcaaggccggagacaacccgtacctcaagtacaaccacgccga
cgccgagttccaggagcggctcaaagaagatacgtcttttgggggcaacctcgggcgag
cagtcttccaggccaaaaagaggcttcttgaacctcttggtctggttgaggaagcggct
aagacggctcctggaaagaagaggcctgtagagcagtctcctcaggaaccggactcctc
cgcgggtattggcaaatcgggtgcacagcccgctaaaaagagactcaatttcggtcaga
ctggcgacacagagtcagtcccagaccctcaaccaatcggagaacctcccgcagccccc
tcaggtgtgggatctcttacaatggcttcaggtggtggcgcaccagtggcagacaataa
cgaaggtgccgatggagtgggtagttcctcgggaaattggcattgcgattcccaatggc
tgggggacagagtcatcaccaccagcacccgaacctgggccctgcccacctacaacaat
cacctctacaagcaaatctccaacagcacatctggaggatcttcaaatgacaacgccta
cttcggctacagcacccccctgggggtattttgacttcaacagattccactgccacttct
caccacgtgactggcagcgactcatcaacaacaactggggattccggcctaagcgactc

aacttcaagctcttcaacattcaggtcaaagaggttacggacaacaatggagtcaagac
catcgccaataaccttaccagcacggtccaggtcttcacggactcagactatcagctcc
cgtacgtgctcgggtcggctcacgagggctgcctcccgccgttcccagcggacgttttc
atgattcctcagtacgggtatctgacgcttaatgatggaagccaggccgtgggtcgttc
gtccttttactgcctggaatatttcccgtcgcaaatgctaagaacgggtaacaacttcc
agttcagctacgagtttgagaacgtacctttccatagcagctacgctcacagccaaagc
ctggaccgactaatgaatccactcatcgaccaatacttgtactatctctcaaagactat
taacggttctggacagaatcaacaaacgctaaaattcagtgtggccggacccagcaaca
tggctgtccagggaagaaactacatacctggacccagctaccgacaacaacgtgtctca
accactgtgactcaaaacaacaacagcgaatttgcttggcctggagcttcttcttgggc
tctcaatggacgtaatagcttgatgaatcctggacctgctatggccagccacaaagaag
gagaggaccgtttctttcctttgtctggatctttaatttttggcaaacaaggaactgga
agagacaacgtggatgcggacaaagtcatgataaccaacgaagaagaaattaaaactac
taacccggtagcaacggagtcctatggacaagtggccacaaaccaccagagtgcccaa**T**
**CTACTACGCTTTATAGTCCT**gcacaggcgcagaccggctgggttcaaaaccaaggaata
cttccgggtatggtttggcaggacagagatgtgtacctgcaaggacccatttgggccaa
aattcctcacacggacggcaactttcacccttctccgctgatgggagggtttggaatga
agcacccgcctcctcagatcctcatcaaaaacacacctgtacctgcggatcctccaacg
gccttcaacaaggacaagctgaactctttcatcacccagtattctactggccaagtcag
cgtggagatcgagtgggagctgcagaaggaaaacagcaagcgctggaacccggagatcc
agtacacttccaactattacaagtctaataatgttgaatttgctgttaatactgaaggt
gtatatagtgaaccccgccccattggcaccagatacctgactcgtaatctg (SEQ ID
NO:10)

The AAV sequences can be, e.g., at least 80, 85, 90, 95, 97, or 99% identical to a reference AAV sequence set forth herein, e.g., can include variants, preferable that do not reduce the ability of the AAV to mediate transgene expression in a cell. To determine the percent identity of two amino acid sequences, or of two nucleic acid sequences, the sequences are aligned for optimal comparison purposes (e.g., gaps can be introduced in one or both of a first and a second amino acid or nucleic acid sequence for optimal alignment and non-homologous sequences can be disregarded for comparison purposes). In a preferred embodiment, the length of a reference sequence aligned for comparison

purposes is at least 80% of the length of the reference sequence, and in some embodiments is at least 90% or 100%. The amino acid residues or nucleotides at corresponding amino acid positions or nucleotide positions are then compared. When a position in the first sequence is occupied by the same amino acid residue or nucleotide as the corresponding position in the second sequence, then the molecules are identical at that position (as used herein amino acid or nucleic acid "identity" is equivalent to amino acid or nucleic acid "homology"). The percent identity between the two sequences is a function of the number of identical positions shared by the sequences, taking into account the number of gaps, and the length of each gap, which need to be introduced for optimal alignment of the two sequences.

The comparison of sequences and determination of percent identity between two sequences can be accomplished using a mathematical algorithm. For example, the percent identity between two amino acid sequences can determined using the Needleman and Wunsch ((1970) J. Mol. Biol. 48:444-453 ) algorithm which has been incorporated into the GAP program in the GCG software package (available on the world wide web at gcg.com), using the default parameters, e.g., a Blossum 62 scoring matrix with a gap penalty of 12, a gap extend penalty of 4, and a frameshift gap penalty of 5.

*Transgenes*

In some embodiments, the AAV also includes a transgene sequence (i.e., a heterologous sequence), e.g., a transgene encoding a therapeutic agent, e.g., as described herein or as known in the art, or a reporter protein, e.g., a fluorescent protein, an enzyme that catalyzes a reaction yielding a detectable product, or a cell surface antigen. The transgene is preferably linked to sequences that promote/drive expression of the transgene in the target tissue.

Exemplary transgenes for use as therapeutics include neuronal apoptosis inhibitory protein (NAIP), nerve growth factor (NGF), glial-derived growth factor (GDNF), brain-derived growth factor (BDNF), ciliary neurotrophic factor (CNTF), tyrosine hydroxlase (TH), GTP-cyclohydrolase (GTPCH), amino acid decarboxylase (AADC), aspartoacylase (ASPA), blood factors, such as β-globin, hemoglobin, tissue plasminogen activator, and coagulation factors; colony stimulating factors (CSF);

interleukins, such as IL-1, IL-2, IL-3, IL-4, IL-5, IL-6, IL-7, IL-8, IL-9, etc.; growth factors, such as keratinocyte growth factor (KGF), stem cell factor (SCF), fibroblast growth factor (FGF, such as basic FGF and acidic FGF), hepatocyte growth factor (HGF), insulin-like growth factors (IGFs), bone morphogenetic protein (BMP), epidermal growth factor (EGF), growth differentiation factor-9 (GDF-9), hepatoma derived growth factor (HDGF), myostatin (GDF-8), nerve growth factor (NGF), neurotrophins, platelet-derived growth factor (PDGF), thrombopoietin (TPO), transforming growth factor alpha (TGF-α), transforming growth factor beta (TGF-β), and the like; soluble receptors, such as soluble TNF-α receptors, soluble VEGF receptors, soluble interleukin receptors (e.g., soluble IL-1 receptors and soluble type II IL-1 receptors), soluble gamma/delta T cell receptors, ligand-binding fragments of a soluble receptor, and the like; enzymes, such as α-glucosidase, imiglucarase, and β-glucocerebrosidase; enzyme activators, such as tissue plasminogen activator; chemokines, such as IP-10, monokine induced by interferon-gamma (Mig), Groa/IL-8, RANTES, MIP-1α, MIP-1β, MCP-1, PF-4, and the like; angiogenic agents, such as vascular endothelial growth factors (VEGFs, e.g., VEGF121, VEGF165, VEGF-C, VEGF-2), transforming growth factor-beta, basic fibroblast growth factor, glioma-derived growth factor, angiogenin, angiogenin-2, and the like; anti-angiogenic agents, such as a soluble VEGF receptor; protein vaccine; neuroactive peptides, such as nerve growth factor (NGF), bradykinin, cholecystokinin, gastin, secretin, oxytocin, gonadotropin-releasing hormone, beta-endorphin, enkephalin, substance P, somatostatin, prolactin, galanin, growth hormone-releasing hormone, bombesin, dynorphin, warfarin, neurotensin, motilin, thyrotropin, neuropeptide Y, luteinizing hormone, calcitonin, insulin, glucagons, vasopressin, angiotensin II, thyrotropin-releasing hormone, vasoactive intestinal peptide, a sleep peptide, and the like; thrombolytic agents; atrial natriuretic peptide; relaxin; glial fibrillary acidic protein; follicle stimulating hormone (FSH); human alpha-1 antitrypsin; leukemia inhibitory factor (LIF); transforming growth factors (TGFs); tissue factors, luteinizing hormone; macrophage activating factors; tumor necrosis factor (TNF); neutrophil chemotactic factor (NCF); nerve growth factor; tissue inhibitors of metalloproteinases; vasoactive intestinal peptide; angiogenin; angiotropin; fibrin; hirudin; IL-1 receptor antagonists; and the like. Some other examples of protein of interest include ciliary neurotrophic factor

(CNTF); neurotrophins 3 and 4/5 (NT-3 and 4/5); glial cell derived neurotrophic factor (GDNF); aromatic amino acid decarboxylase (AADC); hemophilia related clotting proteins, such as Factor VIII, Factor IX, Factor X; dystrophin or nini-dystrophin; lysosomal acid lipase; phenylalanine hydroxylase (PAH); glycogen storage disease-related enzymes, such as glucose-6-phosphatase, acid maltase, glycogen debranching enzyme, muscle glycogen phosphorylase, liver glycogen phosphorylase, muscle phosphofructokinase, phosphorylase kinase (e.g., PHKA2), glucose transporter (e.g., GLUT2), aldolase A, β-enolase, and glycogen synthase; lysosomal enzymes (e.g., beta-N-acetylhexosaminidase A); and any variants thereof.

The transgene can also encode an antibody, e.g., an immune checkpoint inhibitory antibody, e.g., to PD-L1, PD-1, CTLA-4 (Cytotoxic T-Lymphocyte-Associated Protein-4; CD152); LAG-3 (Lymphocyte Activation Gene 3; CD223); TIM-3 (T-cell Immunoglobulin domain and Mucin domain 3; HAVCR2); TIGIT (T-cell Immunoreceptor with Ig and ITIM domains); B7-H3 (CD276); VSIR (V-set immunoregulatory receptor, aka VISTA, B7H5, C10orf54); BTLA 30 (B- and T-Lymphocyte Attenuator, CD272); GARP (Glycoprotein A Repetitions; Predominant; PVRIG (PVR related immunoglobulin domain containing); or VTCN1 (Vset domain containing T cell activation inhibitor 1, aka B7-H4).

Other transgenes can include small or inhibitory nucleic acids that alter/reduce expression of a target gene, e.g., siRNA, shRNA, miRNA, antisense oligos, or long non-coding RNAs that alter gene expression (see, e.g., WO2012087983 and US20140142160), or CRISPR Cas9/cas12a and guide RNAs.

The virus can also include one or more sequences that promote expression of a transgene, e.g. one or more promoter sequences; enhancer sequences, e.g. 5' untranslated region (UTR) or a 3' UTR; a polyadenylation site; and/or insulator sequences. In some embodiments, the promoter is a brain tissue specific promoter, e.g. a neuron-specific or glia-specific promoter. In certain embodiments, the promoter is a promoter of a gene selected from: neuronal nuclei (NeuN), glial fibrillary acidic protein (GFAP), MeCP2, adenomatous polyposis coli (APC), ionized calcium-binding adapter molecule 1 (Iba-1), synapsin I (SYN), calcium/calmodulin-dependent protein kinase II, tubulin alpha I, neuron-specific enolase and platelet-derived growth factor beta chain. In some

embodiments, the promoter is a pan-cell type promoter, e.g., cytomegalovirus (CMV), beta glucuronidase, (GUSB), ubiquitin C (UBC), or rous sarcoma virus (RSV) promoter. The woodchuck hepatitis virus posttranscriptional response element (WPRE) can also be used.

In some embodiments, the AAV also has one or more additional mutations that increase delivery to the target tissue, e.g., the CNS, or that reduce off-tissue targeting, e.g., mutations that decrease liver delivery when CNS, heart, or muscle delivery is intended (e.g., as described in Pulicherla et al. (2011) Mol Ther 19:1070-1078); or the addition of other peptides, e.g., as described in Chen et al. (2008) Nat Med 15:1215-1218 or Xu et al., (2005) Virology 341:203-214 or US9102949; US 9585971; and US20170166926. See also Gray and Samulski (2011) "Vector design and considerations for CNS applications," in *Gene Vector Design and Application to Treat Nervous System Disorders* ed. Glorioso J., editor. (Washington, DC: Society for Neuroscience; ) 1–9, available at sfn.org/~/media/SfN/Documents/Short%20Courses/2011%20Short%20Course%20I/2011_SC1_Gray.ashx.

**Methods of Use**

The methods and compositions described herein can be used to deliver any composition, e.g., a sequence of interest to a tissue, e.g., to the central nervous system (brain), heart, muscle, peripheral nervous system (e.g., dorsal root ganglion or spinal cord), or to the inner ear or retina. In some embodiments, the methods include delivery to specific brain regions, e.g., cortex, cerebellum, hippocampus, substantia nigra, amygdala. In some embodiments, the methods include lumbar delivery, e.g., into the subarachnoid space or epidural space. In some embodiments, the methods include delivery to neurons, astrocytes, or glial cells. In some embodiments, the methods include delivery to inner and/or outer hair cells, spiral ganglion neurons, supporting cells, or fibrocytes of the inner ear. In some embodiments, the methods include delivery to the photoreceptors, interneurons, retinal ganglion cells (e.g., using AAV-F), or retinal pigment epithelium (RPE) (e.g., using AAV-S) of the retina.

In some embodiments, the methods and compositions, e.g., AAVs, are used to deliver a nucleic acid sequence to a subject who has a disease, e.g., a disease of the CNS;

see, e.g., US9102949; US 9585971; and US20170166926. In some embodiments, the subject has a condition listed in Tables 1-3; in some embodiments, the vectors are used to deliver a therapeutic agent listed in Tables 1-3 for treating the corresponding disease listed in Tables 1-3. The therapeutic agent can be delivered as a nucleic acid, e.g. via a viral vector, wherein the nucleic acid encodes a therapeutic protein or other nucleic acid such as an antisense oligo, siRNA, shRNA, and so on; or as a fusion protein/complex with a peptide as described herein.

The methods and compositions described herein can be used to treat these conditions in a subject in need thereof, by administration of a therapeutically effective amount of an AAV carrying a therapeutic transgene, sufficient to ameliorate, reduce risk of, or delay onset of one or more symptoms of the condition.

**Table 1. CNS Targets (AAV-F, AAV-S)**

| Disease | Target genes | Target cells/tissues | Reference |
|---|---|---|---|
| **Alzheimer's Disease** | *CD33, APOE, BACE,* | Brain | (Griciuc et al., 2013) |
| **Parkinson's Disease** | *GDNF, AADC* | Brain<br>Neurons | (Christine et al., 2019) |
| **X-linked Adrenoleukodystrophy** | *ABCD1* | Brain/spinal cord<br>Neurons/astrocytes/microglia/ endothelial cells | (Eichler et al., 2017; Gong et al., 2015) |
| **Canavan's** | *ASPA* | Brain | (Leone et al., 2012) |
| **Niemann Pick** | *NPC1* | Brain | (Hughes et al., 2018) |
| **Spinal muscular atrophy** | *SMN* | Motor neurons | (Al-Zaidy et al., 2019) |
| **Huntington's Disease** | *HTT* | Brain<br>neurons | (Caron et al., 2020; Keskin et al., 2019) |

**Table 2. Inner Ear targets (AAV-S)**

| Disease | Target genes | Target cells/tissues | Reference |
|---|---|---|---|
| **Connexin-26** | ***GJB2*** | **Inner ear- cochlea Fibrocytes/supporting cells** | ARO 2020 |
| **Usher Type 3A*** | ***CLRN1*** | **Inner ear- cochlea *Hair cells (inner and outer)*** | **(György et al., 2019)** |
| **Usher Type 2D*** | ***WHLN*** | **Inner ear- cochlea *Hair cells (inner and outer)*** | **(Isgrig et al., 2017)** |
| **Hair cell-related hearing loss** | ***ATOH1*** | **Inner ear- cochlea** Supporting cells (for HC regeneration) | **(Tan et al., 2019)** |
| **Hair cell-related hearing loss (DFNB7/11)** | ***TMC1*** | **Inner ear- cochlea *Hair cells (inner and outer)*** | **(Nist-Lund et al., 2019)** |
| **Inner hair cell-related hearing loss (DFNB9)** | ***OTOF*** | **Inner ear- cochlea *Inner hair cells*** | **(Akil et al., 2019)** |
| **Usher Type 1F*** | ***PCDH15*** | **Inner ear – cochlea *Hair cells (inner and outer)*** | Reviewed in **(Zhang et al., 2018)** |
| **Usher Type 1B*** | ***Myo7a*** | **Inner ear – cochlea *Hair cells (inner and outer)*** | Reviewied in **(Lopes and Williams, 2015)** |

*Usher syndrome results in both deafness as above, and in blindness via retinitis pigmentosa

**Table 3. Peripheral targets (AAV-F, AAV-S)**

| Disease | Target genes | Target cells/tissues | Reference |
|---|---|---|---|
| **Retinitis pigmentosa (RP; non-syndromic)** | ***RHO, RPGR, RP2, NRL*** **others** | **Retina (photoreceptors)** | **(Cehajic-Kapetanovic et al., 2020; Millington-Ward et al., 2011; Mookherjee et al., 2015; Yu et al., 2017)** |
| **Leber congenital amaurosis** | ***RPE65*** | **Retina (retinal pigment epithelium)** | **(Maguire et al., 2019)** |
| **Leber Hereditary Optic Neuropathy** | ***ND1-6*** **(mitochondrial)** | **Retina (retinal ganglion cells)** | **(Wan et al., 2016; Yang et al., 2016)** |
| **Usher Syndrome (RP; syndromic with deafness)** | **Usher genes listed above** | **Retina (photoreceptors)** | As above |
| **Duchenne Muscular Dystrophy** | **Dystrophin** | **Muscle** | Reviewed in **(Duan, 2018)** |
| **Allograft vasculopathy** | ***TIMP-1*** | **Heart** | **(Remes et al., 2020)** |
| **Hemophilia A and B** | ***FVIII, FIX*** | **Liver** | Reviewed in **(Nathwani, 2019)** |

**Pharmaceutical Compositions and Methods of Administration**

The methods described herein include the use of pharmaceutical compositions comprising the AAVs as an active ingredient.

Pharmaceutical compositions typically include a pharmaceutically acceptable carrier. As used herein the language "pharmaceutically acceptable carrier" includes saline, solvents, dispersion media, coatings, antibacterial and antifungal agents, isotonic and absorption delaying agents, and the like, compatible with pharmaceutical administration.

Pharmaceutical compositions are typically formulated to be compatible with its intended route of administration. Examples of routes of administration include parenteral, e.g., intravenous, intraarterial, subcutaneous, intraperitoneal, intrathecal, intramuscular, or injection or infusion administration. Delivery can thus be systemic or localized. For example, for delivery into the inner ear, delivery into the cochlea through application over or through the round window membrane, through a surgically drilled cochleostomy adjacent to the round window, a fenestra in the bony oval window, or a semicircular canal can be used (see, e.g., Kim et al., Mol Ther Methods Clin Dev. 2019 Jan 11;13:197-204; Ren et al., Front Cell Neurosci. 2019; 13: 323); for delivery into the retina, subretinal or intravitreal injections can be used (see, e.g., Ochakovski et al., Front Neurosci. 2017; 11: 174; Xue et al., Eye (Lond). 2017 Sep;31(9):1308-1316).

Methods of formulating suitable pharmaceutical compositions are known in the art, see, e.g., *Remington: The Science and Practice of Pharmacy*, 21st ed., 2005; and the books in the series *Drugs and the Pharmaceutical Sciences: a Series of Textbooks and Monographs* (Dekker, NY). For example, solutions or suspensions used for parenteral application can include the following components: a sterile diluent such as water for injection, saline solution, fixed oils, polyethylene glycols, glycerine, propylene glycol or other synthetic solvents; antibacterial agents such as benzyl alcohol or methyl parabens; antioxidants such as ascorbic acid or sodium bisulfite; chelating agents such as ethylenediaminetetraacetic acid; buffers such as acetates, citrates or phosphates and agents for the adjustment of tonicity such as sodium chloride or dextrose. pH can be adjusted with acids or bases, such as hydrochloric acid or sodium hydroxide. The

parenteral preparation can be enclosed in ampoules, disposable syringes or multiple dose vials made of glass or plastic.

Pharmaceutical compositions suitable for injectable use can include sterile aqueous solutions (where water soluble) or dispersions and sterile powders for the extemporaneous preparation of sterile injectable solutions or dispersion. For intravenous administration, suitable carriers include physiological saline, bacteriostatic water, Cremophor EL™ (BASF, Parsippany, NJ) or phosphate buffered saline (PBS). In all cases, the composition must be sterile and should be fluid to the extent that easy syringability exists. It should be stable under the conditions of manufacture and storage and must be preserved against the contaminating action of microorganisms such as bacteria and fungi. The carrier can be a solvent or dispersion medium containing, for example, water, ethanol, polyol (for example, glycerol, propylene glycol, and liquid polyetheylene glycol, and the like), and suitable mixtures thereof. The proper fluidity can be maintained, for example, by the use of a coating such as lecithin, by the maintenance of the required particle size in the case of dispersion and by the use of surfactants. Prevention of the action of microorganisms can be achieved by various antibacterial and antifungal agents, for example, parabens, chlorobutanol, phenol, ascorbic acid, thimerosal, and the like. In many cases, it will be preferable to include isotonic agents, for example, sugars, polyalcohols such as mannitol, sorbitol, sodium chloride in the composition. Prolonged absorption of the injectable compositions can be brought about by including in the composition an agent that delays absorption, for example, aluminum monostearate and gelatin.

Sterile injectable solutions can be prepared by incorporating the active compound in the required amount in an appropriate solvent with one or a combination of ingredients enumerated above, as required, followed by filtered sterilization. Generally, dispersions are prepared by incorporating the active compound into a sterile vehicle, which contains a basic dispersion medium and the required other ingredients from those enumerated above. In the case of sterile powders for the preparation of sterile injectable solutions, the preferred methods of preparation are vacuum drying and freeze-drying, which yield a powder of the active ingredient plus any additional desired ingredient from a previously sterile-filtered solution thereof.

In one embodiment, the therapeutic compounds are prepared with carriers that will protect the therapeutic compounds against rapid elimination from the body, such as a controlled release formulation, including implants and microencapsulated delivery systems. Biodegradable, biocompatible polymers can be used, such as ethylene vinyl acetate, polyanhydrides, polyglycolic acid, collagen, polyorthoesters, and polylactic acid. Such formulations can be prepared using standard techniques, or obtained commercially, e.g., from Alza Corporation and Nova Pharmaceuticals, Inc. Liposomal suspensions (including liposomes targeted to selected cells with monoclonal antibodies to cellular antigens) can also be used as pharmaceutically acceptable carriers. These can be prepared according to methods known to those skilled in the art, for example, as described in U.S. Patent No. 4,522,811.

The pharmaceutical compositions can be included in a kit, container, pack, or dispenser together with instructions for administration. For example, the kit can include compositions comprising an AAV comprising a peptide as described herein.

## EXAMPLES

The invention is further described in the following examples, which do not limit the scope of the invention described in the claims.

### Materials and Methods

The following materials and methods were used in the Examples below, unless otherwise noted.

*AAV library construction.*

*iTransduce plasmid: pAAV-CBA-Cre-$^{mut}$-p41-Cap9del*

We constructed the iTransduce library backbone plasmid called pAAV-CBA-Cre$^{mut}$-p41-Cap9del, containing two expression cassettes in-cis: 1) the CBA-Cre$^{mut}$ in which we introduced a mutant Cre cDNA (CCG ->CCT encoding the Pro15 amino acid to eliminate the AgeI site initially present) under the ubiquitous promoter CBA, 2) the p41-Cap9del composed of the AAV9 capsid gene under the AAV5 p41 promoter (residues 1680-1974 of GenBank AF085716.1) and splicing sequences of the AAV2 rep gene (similar as described in[12]).

Both the mutant Cre cDNA ($Cre^{mut}$) flanked by KpnI and SalI restriction sites and the p41-CAP9(del)-polyA fragment were synthesized by GenScript and cloned into a puC57 backbone. We constructed first the pAAV-CBA-$Cre^{mut}$-polyA plasmid by subcloning the mutant Cre cDNA (fragment KpnI-blunt, SalI) in place of eGFP-WPRE in our pAAV-CBA-WPRE backbone (opened with NcoI-blunt/SalI, which eliminated the eGFP-WPRE fragment initially present). We then introduced the p41-Cap9del fragment harbouring a K449R mutation in the Cap9 sequence allowing the creation of a unique XbaI site, and in which the 447 bp Cap sequence between XbaI and AgeI restriction sites had been deleted.

*Plasmid for generating random 7-mer peptide cap fragments and subcloning the CAP9 fragments retrieved by PCR: pUC57-Cap9-XbaI/KpnI/AgeI.*

We first had the 447 bp region of the AAV9 capsid sequence between the XbaI/AgeI sites (sequence that is missing in pAAV-CBA-$Cre^{mut}$-p41-Cap9del) synthesized by Genscript (Piscataway, NJ) and subcloned into a pUC57-Kan plasmid. This capsid sequence contains the same removal of the EarI site in this 447 bp region WT AAV9 cap that allows restriction digest removal of WT AAV9 as described by Deverman et al. 2015. This also creates a unique KpnI site. The cap fragment of *pUC57-Cap9-XbaI/KpnI/AgeI* was used to generate the initial library of random 21-mer nucleotide sequences (encoding for 7-mer peptides) inserted between nucleotides encoding amino acids 588 and 589 of AAV9 VP1. We used a strategy similar to that of Deverman et al. (2015). Briefly, *pUC57-Cap9-XbaI/KpnI/AgeI* served as template to amplify the cap DNA and insert random 21-mer sequences using a forward and reverse primer. Primer information: XF-extend (5'GTACTATCTCTCTAGAACtattaacggttc3'; SEQ ID NO:11) and reverse primer 588iRev 5' (GTATTCCTTGGTTTTGAACCCAACCGGTCTGCGCCTGTGCXMNNMNNMNNMNNNMNNMNNTTGGGCACTCTGGTGGTTTGTG 3'; SEQ ID NO:12) in which the MNN repeat refers to the the randomized 21-mer nucleotides (purchased from IDT). XF-extend and 588iRev were used in a PCR with Phusion polymerase (NEB) and *pUC57-Cap9-XbaI/KpnI/AgeI* as template. The 447 bp PCR product was digested with XbaI and AgeI overnight at 37°C and then gel-purified the product (Qiagen). Similarly, *pAAV-CBA-Cre-$^{mut}$-p41-Cap9del* was digested with XbaI and AgeI and gel purified.

Next, a ligation reaction (1h at room temperature) with T4 DNA ligase (NEB) was performed using a 3:1 cap insert to vector molar ratio. The subsequent ligated plasmid was called *pAAV-CBA-Cre-$^{mut}$-p41-Cap9-7mer* and contained a pool of plasmids with random 7-mer peptides inserted in the cap gene between nucleotides encoding 588 and 589 of AAV9 VP1.

This plasmid (*pUC57-Cap9-XbaI/KpnI/AgeI)* was also used as our recipient plasmid for subcloning the CAP9 fragments amplified by PCR from brain tissue. We removed an upstream KpnI site in the pUC57 plasmid by digestion with SacI and NsiI and ligation. This allowed the KpnI site in the capsid fragment to be unique. See below in

*Rep expression plasmid.*

We constructed a *rep* expression plasmid called pAR9-Cap9-stop/AAP/Rep using a similar strategy to that as Deverman et al.[12]. The entire cDNA was synthesized by Genscript and cloned into a pUC57-Kan plasmid. Stop codons were inserted in place of start codons for VP1, VP2, VP3 so that no parental AAV9 capsids were produced, while maintaining AAP and rep expression.

*AAV library production and purification.*

For each production, we plated 15-cm tissue culture dishes with $1.5x10^7$ 293T cells/dish. The next day cells were transfected using the calcium phosphate method, with the adenovirus helper plasmid (pAdΔF6, 26 μg per plate), rep plasmid (pAR9-Cap9-stop/AAP/Rep, 12 μg per plate) and ITR-flanked AAV library (pAAV-CBA-Cre-mut/p41-Cap9-7mer, 1 μg per plate) to induce production of AAV. The day after transfection, medium was changed to DMEM containing 2% FBS. AAV was purified from the cell lysate using iodixanol density-gradient ultracentrifugation. Buffer exchange to PBS was done using ZEBA spin columns (7K MWCO; Thermo Fisher Scientific) and further concentration was performed using Amicon Ultra 100kDa MWCO ultrafiltration centrifugal devices (Millipore). Vectors were stored at -80 °C until use. We quantified AAV genomic copies (vg) in AAV preparations using TaqMan qPCR with ITR-sequence specific primers and probes[20, 21].

*Next generation sequencing of library.*

Next generation sequencing was performed on the plasmid AAV9 library pool, as well as following packaging of capsids. Sequencing was also performed following PCR

rescue of the cap fragment (either from brain tissue or from isolated tdTomato-positive cells sorted by flow cytometry). For each round of selection viral DNA corresponding to the insert-containing region was amplified by PCR using the Phusion High-Fidelity PCR kit from New England Biolabs (Forward primer: 5'-AATCCTGGACCTGCTATGGC-3' (SEQ ID NO:13), reverse primer: 5'-TGCCAAACCATACCCGGAAG-3' (SEQ ID NO:14)). PCR amplification was performed using Q5 polymerase (New England Biolabs). Unique barcode adapters were annealed to each sample, and samples were sequenced on an Illumina Miseq (150bp reads). Approximately 50-100,000 reads per sample were analysed. Sequence output files were quality-checked initially using FastQC (bioinformatics.babraham.ac.uk/projects/fastqc/), and analyzed on a program custom-written in Python. Briefly, sequences were binned based on the presence or absence of insert; insert-containing sequences were then compared to a baseline reference sequence and error-free reads were tabulated based on incidences of each detected unique insert. Inserts were translated and normalized.

*Animals.*

All animal experiments were approved by the Massachusetts General Hospital Subcommittee on Research Animal Care following guidelines set forth by the National Institutes of Health Guide for the Care and Use of Laboratory Animals. We used adult age (8-10 week old) Ai9 (strain # 007909), C57BL/6 (strain # 000664), and BALB/c (strain # 000651) mice all from The Jackson Laboratory, Bar Harbor, ME.All animals were euthanized three weeks post-injection, perfused transcardially and tissues were harvested and either fixed in 4% paraformaldehyde in PBS, snap frozen in liquid nitrogen or dissociated for flow cytometry.

*In vivo selection of brain-tropic capsids.*

Ai9 mice were injected intravenously (tail vein) with the dose in vg indicated in the results section and 3weeks post injection, mice were euthanized, and tissue harvested.

Mice were deeply anesthetized by isofluorane and decapitated. For round 1, the brain was rapidly dissected and two coronal sections (2 mm thick) were harvested. One section was used for extracting whole brain DNA (DNeasy Blood and Tissue Kits, Qiagen, Hilden, Germany). The other coronal section was fixed in 4% PFA and paraffin embedded for immunohistology (tdtomato-positive cells were detected after each round

of selection by DAB staining using a rabbit anti-RFP antibody from Rockland Immunochemicals). For round 2, brain tissue was then cut with a razor blade into 1 mm3 pieces and neural cells were isolated by papain dissociation (Papain Dissociation System, Worthington), according to the manufacturer's instructions. Following dissociation, myelin was removed (Myelin Removal Beads II, human, mouse, rat from Miltenyi) and the Td-tomato positive cells were sorted by a S3eTM Cell Sorter (Bio-Rad). Cells were sorted by first setting gates to exclude cellular debris and select for singlets only. Cell suspensions from an AAV9-PHP.B-Cre injected Ai9 (positive control) and a PBS injected Ai9 mouse (negative control) were used to set gates to sort tdTomato-positive and negative cells. After sorting, the tdTomato-positive cells were immediately pelleted by centrifugation, and DNA was extracted using the ARCTURUS PicoPure DNA extraction kit (ThermoFisher).

After DNA extraction, the Cap9 inserts (containing the 21-mer sequence encoding the 7mer peptides) were amplified using the following primers: Cap9_Kpn/Age_For: 5'-AGCTACCGACAACAACGTGT-3' (SEQ ID NO:15)and Cap9_ Kpn/Age_Rev: 5'-AGAAGGGTGAAAGTTGCCGT-3' (SEQ ID NO:16) (Phusion High-Fidelity PCR kit, New England Biolabs). The amplicons were then purified (Monarch PCR & DNA Cleanup kit, New England Biolabs), digested by KpnI, AgeI and BanII and the Cap9 KpnI-AgeI fragments (144 bp) were agarose gel purified (Monarch DNA Gel Extraction kit, New England Biolabs) before ligation in the pUC57-Cap9-XbaI/AgeI/KpnI plasmid (opened with KpnI and AgeI and dephosphorylated with Calf Inositol Phosphatase, New England Biolabs). The ligation products were transformed into electrocompetent DH5alpha bacteria (New England Biolabs) and the entire transformation was grown overnight in LB-ampicillin medium. pUC57-Cap9-XbaI/AgeI/KpnI plasmid was purified by maxi prep (Qiagen). Plasmid was digested by XbaI/AgeI to release the 447 bp cap fragment which was gel purified and ligated with similarly cut pAAV-CBA-Cre-mut/p41-Cap9del for the next round of AAV library production.

*AAV rep/cap plasmids containing AAV-F and AAV-S peptide inserts for vector production.*

To create *rep/cap* plasmids encoding AAV9 capsids displaying the peptide insert of interest for production of vectors encoding a transgene of interest (e.g. GFP), we

digested an AAV9 *rep/cap* plasmid with BsiWI and BaeI which removes a fragment flanking the VP3 amino acid 588 site for peptide sequence insertion. Next we ordered a 997 bp dsDNA fragment from Integrated DNA Technologies (IDT, Coralville, IA), which contains overlapping Gibson homology arms with the BsiWI/BaeI cut AAV9 as well as the 21-mer nucleotide sequence encoding the peptide of interest in frame after amino acid 588 of VP3. Last, we performed Gibson assembly using the Gibson Assembly® Master Mix (NEB, Ipswich, MA) to ligate the peptide containing insert into the AAV9 *rep/cap* plasmid.

*AAV vectors for transduction analysis.*

For each production, we plated 15-cm tissue culture dishes with $1.5x10^7$ 293T cells/dish. The next day cells were transfected using the calcium phosphate method, with the adenovirus helper plasmid (pAdΔF6, 26 μg per plate), rep/cap plasmid (AAV9, AAV-F, AAV-S; 12 μg per plate) and ITR-flanked transgene cassette plasmid (single-stranded AAV-CBA-GFP-WPRE[22] , 10 μg/plate) to induce production of AAV. The day after transfection, medium was changed to DMEM containing 2% FBS. AAV was purified from the cell lysate using iodixanol density-gradient ultracentrifugation. Buffer exchange to PBS was done using ZEBA spin columns (7K MWCO; Thermo Fisher Scientific) and further concentration was performed using Amicon Ultra 100kDa MWCO ultrafiltration centrifugal devices (Millipore). Vectors were stored at -80 °C until use. We quantified AAV genomic copies in AAV preparations using TaqMan qPCR with BGH polyA-sequence specific primers and probe[23].

*Animal euthanasia and tissue harvesting*

Mice (strain indicated in each FIGure) were slowly injected via the lateral tail vein with 200 μl of the tested AAV vector diluted in sterile PBS (low dose: $4x10^{12}$vg/kg and high dose: $3.2x10^{13}$vg/kg), before gently finger-clamping the injection site until bleeding stopped. Three weeks post injection mice were euthanized and perfused transcardially with sterile cold phosphate buffered saline (PBS). Next the brain was longitudinally bisected into two hemispheres. One hemisphere was post-fixed in 15% Glycerol/4% paraformaldehyde diluted in PBS for 48 hours, followed by 30% glycerol for cryopreservation for another 48-72 hours. For the high-dose cohort, a small piece of heart, muscle (gastrocnemius) and the retina were also processed for immunohistology.

We made 3 independent preparations of AAV-S, AAV-F, and AAV9 (Table I). The transduction results in mice were from one preparation of each vector, however we have replicated these results in two more independent experiments.

*Immunohistology and high-magnification imaging of AAV-CBA-GFP transduced neural and neuronal cell populations*

Coronal floating sections (40μm) were cut using a cryostat microtome. After rinsing off the glycerol in tris-buffered saline (TBS) buffer, cryosections were permeabilized with 0.5% Triton X-100 (AmericanBio) in TBS for 30 minutes at room temperature and blocked with 5% normal goat serum (or normal donkey serum) and 0.05% Triton in TBS for 1 hour at room temperature. Primary antibodies were incubated overnight at 4°C in 2.5% NGS and 0.05% Triton in TBS, while Alexa Fluor 488 or -Cy3 conjugated secondary antibodies (Jackson ImmunoResearch laboratories, Baltimore, USA) were incubated for 1 hour the next day. Primary antibodies used for this study were: chicken anti-GFP (Aves Labs, Tigard, USA), Mouse anti-NeuN (EMD Millipore, Burlington, USA); rabbit anti-Glutamine Synthetase (Abcam, Cambridge, USA); rabbit anti-Olig2 (EMD Millipore, Burlington, USA); rabbit anti-Iba1 (Wako, Japan); rabbit anti-CamKII (Abcam, Cambridge, USA); mouse anti-GAD67 (EMD Millipore, Burlington, USA); rabbit anti-ChAT (EMD Millipore, Burlington, USA); mouse anti-calbindin (Abcam, Cambridge, USA) and rabbit anti-TH (Novus Biologicals, Littleton, USA). Sections were mounted with Vectashield mounting medium with DAPI (Vector Laboratories, Burlingame, USA).

To identify the neural cell types transduced by each vector and investigate the various neuronal sub-types targeted by AAV-F, a Zeiss Axio Imager Z epifluorescence microscope equipped with AxioVision software and a 60X objective was used to take high-resolution images showing colocalization between GFP and each cell marker.

*Imaging and quantification of global GFP signal coverage*

To quantify the overall native GFP fluorescence signal in brain and liver section, a robotic slide scanner Virtual slide microscope VS120 (Olympus) was used to image the entire batch of slides on one go using an Olympus UPLSAPO 10x objective. In order to reduce variability, the entire batch of slides was imaged in one session. The initial exposure time for GFP was set up so that the fluorescent signal was neither under- no

over-saturated across all experimental group and remained unchanged throughout the entire batch scan. The order of the slides was randomized and remained blinded until final statistical analysis. The Olympus cellSens Standard software was then used to analyze the percent GFP coverage in each brain section. A region of interest (ROI) was initially defined using the "ROI-polygon" tool and we quantified the GFP-positive area within this initial ROI, after applying a similar detection threshold on the GFP channel for all the slides analyzed (the threshold was set at a similar level for the analysis of all mouse brain sections, but a different threshold was applied for the analysis of all mouse liver sections and all rat brain sections). The percentage of GFP-positive area accordingly to the total surface of the ROI was then calculated. The autofluorescence signal was taken into account in our analysis as we set the threshold for eGFP fluorescence intensity above the autofluorescence level (making sure that only the signal from AAV-GFP transduced cells was taken into account). In addition, we drew each ROI for each brain section avoiding the very edges of the section, as those could also present with a high level of autofluorescence. The ventricular space was also excluded from our analysis. Finally, three technical replicates (brain sections) were measured per mouse and all measurements were done blind until the final step of the analysis.

*Stereology-based quantitative analyses of the percentages of transduced astrocytes and neurons*

Stereology-based studies were performed as previously described[24, 25], after co-staining the brain sections for GFP and NeuN (neuronal marker) or GFP and GS (Glutamine synthetase, pan-astrocytic marker). We did not include microglia and oligodendrocytes in this analysis as those cell types were not transduced to an appreciable amount. Stereological evaluation of the percentages of AAV-transduced neurons and astrocytes was done blindly after de-identification of the vector initially injected, using a motorized stage of an Olympus BX51 epifluorescence microscope equipped with a DP70 digital CCD camera, an X-Cite fluorescent lamp, and the associated CAST stereology software version 2.3.1.5 (Olympus, Tokyo, Japan). The cortex was initially outlined under the 4x objective. Random sampling of the selected area was defined using the optical dissector probe of the CAST software. To evaluate the percentage of AAV9, AAV9-PHP.B, AAV-S and AAV-F transduced astrocytes or neurons, the stereology-

based counts were performed under the 20X objective, with a meander sampling of 10% for the surface of cortex for the "high transduction" AAVs, and 20% for "low transduction" AAVs (considering the infrequency of GFP positive cells in those cases ). For each counting frame, the total number of astrocytes (GS positive cells) or neurons (NeuN positive cells) were evaluated, and, among each of those populations, the percentages of GFP positive cells. Only glial and neuronal cells with DAPI-positive nucleus within the counting frame were considered.

*Vector genome quantification in the brain and liver*

One brain hemisphere and a small piece of liver were fresh frozen for AAV genome isolation for vector genome biodistribution. For the fresh frozen brain and liver samples, we isolated genomic and AAV vector DNA from 10 mg of tissue using the DNeasy Blood and Tissue Kit (Qiagen) according to manufacturer's instructions. DNA was quantitated using a NanoDrop ND-1000 Spectrophotometer (Thermo Scientific). Next using 50 ng of genomic DNA as template, we performed a Taqman qPCR using probe and primers to the polyA region of the transgene expression cassette (same assay used to titer the purified AAV vectors). To ensure equal genomic DNA input for each sample, we performed a separate qPCR on each sample using a Taqman probe and primer set that detects GAPDH genomic DNA (Thermo Fisher Scientific, Assay ID Mm01180221_g1; gene symbol Gm12070). For each organ/tissue, we adjusted the AAV vector genome copies for each sample by taking into account any differences in GAPDH Ct values using the following formula: (AAV vector genome copies)/($2^{\Delta Ct}$). The ΔCt value was calculated by the following formula: GAPDH Ct value of sample of interest - average GAPDH Ct value of sample which had the lowest amount of GAPDH (highest Ct value). Data was expressed as AAV vector genomes per 50 ng genomic DNA.

*Human neuron transduction:*

Primary human fetal neural stem cells (NSCs) were obtained from the Birth Defects Research Laboratory (University of Washington, Seattle, WA) in full compliance with the NIH ethical guidelines. The isolation procedure has been detailed previously[26] with slight modifications. Briefly, brain tissue was incubated in 0.25% trypsin, DNase (90Units/mL), diluted in Hank's balanced salt solution (HBSS) for 45 min. Tissue was titrated, transferred into 4°C heat-inactivated fetal bovine serum and centrifuged at

500*g* for 20 min. The pellet was resuspended in NSC complete media consisting of x-Vivo 15 (without phenol red and gentamicin; Lonza) supplemented with 10 μg of basic fibroblast growth factor (Life Technologies), 100 μg of epidermal growth factor (Life Technologies), 5 μg of leukemia inhibitory factor (EMD Millipore), 60 ng/mL of *N*-acetylcysteine (Sigma-Aldrich), 4 mL of neural survival factor-1 supplement (Lonza), 5 mL of 100× N-2 supplement (Life Technologies), 100 U of penicillin, 100 μg/mL of streptomycin (Life Technologies), and 2.5 μg/mL of fungizone (Life Technologies). Supernatants were then filtered through a 40-μm cell strainer (Corning Life Science). Neurospheres larger than 40 μm in diameter were dissociated with Accutase (10 min). Neural Differentiation Medium consisted of 1× Neurobasal Medium, 2% B-27 serum-free supplement, and 2 mM GlutaMAX-I supplement (all from Invitrogen) and supplemented with human recombinant brain-derived neurotrophic factor (BDNF) (10 ng/mL; Peprotech).

Differentiating NSCs were grown in chamber slides in differentiation media for 2 weeks and then treated with the indicated AAV vector encoding GFP ($7x10^{9}$ vg/well added, 150 vg/cell). One week after transduction, cells were fixed with 4% paraformaldehyde and permeabilized with 0.05% Triton X-100 (Sigma-Aldrich) in 1x phosphate-buffered saline (PBS; Invitrogen). Cells were stained with a primary monoclonal antibody (TU-20) to neuron-specific class III β-Tubulin (1:50; Abcam). Secondary antibodies conjugated to Alexa Fluor 594 (diluted 1:200; Invitrogen) were added for 1 h, followed by DAPI for 30 min. The slides were then mounted with a ProLong antifade reagent (Invitrogen). Max projection Images were generated form captured Z-stacks using the Nikon A1R confocal microscope.

Z-stacks were loaded in Imaris, the surface module was used to render the images into 3D volumes. GFP+ neurons were counted (under channel 1-green) and Class III β-Tubulin positive neurons (under channel 2-red). Using Imaris' colocalization module, the population of neurons double positive for the above was determined.

*Statistics*

Statistical analysis of data was performed using GraphPad Prism software (version 8.00). A one-way ANOVA test followed by a Tukey's multiple comparisons test was performed, across the different groups AAV9, AAV9-PHP.B, AAV-S and AAV-F.

A value of $p<0.05$ was considered to be statistically significant. Results are shown as the mean ± S.E.M. Similar analyses were performed the biodistribution assay of AAV genomes in brain and liver, as well as transduction of human neurons.

*Direct stereotactic injection of vectors*

Adult C57BL/6 mice were anesthetized by intraperitoneal injection of ketamine/xylazine (100mg/kg and 50mg/kg body weight, respectively) and positioned on a stereotactic frame (Kopf Instruments, Tujunga, USA). Injections of vectors were performed in the cortex (somatosensory cortex) and the hippocampus. A total of 3µl of viral suspension was injected ($1.65x10^{10}$ and $5.6x10^{10}$gc per injection site for AAV-F and AAV-S, respectively) at a rate of 0.15µl/minute) and using a 33-gauge sharp needle attached to a 10-µl Hamilton syringe (Sigma-Aldrich, St. Louis, USA). Stereotactic coordinates of injection sites were calculated from bregma (Cortex coordinates: anteroposterior -1mm, mediolateral ± 1mm and dorsoventral -0.8mm; Hippocampus coordinates: anteroposterior -2mm, mediolateral ± 1.7mm and dorsoventral -2.5mm).

*Intrathecal bolus delivery (IT bolus)*

Adult C57BL/6 mice were put under anesthesia by isoflurane. After the skin over the lumbar region was shaved and cleaned, a 3~4 cm mid-sagittal incision was made through the skin exposing the muscle and spine. A catheter was inserted between L4-L5 spine region and attached to a gas-tight Hamilton syringe with a 33-gauge steel needle. Ten microliters of AAV9-CBA-GFP ($1.25X10^{11}$ vg) vectors or AAV-F-CBA-GFP ($8.8x10^{10}$ vg) were slowly injected at a rate of 2 µl /min. Mice were killed three weeks post injection.

For low magnification imaging of whole spinal cord and brain sections, we stained overnight with anti-GFP (Invitrogen, cat no. G10362, dilution 1:250) followed by secondary antibody staining and imaging as for FIGure 3.

For immunostaining of cell types in brain and spinal cord, fixed tissue sections were washed with PBS, blocked with goat serum and permeabilized with 0.3% Triton in PBS. Target antibodies were diluted in blocking buffer and incubated at 4°C overnight.

Primary antibodies: anti-GFP: catalog no. ab1218 (abcam): Dilution, 1:1000
GFAP: catalog no catz0334, (Dako); Dilution, 1:500
NeuN: catalog no ab177487, (abcam); Dilution, 1:300

After overnight incubation slides were washed extensively with PBS with 0.1%Tween. Fluorochrome-conjugated secondary antibodies (1:500 dilution) were added and incubated for 1h at RT. After washing slides were washed with PBS and mounted using DAPI mounting solution (ThermoFisher, cat no. P36931). Slides were imaged using a Zeiss LSM 800 confocal laser scanning microscope.

*Transmission electron microscopy*

Carbon-coated grids (Electron Microscopy Sciences, EMS) was rendered hydrophilic by exposure to a 25 mA glow discharge for 20 s. For each AAV vector pre, 5µl was adsorbed onto a grid for 1 minute, and stained with 1% uranyl acetate (EMS #22400) for 20s. Grids were examined in a TecnaiG$^2$ Spirit BioTWIN and imaged with an AMT 2k CCD camera. Work was carried out at the Harvard Medical School Electron Microscopy Facility. Counts were performed as follows: 5 representative images of each vector prep were taken; all full and empty capsids were counted using the Count tool in Photoshop (CS6). Empty capsid percentage was calculated for each image, and plotted.

**Example 1. Design of iTransduce- an expression-based AAV library**

First, we constructed an AAV library plasmid which consisted of an AAV2 ITR-flanked expression cassette comprised of a chicken beta actin (CBA)-driven Cre recombinase and a p41promoter-driven AAV9 capsid (schematic in **FIG. 1a**). Pseudorandom 21-base nucleotides were inserted between AAV9 VP1 nucleotides encoding amino acids 588/589 via PCR. Before viral packaging, we sequenced this plasmid library using low-depth next-generation sequencing (NGS) and confirmed the presence of 21-mer inserts in the vast majority of plasmids and the lack of variant bias (data not shown). We then packaged the capsid library and performed NGS to validate that the vector creation process maintained a sufficient diversity for selection. iTransduce relies on each unique capsid carrying both its own *cap* gene as well as a Cre-expressing construct (**FIG.1b**). Transgenic mice (Ai9) carrying a floxed-STOP tdTomato cassette are injected intravenously with the AAV library (**FIG. 1b-i**). Those capsids that successfully transduce cells enable tdTomato expression in any target organ or cell type (without being dependent upon the availability of specific Cre transgenic mouse lines); these tdTomato-positive cells can then be flow sorted from the tissue of interest

(optionally, alongside cell-specific markers, **FIG. 1b-ii**). Viral DNA rescued from these cells should correspond to capsid variants that can effectively overcome all of the extracellular and intracellular biological barriers to transgene expression (**FIG. 1b-iii**).

**Example 2. Selection of new AAV9 capsid variants using transgene expression to identify functional capsids**

To test the iTransduce library strategy, we performed a proof-of-concept selection to attempt to isolate AAV capsid variants with the ability to transduce brain cells after systemic injection. $1.27x10^{11}$ vector genomes (vg, $5x10^{12}$vg/kg) of the library were injected intravenously through the tail vein of one adult male and one female Ai9 mouse and three weeks post-injection the mice were killed; a section of liver, brain, spleen, and kidney were cut and immunostaining of tdTomato was performed. We readily detected tdTomato positive cells (likely hepatocytes) in the liver, with scattered tdTomato positive cells (both neurons and astrocytes) in the brain as well as the other organs (**FIG. 7a**). We also tested whether we could rescue the *cap* DNA containing the 21-base insert by PCR, and we detected specific bands in 10 organs/tissues in mice injected with the library, but not in control, non-injected mice (**FIG. 7b**).We pooled the remaining brain tissue from the female and male mice, and DNA was extracted, initially from total brain tissue for the first round of selection. We amplified *cap* DNA containing the 21-mer insert and analyzed their identity and read counts using NGS. We observed substantial enrichment of specific peptides in the library population harvested from brain tissue following a single round of selection when compared to the unselected library and with the variants retrieved from liver (**FIG. 7c** and data not shown). Next, we isolated the insert-containing region of viral DNA and re-cloned it back into the AAV plasmid backbone and repackaged capsids ("brain-enriched capsid library") for a second round of selection.

For the second round of selection, two Ai9 mice (one male, one female) were injected with the library rescued from round 1 (dose of $1.91x10^{10}$ vg, $7.64x10^{11}$vg/kg) and sacrificed after three weeks. Prior to injection, sequence containing the variant region was amplified and sequenced by NGS to ensure a pre-existing bias had not been introduced into the vector pool (**FIG. 2**). The brain tissue was dissociated to obtain a cell suspension for sorting tdTomato-positive cells by flow cytometry. We flow sorted 3,834

tdTomato-positive cells (0.043% of the initial cell suspension), which were indicative of successful transduction (**FIG. 8a-b**). Viral DNA from tdTomato sorted cells was amplified and sequenced as previously done (**FIG. 2**). Viral DNA isolated from tdTomato-positive cells showed 97% of reads represented by just three peptides, STTLYSP, FVVGQSY, and FQPCP* (where * indicates a stop codon) (**FIG. 2b**). We selected two of these, STTLYSP (termed AAV-S) and FVVGQSY (termed AAV-F), for functional evaluation *in vivo* (we excluded evaluation of FQPCP* as it was likely a product of cross-packaging). As seen in **FIG. 2**, both of these sequences were detectable in the round 2 library at low levels (~0.4% of reads for each variant), but were highly enriched in the brain after selection.

**Example 3. AAV-F capsid mediates efficient transgene expression in the murine CNS.**

To test whether these peptides expressed on the capsid of AAV could mediate efficient transgene expression by an AAV vector, we produced these capsids (AAV-S and AAV-F), packaging a single-stranded CBA promoter-driven GFP expression cassette (**FIG. 3a**). For comparison, we included the parental AAV9 vector and AAV9-PHP.B, the most widely studied AAV9 variant with an 7-mer peptide insertion (TLAVPFK) generated by directed evolution[12]. All vectors produced well and gave slightly lower production efficiencies than AAV9 (**Table 4).**

**Table 4**. Production efficiency of AAV capsids*

| AAV capsid | Titer (vg/ml) | Production Efficiency (vg/cell) |
|---|---|---|
| *AAV9* | $3.20\times10^{13}$ ($\pm2.55\times10^{13}$) | $3.06\times10^{4}$ ($\pm1.39\times10^{4}$) |
| *AAV-F* | $5.51\times10^{12}$ ($\pm4.23\times10^{12}$) | $9.57\times10^{3}$ ($\pm8.00\times10^{3}$) |
| *AAV-S* | $1.88\times10^{13}$ ($1.38\times10^{13}$) | $2.09\times10^{4}$ ($\pm5.65\times10^{3}$) |

*All capsids packaged a single-stranded AAV2 ITR-flanked AAV-CBA-GFP-WPRE transgene cassette

Adult male C57BL/6J mice were injected via the lateral tail vein with a low dose or a high dose ($1x10^{11}$ vg and $8x10^{11}$ vg of vector, respectively; approximately $4x10^{12}$ and $3.2x10^{13}$ vg/kg) of one of the following vectors: AAV9, AAV9-PHP.B, AAV-S and AAV-F (n=3 each). Three weeks post injection, mice were killed and organs harvested for endogenous (unstained) GFP fluorescence analysis. We quantitated the percent coverage of GFP signal in serial sagittal brain sections (3 sections were analyzed per animal). Remarkably, AAV-F demonstrated a 119-fold ($p<0.0001$) and 68-fold ($p=0.0004$) increased GFP fluorescence coverage compared to the parental AAV9 vector at $1x10^{11}$ vg and $8x10^{11}$ vg, respectively (**FIG. 3b, c, e, f; FIG. 9A-B**). AAV9 and AAV-S displayed similar GFP coverage levels (**FIG. 3b, c, e, f**). AAV9-PHP.B gave slightly higher GFP coverage at the low dose compared to AAV-F, while similar levels of GFP coverage was observed at the $8x10^{11}$ vg dose (**FIG. 3b, c, e, f).** Similar to AAV9-PHP.B, AAV-F transduced the spinal cord with remarkable efficiency (**FIG. 3d**). Most areas of the brain were effectively targeted by AAV-F and robust GFP signal was observed in the cortex, hippocampus, striatum, cerebellum and olfactory bulb (**FIG. 3f**).

In order to get a detailed appreciation of the cell types being targeted by AAV-S and AAV-F, we next performed a series of co-immunostaining with GFP and markers of neurons (NeuN), astrocytes (Glutamine Synthetase, GS), microglia (Iba-1) and oligodendrocytes (Olig2). AAV-F and AAV-S, similar to the other two reference vectors, mainly transduced neurons and astrocytes (none of the variants appeared to effectively transduce microglial or oligodendroglial cells, **FIG. 4a, b**). Stereological quantitation of neurons and astrocytes in the cortex at the $1x10^{11}$ vg dose confirmed the efficient transduction potential of AAV-F as compared with conventional AAV9 by a factor of 65 in astrocytes and 171 in neurons, while the difference between AAVS and AAV9 was not significant (the percent of GFP positive astrocytes was 0.63%±0.24% for AAV9 and 0.36±0.15% for AAV-S, respectively; and the percent of GFP positive neurons was 0.039%±0.0.02% for AAV9 and 0.029±0.002% for AAV-S; all ± numbers represent standard error of the mean, SEM). Of note, AAV-F targeted significantly more astrocytes (40.78±0.73%) than AAV9-PHP.B (28.21±0.25%) and the reverse was true for neurons (6.67±0.5% for AAV-F and 10.59±0.16%for AAV9-PHP.B, **FIG. 4c**), suggestive of a slightly different tropism between those two vectors in mice. In addition,

AAV-F transduced a variety of neuronal sub-types, including excitatory (CamKII positive) and inhibitory (GAD67 positive) cortical neurons, dopaminergic neurons in the striatum (expressing Tyrosine Hydroxylase, TH), Purkinje neurons in the cerebellum (calbindin positive) and motor neurons in the spinal cord (expressing the Choline acetyltransferase marker, ChAT, **FIG. 10a.)** Consistent with the stereological counts in the cortex (**FIG. 4c**) and with the images of the high dose of AAV-F vs AAV9 (**FIG. 3f**), we observed efficient transduction of neurons and astrocytes with AAV-F and not AAV9 at the dose of $1x10^{11}$ vg/mouse in the striatum, hippocampus, and cerrebellum (**FIG. 10b**).

To better understand whether the high levels of GFP transgene expression in the brain with AAV-F corresponded to higher levels of AAV genomes in the brain, we isolated vector and murine genomic DNA from liver and brain and performed a qPCR on the $8x10^{11}$ vg dosed mice. AAV-F displayed a 20-fold enhancement ($p<0.0001$) in AAV genomes in the brain compared to AAV9 (**FIG 4d**). As reported, AAV9-PHP.B had a much higher (25-fold) amount of AAV genomes in the brain compared to AAV9, while AAV-S had a low level, similar to the GFP fluorescence data (**FIG. 3**). PHP.B showed expression levels in the liver that were slightly lower than AAV9 and AAV-F (although not AAV-S; **FIG. 4d**). AAV-F showed levels in the liver similar to AAV9, and AAV-S showed a lower, but non-significant trend downwards. We also examined the biodistribution of AAV-F compared to AAV9 in several other organs – skeletal muscle, heart, and spinal cord (**FIG. 11**). We observed no significant difference between the two vectors in muscle and heart (although an upward trend was seen with respect to AAV-F in the heart). As would be expected from expression in the brain, AAV-F showed significantly higher expression levels in the spinal cord compared to AAV9 ($p < 0.05$, t-test).

To investigate transgene expression in peripheral organs after systemic injection, we analyzed GFP fluorescence in the liver, heart, skeletal muscle, and retina (**FIG. 4e).** Not surprisingly, all vectors transduced liver efficiently. In the heart and skeletal muscle, AAV-S yielded higher numbers of bright GFP signal/section than AAV9 and AAV-F. All capsids mediated low transduction of the retina, as expected with intravenous delivery. Interestingly, while AAV-9 and AAV-S did not transduce the neuronal retina, consistent

expression was observed in the retinal pigment epithelium (RPE). Both AAV9-PHP.B and AAV-F transduced multiple layers in the retina, most notably cells in the ganglion cell layer (GCL). GFP expression was also observed in the inner nuclear layer (INL), with substantial expression shown in the outer plexiform layer (OPL), which may reflect bipolar or inhibitory horizontal cell transduction.

Since transduction by AAV vectors in mice can vary substantially between sex and mouse strain, we examined whether the most efficient capsid, AAV-F could efficiently transduce brain after systemic injection of female C57BL/6 as well as male BALB/c. Mice were injected with $1x10^{11}$ vg ($4x10^{12}$ vg/kg), and we observed robust and efficient transduction independent of strain or sex (**FIG. 5a-c**). These results contrasted with the lack of efficacy of AAV9-PHP.B at transducing the central nervous system after systemic delivery in the BALB/c strain, as previously reported (**FIG. 5b, c**.) [13, 14]

While iodixanol density gradient purification removes the majority of empty capsids, to examine if an excess of empty capsids in AAV-F could explain its increased biodistribution to the brain compared to AAV9, we performed transmission electron microscopy (TEM) on two separate preparations of AAV-F, and compared them to two independent preparations of AAV9. As seen in **FIGs. 12A-E**, we observed no significant difference in empty capsid levels between AAV-F and AAV9 (mean 4.63±1.99% vs. 5.2±2.18% empty capsids for AAV9 and AAV-F respectively, mean ± SD, $p = 0.54$, unpaired t-test).

Next, we tested whether AAV-F would have utility as a vector for CNS transduction via other routes of administration. We first tested AAV-S and AAV-F to mediate transgene expression in the brain after direct hippocampal injection of adult C57BL/6 mice. We found that both capsids achieve a widespread expression of GFP after direct injection, primarily in neurons (**FIG. 13**). Intrathecal injection of AAV vectors to transduce the spinal cord, has shown promise to treat this compartment. One drawback is limited spread of the vector to the brain after lumbar injection of vector. We compared AAV9 and AAV-F after bolus intrathecal injection of vector into the lumbar region of the spinal cord in adult C57BL/6 mice. Three weeks post injection, mice were killed and spinal cords and brains analyzed. Remarkably, AAV-F resulted in much more intense GFP expression throughout the spinal cord compared to AAV9, transducing both white

and gray matter. Meanwhile AAV9 transduction was mainly restricted to the white matter. Strikingly, we also detected transduction of astrocytes and neurons in the brain of mice injected with AAV-F, but not AAV9 (**FIG. 14**).

**Example 4. AAV-F mediates enhanced transduction of human neurons**

Since the selection was performed in mice, we analyzed if the robust transduction characteristics of AAV-F also translated to human cells. Primary human stem cell-derived neurons were transduced with equal doses of AAV9, AAV-S and AAV-F, all encoding GFP. One week later they were fixed, stained with Class III β Tubulin and analyzed for the percentage of GFP positive neurons. Remarkably, AAV-F transduced 62% of neurons, 3-fold higher than AAV9 ($p<0.05$) (**FIG. 6a, b**). AAV-S yielded a slight, yet statistically significant ($p<0.05$) increase in transduction efficiency over AAV9 (**FIG. 6a**).

**Example 5. AAV-S transduces the inner ear with high efficiency**

Recent years have seen the development of new AAV vectors, designed to target specific organs and cell types with high efficacy. Many of these utilize 7-mer peptide insertions that modify the transduction properties of a particular AAV serotype. However, these vectors can often be repurposed to transduce other tissues, including those that are difficult to treat, such as the inner ear. Transducing certain cell types in the inner ear - such as hair cells - remains a challenge, with many conventional AAV vectors failing to consistently target one class of hair cells, outer hair cells (OHCs).

As noted above, one (AAV-F) showed great promise and high CNS expression after systemic injection, whereas the other (AAV-S) did not. While systemically injected AAV-S did not cross the blood-brain barrier effectively, it transduced a variety of tissues including heart, liver, and muscle. After direct injection into the brain, AAV-S displayed high local transduction efficiency in neurons, even at relatively low doses. To assay its transduction properties in the inner ear, we produced AAV-S encoding a single-stranded expression cassette driving EGFP under the CBA promoter, and injected it in neonatal (P1) mice via the round window. We found that AAV-S transduces hair cells of the cochlea extremely well. Both inner and outer hair cells were transduced with efficiencies of up to 100% and 99% (**FIGs. 15a, b**) at the dose tested ($2x10^{10}$ VG). We also observed

significant transduction of the spiral limbus and spiral ganglion (**FIGs. 15c, d**). Overall, we show here that AAV-S can be used for genetic therapies of the inner ear.

**Example 6. Using the iTransduce system for selections in non-transgenic adult primates to isolate capsids that transduce fibrocytes efficiently**

2-3 rounds of selection for fibrocyte-targeting AAV capsids are performed in non-human primates, e.g., cynomolgus monkeys. To identify fibrocyte-selective, transduction-competent AAV capsid selection is performed by co-injecting the iTransduce AAV library along with AAV9-PHP.B which encodes a *GJB2*-floxed-STOP-tdTomato cassette (size fits inside AAV capsid). In NHP inner ear, AAV9-PHP.B-CBA-GFP transduces many cells of the cochlea including fibrocytes, HCs, and spiral ganglion neuron region. In this selection strategy (see **FIG. 16A**), tdTomato expression is restricted to fibrocytes under the GJB2 promoter, essentially creating an inner ear transgenic NHP. AAV capsids that enter fibrocytes and turn on tdTomato are flow sorted from dissociated cochlea and capsid DNA rescued for NGS and cloning to identify peptide sequences that allow AAV mediated expression in fibrocytes. Individual peptide enrichment is followed by deep-sequencing as described above to inform when to stop additional rounds of selection (likely when a particular peptide represents >25% of reads).

Alternatively or in addition, 2-3 rounds of selection for spinal cord cell targeting AAV capsids are performed in non-human primates, e.g., cynomolgus monkeys. To identify spinal cord-selective, transduction-competent AAV capsids, selection is performed by co-injecting the iTransduce AAV library along with AAV9 which encodes a *CBA*-floxed-STOP-mPlum cassette (size fits inside AAV capsid). In NHP spinal cord, AAV9- transduces cells including neurons and astrocytes. In this selection strategy (see **FIG. 16B**), AAV capsids that enter spinal cord cells and turn on mPlum fluorescence are flow sorted from dissociated spinal cord and capsid DNA rescued for NGS and cloning to identify peptide sequences that allow AAV mediated expression in cells of the spinal cord. Individual peptide enrichment is followed by deep-sequencing as described above to inform when to stop additional rounds of selection (likely when a particular peptide represents >25% of reads).

Once candidate capsids clones are identified, the capsids are vectorized as before, encoding a GFP cassette. Next, the capsids are tested for transduction of target cells after direct round window membrane (RMW) injection (e.g., as shown in 16A), or intrathecal injection (e.g., as shown in 16B).

**References**

1. Mendell, J.R., S. Al-Zaidy, R. Shell, W.D. Arnold, L.R. Rodino-Klapac, T.W. Prior, L. Lowes, L. Alfano, K. Berry, K. Church, J.T. Kissel, S. Nagendran, J. L'Italien, D.M. Sproule, C. Wells, J.A. Cardenas, M.D. Heitzer, A. Kaspar, S. Corcoran, L. Braun, S. Likhite, C. Miranda, K. Meyer, K.D. Foust, A.H.M. Burghes, and B.K. Kaspar, Single-Dose Gene-Replacement Therapy for Spinal Muscular Atrophy. N Engl J Med, 2017. 377(18): p. 1713-1722.

2. Manno, C.S., G.F. Pierce, V.R. Arruda, B. Glader, M. Ragni, J.J. Rasko, M.C. Ozelo, K. Hoots, P. Blatt, B. Konkle, M. Dake, R. Kaye, M. Razavi, A. Zajko, J. Zehnder, P.K. Rustagi, H. Nakai, A. Chew, D. Leonard, J.F. Wright, R.R. Lessard, J.M. Sommer, M. Tigges, D. Sabatino, A. Luk, H. Jiang, F. Mingozzi, L. Couto, H.C. Ertl, K.A. High, and M.A. Kay, Successful transduction of liver in hemophilia by AAV-Factor IX and limitations imposed by the host immune response. Nat Med, 2006. 12(3): p. 342-7.

3. Hinderer, C., N. Katz, E.L. Buza, C. Dyer, T. Goode, P. Bell, L.K. Richman, and J.M. Wilson, Severe Toxicity in Nonhuman Primates and Piglets Following High-Dose Intravenous Administration of an Adeno-Associated Virus Vector Expressing Human SMN. Hum Gene Ther, 2018. 29(3): p. 285-298.

4. Paulk, N.K., K. Pekrun, G.W. Charville, K. Maguire-Nguyen, M.N. Wosczyna, J. Xu, Y. Zhang, L. Lisowski, B. Yoo, J.G. Vilches-Moure, G.K. Lee, J.B. Shrager, T.A. Rando, and M.A. Kay, Bioengineered Viral Platform for Intramuscular Passive Vaccine Delivery to Human Skeletal Muscle. Mol Ther Methods Clin Dev, 2018. 10: p. 144-155.

5. Paulk, N.K., K. Pekrun, E. Zhu, S. Nygaard, B. Li, J. Xu, K. Chu, C. Leborgne, A.P. Dane, A. Haft, Y. Zhang, F. Zhang, C. Morton, M.B. Valentine, A.M.

Davidoff, A.C. Nathwani, F. Mingozzi, M. Grompe, I.E. Alexander, L. Lisowski, and M.A. Kay, Bioengineered AAV Capsids with Combined High Human Liver Transduction In Vivo and Unique Humoral Seroreactivity. Mol Ther, 2018. 26(1): p. 289-303.

6. Gray, S.J., B.L. Blake, H.E. Criswell, S.C. Nicolson, R.J. Samulski, T.J. McCown, and W. Li, Directed evolution of a novel adeno-associated virus (AAV) vector that crosses the seizure-compromised blood-brain barrier (BBB). Mol Ther, 2010. 18(3): p. 570-8.

7. Tse, L.V., K.A. Klinc, V.J. Madigan, R.M. Castellanos Rivera, L.F. Wells, L.P. Havlik, J.K. Smith, M. Agbandje-McKenna, and A. Asokan, Structure-guided evolution of antigenically distinct adeno-associated virus variants for immune evasion. Proc Natl Acad Sci U S A, 2017. 114(24): p. E4812-E4821.

8. Koerber, J.T., N. Maheshri, B.K. Kaspar, and D.V. Schaffer, Construction of diverse adeno-associated viral libraries for directed evolution of enhanced gene delivery vehicles. Nat Protoc, 2006. 1(2): p. 701-6.

9. Korbelin, J., T. Sieber, S. Michelfelder, L. Lunding, E. Spies, A. Hunger, M. Alawi, K. Rapti, D. Indenbirken, O.J. Muller, R. Pasqualini, W. Arap, J.A. Kleinschmidt, and M. Trepel, Pulmonary Targeting of Adeno-associated Viral Vectors by Next-generation Sequencing-guided Screening of Random Capsid Displayed Peptide Libraries. Mol Ther, 2016. 24(6): p. 1050-1061.

10. Sallach, J., G. Di Pasquale, F. Larcher, N. Niehoff, M. Rubsam, A. Huber, J. Chiorini, D. Almarza, S.A. Eming, H. Ulus, S. Nishimura, U.T. Hacker, M. Hallek, C.M. Niessen, and H. Buning, Tropism-modified AAV vectors overcome barriers to successful cutaneous therapy. Mol Ther, 2014. 22(5): p. 929-39.

11. Berry, G.E. and A. Asokan, Cellular transduction mechanisms of adeno-associated viral vectors. Curr Opin Virol, 2016. 21: p. 54-60.

12. Deverman, B.E., P.L. Pravdo, B.P. Simpson, S.R. Kumar, K.Y. Chan, A. Banerjee, W.L. Wu, B. Yang, N. Huber, S.P. Pasca, and V. Gradinaru, Cre-dependent selection yields AAV variants for widespread gene transfer to the adult brain. Nat Biotechnol, 2016. 34(2): p. 204-9.

13. Matsuzaki, Y., M. Tanaka, S. Hakoda, T. Masuda, R. Miyata, A. Konno, and H. Hirai, Neurotropic Properties of AAV-PHP.B Are Shared among Diverse Inbred Strains of Mice. Mol Ther, 2019. 27(4): p. 700-704.

14. Hordeaux, J., Q. Wang, N. Katz, E.L. Buza, P. Bell, and J.M. Wilson, The Neurotropic Properties of AAV-PHP.B Are Limited to C57BL/6J Mice. Mol Ther, 2018. 26(3): p. 664-668.

15. Nonnenmacher, M., H. van Bakel, R.J. Hajjar, and T. Weber, High capsid-genome correlation facilitates creation of AAV libraries for directed evolution. Mol Ther, 2015. 23(4): p. 675-82.

16. Hordeaux, J., Y. Yuan, P.M. Clark, Q. Wang, R.A. Martino, J.J. Sims, P. Bell, A. Raymond, W.L. Stanford, and J.M. Wilson, The GPI-Linked Protein LY6A Drives AAV-PHP.B Transport across the Blood-Brain Barrier. Mol Ther, 2019. 27(5): p. 912-921.

17. Igarashi, H., K. Koizumi, R. Kaneko, K. Ikeda, R. Egawa, Y. Yanagawa, S. Muramatsu, H. Onimaru, T. Ishizuka, and H. Yawo, A Novel Reporter Rat Strain That Conditionally Expresses the Bright Red Fluorescent Protein tdTomato. PLoS One, 2016. 11(5): p. e0155687.

18. Park, J.E., X.F. Zhang, S.H. Choi, J. Okahara, E. Sasaki, and A.C. Silva, Generation of transgenic marmosets expressing genetically encoded calcium indicators. Sci Rep, 2016. 6: p. 34931.

19. Sasaki, E., H. Suemizu, A. Shimada, K. Hanazawa, R. Oiwa, M. Kamioka, I. Tomioka, Y. Sotomaru, R. Hirakawa, T. Eto, S. Shiozawa, T. Maeda, M. Ito, R. Ito, C. Kito, C. Yagihashi, K. Kawai, H. Miyoshi, Y. Tanioka, N. Tamaoki, S. Habu, H. Okano, and T. Nomura, Generation of transgenic non-human primates with germline transmission. Nature, 2009. 459(7246): p. 523-7.

20. D'Costa, S., V. Blouin, F. Broucque, M. Penaud-Budloo, A. Francois, I.C. Perez, C. Le Bec, P. Moullier, R.O. Snyder, and E. Ayuso, Practical utilization of recombinant AAV vector reference standards: focus on vector genomes titration by free ITR qPCR. Mol Ther Methods Clin Dev, 2016. 5: p. 16019.

21. Aurnhammer, C., M. Haase, N. Muether, M. Hausl, C. Rauschhuber, I. Huber, H. Nitschko, U. Busch, A. Sing, A. Ehrhardt, and A. Baiker, Universal real-time

PCR for the detection and quantification of adeno-associated virus serotype 2-derived inverted terminal repeat sequences. Hum Gene Ther Methods, 2012. 23(1): p. 18-28.

22. Gyorgy, B., E.J. Meijer, M.V. Ivanchenko, K. Tenneson, F. Emond, K.S. Hanlon, A.A. Indzhykulian, A. Volak, K.D. Karavitaki, P.I. Tamvakologos, M. Vezina, V.K. Berezovskii, R.T. Born, M. O'Brien, J.F. Lafond, Y. Arsenijevic, M.A. Kenna, C.A. Maguire, and D.P. Corey, Gene Transfer with AAV9-PHP.B Rescues Hearing in a Mouse Model of Usher Syndrome 3A and Transduces Hair Cells in a Non-human Primate. Mol Ther Methods Clin Dev, 2019. 13: p. 1-13.

23. Maguire, C.A., L. Balaj, S. Sivaraman, M.H. Crommentuijn, M. Ericsson, L. Mincheva-Nilsson, V. Baranov, D. Gianni, B.A. Tannous, M. Sena-Esteves, X.O. Breakefield, and J. Skog, Microvesicle-associated AAV vector as a novel gene delivery system. Mol Ther, 2012. 20(5): p. 960-71.

24. Hudry, E., C. Martin, S. Gandhi, B. Gyorgy, D.I. Scheffer, D. Mu, S.F. Merkel, F. Mingozzi, Z. Fitzpatrick, H. Dimant, M. Masek, T. Ragan, S. Tan, A.R. Brisson, S.H. Ramirez, B.T. Hyman, and C.A. Maguire, Exosome-associated AAV vector as a robust and convenient neuroscience tool. Gene Ther, 2016. 23(4): p. 380-92.

25. Dashkoff, J., E.P. Lerner, N. Truong, J.A. Klickstein, Z. Fan, D. Mu, C.A. Maguire, B.T. Hyman, and E. Hudry, Tailored transgene expression to specific cell types in the central nervous system after peripheral injection with AAV9. Mol Ther Methods Clin Dev, 2016. 3: p. 16081.

26. Watters, A.K., S. Rom, J.D. Hill, M.K. Dematatis, Y. Zhou, S.F. Merkel, A.M. Andrews, J. Cena, R. Potula, A. Skuba, Y.J. Son, Y. Persidsky, and S.H. Ramirez, Identification and dynamic regulation of tight junction protein expression in human neural stem cells. Stem Cells Dev, 2015. 24(12): p. 1377-89.

27. Akil, O., Dyka, F., Calvet, C., Emptoz, A., Lahlou, G., Nouaille, S., De Monvel, J. B., Hardelin, J. P., Hauswirth, W. W., Avan, P., Petit, C., Safieddine, S., and Lustig, L. R. (2019). Dual AAV-mediated gene therapy restores hearing in a DFNB9 mouse model. *Proc. Natl. Acad. Sci. U. S. A.* doi:10.1073/pnas.1817537116.

28. Al-Zaidy, S. A., Kolb, S. J., Lowes, L., Alfano, L. N., Shell, R., Church, K. R., Nagendran, S., Sproule, D. M., Feltner, D. E., Wells, C., Ogrinc, F., Menier, M., L'Italien, J., Arnold, W. D., Kissel, J. T., Kaspar, B. K., and Mendell, J. R. (2019).

AVXS-101 (Onasemnogene Abeparvovec) for SMA1: Comparative Study with a Prospective Natural History Cohort. *J. Neuromuscul. Dis.* doi:10.3233/JND-190403.

29. Caron, N. S., Southwell, A. L., Brouwers, C. C., Cengio, L. D., Xie, Y., Black, H. F., Anderson, L. M., Ko, S., Zhu, X., van Deventer, S. J., Evers, M. M., Konstantinova, P., and Hayden, M. R. (2020). Potent and sustained huntingtin lowering via AAV5 encoding miRNA preserves striatal volume and cognitive function in a humanized mouse model of Huntington disease. *Nucleic Acids Res.* doi:10.1093/nar/gkz976.

30. Cehajic-Kapetanovic, J., Xue, K., Martinez-Fernandez de la Camara, C., Nanda, A., Davies, A., Wood, L. J., Salvetti, A. P., Fischer, M. D., Aylward, J. W., Barnard, A. R., Jolly, J. K., Luo, E., Lujan, B. J., Ong, T., Girach, A., Black, G. C. M., Gregori, N. Z., Davis, J. L., Rosa, P. R., Lotery, A. J., Lam, B. L., Stanga, P. E., and MacLaren, R. E. (2020). Initial results from a first-in-human gene therapy trial on X-linked retinitis pigmentosa caused by mutations in RPGR. *Nat. Med.* doi:10.1038/s41591-020-0763-1.

31. Christine, C. W., Bankiewicz, K. S., Van Laar, A. D., Richardson, R. M., Ravina, B., Kells, A. P., Boot, B., Martin, A. J., Nutt, J., Thompson, M. E., and Larson, P. S. (2019). Magnetic resonance imaging–guided phase 1 trial of putaminal AADC gene therapy for Parkinson's disease. *Ann. Neurol.* doi:10.1002/ana.25450.

32. Duan, D. (2018). Systemic AAV Micro-dystrophin Gene Therapy for Duchenne Muscular Dystrophy. *Mol. Ther.* doi:10.1016/j.ymthe.2018.07.011.

33. Eichler, F., Duncan, C., Musolino, P. L., Orchard, P. J., De Oliveira, S., Thrasher, A. J., Armant, M., Dansereau, C., Lund, T. C., Miller, W. P., Raymond, G. V., Sankar, R., Shah, A. J., Sevin, C., Gaspar, H. B., Gissen, P., Amartino, H., Bratkovic, D., Smith, N. J. C., Paker, A. M., Shamir, E., O'Meara, T., Davidson, D., Aubourg, P., and Williams, D. A. (2017). Hematopoietic stem-cell gene therapy for cerebral adrenoleukodystrophy. *N. Engl. J. Med.* doi:10.1056/NEJMoa1700554.

34. Gong, Y., Mu, D., Prabhakar, S., Moser, A., Musolino, P., Ren, J. Q., Breakefield, X. O., Maguire, C. A., and Eichler, F. S. (2015). Adenoassociated virus serotype 9-mediated gene therapy for X-linked adrenoleukodystrophy. *Mol. Ther.* doi:10.1038/mt.2015.6.

35. Griciuc, A., Serrano-Pozo, A., Parrado, A. R., Lesinski, A. N., Asselin, C. N., Mullin, K., Hooli, B., Choi, S. H., Hyman, B. T., and Tanzi, R. E. (2013). Alzheimer's disease risk gene cd33 inhibits microglial uptake of amyloid beta. *Neuron.* doi:10.1016/j.neuron.2013.04.014.

36. György, B., Meijer, E. J., Ivanchenko, M. V., Tenneson, K., Emond, F., Hanlon, K. S., Indzhykulian, A. A., Volak, A., Karavitaki, K. D., Tamvakologos, P. I., Vezina, M., Berezovskii, V. K., Born, R. T., O'Brien, M., Lafond, J. F., Arsenijevic, Y., Kenna, M. A., Maguire, C. A., and Corey, D. P. (2019). Gene Transfer with AAV9-PHP.B Rescues Hearing in a Mouse Model of Usher Syndrome 3A and Transduces Hair Cells in a Non-human Primate. *Mol. Ther. - Methods Clin. Dev.* doi:10.1016/j.omtm.2018.11.003.

37. Hughes, M. P., Smith, D. A., Morris, L., Fletcher, C., Colaco, A., Huebecker, M., Tordo, J., Palomar, N., Massaro, G., Henckaerts, E., Waddington, S. N., Platt, F. M., and Rahim, A. A. (2018). AAV9 intracerebroventricular gene therapy improves lifespan, locomotor function and pathology in a mouse model of Niemann-Pick type C1 disease. *Hum. Mol. Genet.* doi:10.1093/hmg/ddy212.

38. Isgrig, K., Shteamer, J. W., Belyantseva, I. A., Drummond, M. C., Fitzgerald, T. S., Vijayakumar, S., Jones, S. M., Griffith, A. J., Friedman, T. B., Cunningham, L. L., and Chien, W. W. (2017). Gene Therapy Restores Balance and Auditory Functions in a Mouse Model of Usher Syndrome. *Mol. Ther.* doi:10.1016/j.ymthe.2017.01.007.

39. Keskin, S., Brouwers, C. C., Sogorb-Gonzalez, M., Martier, R., Depla, J. A., Vallès, A., van Deventer, S. J., Konstantinova, P., and Evers, M. M. (2019). AAV5-miHTT Lowers Huntingtin mRNA and Protein without Off-Target Effects in Patient-Derived Neuronal Cultures and Astrocytes. *Mol. Ther. - Methods Clin. Dev.* doi:10.1016/j.omtm.2019.09.010.

40. Leone, P., Shera, D., McPhee, S. W. J., Francis, J. S., Kolodny, E. H., Bilaniuk, L. T., Wang, D. J., Assadi, M., Goldfarb, O., Goldman, H. W., Freese, A., Young, D., During, M. J., Samulski, R. J., and Janson, C. G. (2012). Long-term follow-up after gene therapy for canavan disease. *Sci. Transl. Med.* doi:10.1126/scitranslmed.3003454.

41. Lopes, V. S., and Williams, D. S. (2015). Gene therapy for the retinal degeneration of usher syndrome caused by mutations in MYO7A. *Cold Spring Harb. Perspect. Med.* doi:10.1101/cshperspect.a017319.

42. Maguire, A. M., Russell, S., Wellman, J. A., Chung, D. C., Yu, Z. F., Tillman, A., Wittes, J., Pappas, J., Elci, O., Marshall, K. A., McCague, S., Reichert, H., Davis, M., Simonelli, F., Leroy, B. P., Wright, J. F., High, K. A., and Bennett, J. (2019). Efficacy, Safety, and Durability of Voretigene Neparvovec-rzyl in RPE65 Mutation–Associated Inherited Retinal Dystrophy: Results of Phase 1 and 3 Trials. *Ophthalmology.* doi:10.1016/j.ophtha.2019.06.017.

43. Millington-Ward, S., Chadderton, N., O'Reilly, M., Palfi, A., Goldmann, T., Kilty, C., Humphries, M., Wolfrum, U., Bennett, J., Humphries, P., Kenna, P. F., and Farrar, G. J. (2011). Suppression and Replacement Gene Therapy for Autosomal Dominant Disease in a Murine Model of Dominant Retinitis Pigmentosa. *Mol. Ther.* 19, 642–649. doi:10.1038/mt.2010.293.

44. Mookherjee, S., Hiriyanna, S., Kaneshiro, K., Li, Y., Li, W., Qian, H., Li, T., Colosi, P., Swaroop, A., Wu, Z., Li, L., and Khanna, H. (2015). Long-term rescue of cone photoreceptor degeneration in retinitis pigmentosa 2 (RP2)-knockout mice by gene replacement therapy. *Hum. Mol. Genet.* doi:10.1093/hmg/ddv354.

45. Nathwani, A. C. (2019). Gene therapy for hemophilia. *Hematol. (United States).* doi:10.1182/hematology.2019000007.

46. Nist-Lund, C. A., Pan, B., Patterson, A., Asai, Y., Chen, T., Zhou, W., Zhu, H., Romero, S., Resnik, J., Polley, D. B., Géléoc, G. S., and Holt, J. R. (2019). Improved TMC1 gene therapy restores hearing and balance in mice with genetic inner ear disorders. *Nat. Commun.* doi:10.1038/s41467-018-08264-w.

47. Remes, A., Franz, M., Zaradzki, M., Borowski, C., Frey, N., Karck, M., Kallenbach, K., Müller, O. J., Wagner, A. H., and Arif, R. (2020). AAV-mediated TIMP-1 overexpression in aortic tissue reduces the severity of allograft vasculopathy in mice. *J. Hear. Lung Transplant.* doi:10.1016/j.healun.2020.01.1338.

48. Tan, F., Chu, C., Qi, J., Li, W., You, D., Li, K., Chen, X., Zhao, W., Cheng, C., Liu, X., Qiao, Y., Su, B., He, S., Zhong, C., Li, H., Chai, R., and Zhong, G.

(2019). AAV-ie enables safe and efficient gene transfer to inner ear cells. *Nat. Commun.* doi:10.1038/s41467-019-11687-8.

49. Wan, X., Pei, H., Zhao, M., Yang, S., Hu, W., He, H., Ma, S., Zhang, G., Dong, X., Chen, C., Wang, D., and Li, B. (2016). Efficacy and Safety of rAAV2-ND4 Treatment for Leber's Hereditary Optic Neuropathy. *Sci. Rep.* 6, 1–10. doi:10.1038/srep21587.

50. Yang, S., Ma, S.-Q., Wan, X., He, H., Pei, H., Zhao, M.-J., Chen, C., Wang, D.-W., Dong, X.-Y., Yuan, J.-J., and Li, B. (2016). Long-term outcomes of gene therapy for the treatment of Leber's hereditary optic neuropathy. *EBioMedicine* 10, 258–268. doi:10.1016/j.ebiom.2016.07.002.

51. Yu, W., Mookherjee, S., Chaitankar, V., Hiriyanna, S., Kim, J. W., Brooks, M., Ataeijannati, Y., Sun, X., Dong, L., Li, T., Swaroop, A., and Wu, Z. (2017). Nrl knockdown by AAV-delivered CRISPR/Cas9 prevents retinal degeneration in mice. *Nat. Commun.* doi:10.1038/ncomms14716.

52. Zhang, W., Kim, S. M., Wang, W., Cai, C., Feng, Y., Kong, W., and Lin, X. (2018). Cochlear Gene Therapy for Sensorineural Hearing Loss: Current Status and Major Remaining Hurdles for Translational Success. *Front. Mol. Neurosci.* doi:10.3389/fnmol.2018.00221.

## OTHER EMBODIMENTS

It is to be understood that while the invention has been described in conjunction with the detailed description thereof, the foregoing description is intended to illustrate and not limit the scope of the invention, which is defined by the scope of the appended claims. Other aspects, advantages, and modifications are within the scope of the following claims.

**WHAT IS CLAIMED IS:**

1. An AAV capsid protein comprising an amino acid sequence that comprises at least four contiguous amino acids from the sequence STTLYSP (SEQ ID NO:1) or FVVGQSY (SEQ ID NO:2).

2. The AAV capsid protein of claim 1, comprising an amino acid sequence that comprises at least five contiguous amino acids from the sequence STTLYSP (SEQ ID NO:1) or FVVGQSY (SEQ ID NO:2).

3. The AAV capsid protein of claim 1, comprising an amino acid sequence that comprises at least six contiguous amino acids from the sequence STTLYSP (SEQ ID NO:1) or FVVGQSY (SEQ ID NO:2).

4. The AAV capsid protein of claims 1-3, wherein the AAV is AAV9.

5. The AAV capsid protein of claims 1-4, comprising AAV9 VP1.

6. The AAV capsid protein of claim 5, wherein the sequence is inserted in a position corresponding to amino acids 588 and 589 of SEQ ID NO:6.

7. A nucleic acid encoding the AAV capsid protein of claims 1-6.

8. An AAV comprising the capsid protein of claims 1-6, and preferably not comprising a wild type VP1, VP2, or VP3 capsid protein.

9. The AAV of claim 8, further comprising a transgene, preferably a therapeutic transgene.

10. A method of delivering a transgene to a cell, the method comprising contacting the cell with the AAV of claims 1-9.

11. The method of claim 10, wherein the cell is a neuron (optionally a dorsal root ganglion neuron or spiral ganglion neuron), astrocyte, cardiomyocyte, or myocyte, astrocyte, glial cell, inner hair cell, outer hair cell, supporting cell, fibrocyte of the

inner ear, photoreceptors, interneurons, retinal ganglion, or retinal pigment epithelium.

12. The method of claim 11, wherein the cell is in a living subject.

13. The method of claims 11, wherein the subject is a mammalian subject.

14. The method of claims 10 to 13, wherein the cell is in a tissue selected from the brain, spinal cord, dorsal root ganglion, heart, inner ear, eye, or muscle, and a combination thereof.

15. The method of claim 14, wherein the subject has Alzheimer's Disease; Parkinson's Disease; X-linked Adrenoleukodystrophy; Canavan's ; Niemann Pick; Spinal muscular atrophy; Huntington's Disease; Connexin-26; Usher Type 3A; Usher Type 2D; Hair cell-related hearing loss; Hair cell-related hearing loss (DFNB7/11); Inner hair cell-related hearing loss (DFNB9); Usher Type 1F; Usher Type 1B; Retinitis pigmentosa (RP; non-syndromic); Leber congenital amaurosis; Leber Hereditary Optic Neuropathy; Usher Syndrome (RP; syndromic with deafness); Duchenne Muscular Dystrophy; Allograft vasculopathy; Hemophilia A and B;.

16. The method of any of claims 10 to 13, wherein the cell is in the brain of the subject, and the AAV is administered by parenteral delivery; intracerebral; or intrathecal delivery.

17. The method of claim 16, wherein the intrathecal delivery is via lumbar injection, cisternal magna injection, or intraparenchymal injection.

18. The method of claims 10 to 16, wherein the AAV is delivered by parenteral delivery, preferably via intravenous, intraarterial, subcutaneous, intraperitoneal, or intramuscular delivery.

19. The method of any of claims 10 to 13, wherein the cell is in the eye of the subject, and the AAV is administered by subretinal or intravireal injection.

20. The method of any of claims 10 to 13, wherein the cell is in the inner ear of the subject, and the AAV is administered to the cochlea through application over or through the round window membrane, through a surgically drilled cochleostomy adjacent to the round window, a fenestra in the bony oval window, or a semicircular canal.

21. A library construct AAV comprising:
(i) a sequence encoding a Cre recombinase driven by a promoter;
(ii) a sequence encoding an AAV9 capsid protein with a heptamer peptide inserted between the sequences encoding amino acids (aa) 588-589 of the capsid, driven by a promoter, downstream of the Cre cassette.

22. The library construct AAV of claim 21, wherein the heptamer comprises a random heptamer peptide or a pre-selected heptamer peptide.

23. A library comprising a plurality of the library constructs of claim 21 or 22.

24. The library of claim 23, wherein the library comprises library constructs having sequences encoding all possible variants of the heptamer.

25. A method of identifying an engineered capsid that mediates transgene expression in a pre-selected cell type, the method comprising:
(a) administering the library of claims 23 or 24 to a non-human model animal, preferably a mammal, wherein the cells of the model animal express a loxP-flanked STOP cassette upstream of a reporter sequence;
(b) isolating cells of the pre-selected cell type;
(c) selecting cells in which the reporter sequence is expressed;
(d) isolating at least part of the library construct, preferably a part comprising the heptamer, from the selected cells in which the reporter sequence is expressed from step (c); and
(e) determining identity of the heptamers in the library constructs isolated in step (d), wherein the heptamers that are isolated can mediate transgene expression in the pre-selected cell type.

26. The method of claim 25, wherein the reporter sequence encodes a fluorescent reporter protein.

27. The method of claim 25, wherein the model animal is transgenic for the loxP-flanked STOP cassette upstream of a reporter sequence, or wherein the loxP-flanked STOP cassette upstream of a reporter sequence can be expressed from a second construct.

28. The method of claim 25, wherein determining identity of the heptamers in the library constructs comprises using DNA sequencing analysis.

29. The method of claim 25, further comprising before and/or after step (e):
using PCR to amplify sequences comprising the heptamer sequences, optionally comprising full capsid sequences, from the library constructs isolated in step (d);
cloning the amplified sequences back to a second set of library vectors;
repackaging the second set of library vectors; and
performing steps (a)-(d) or (a)-(e) on the second set of library vectors.

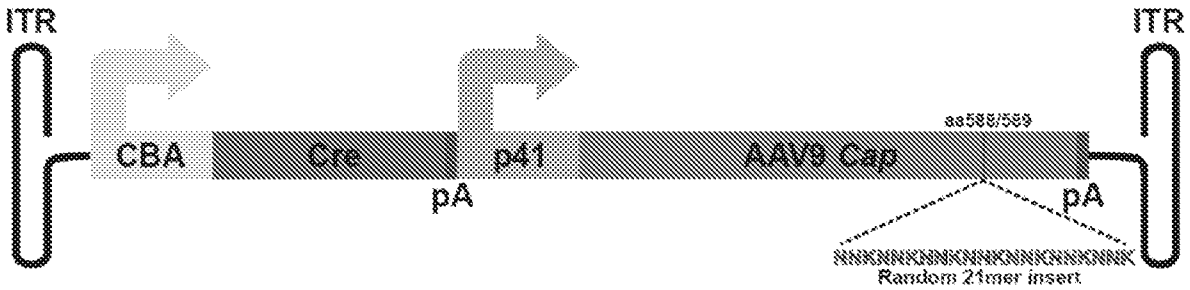


FIG. 1A

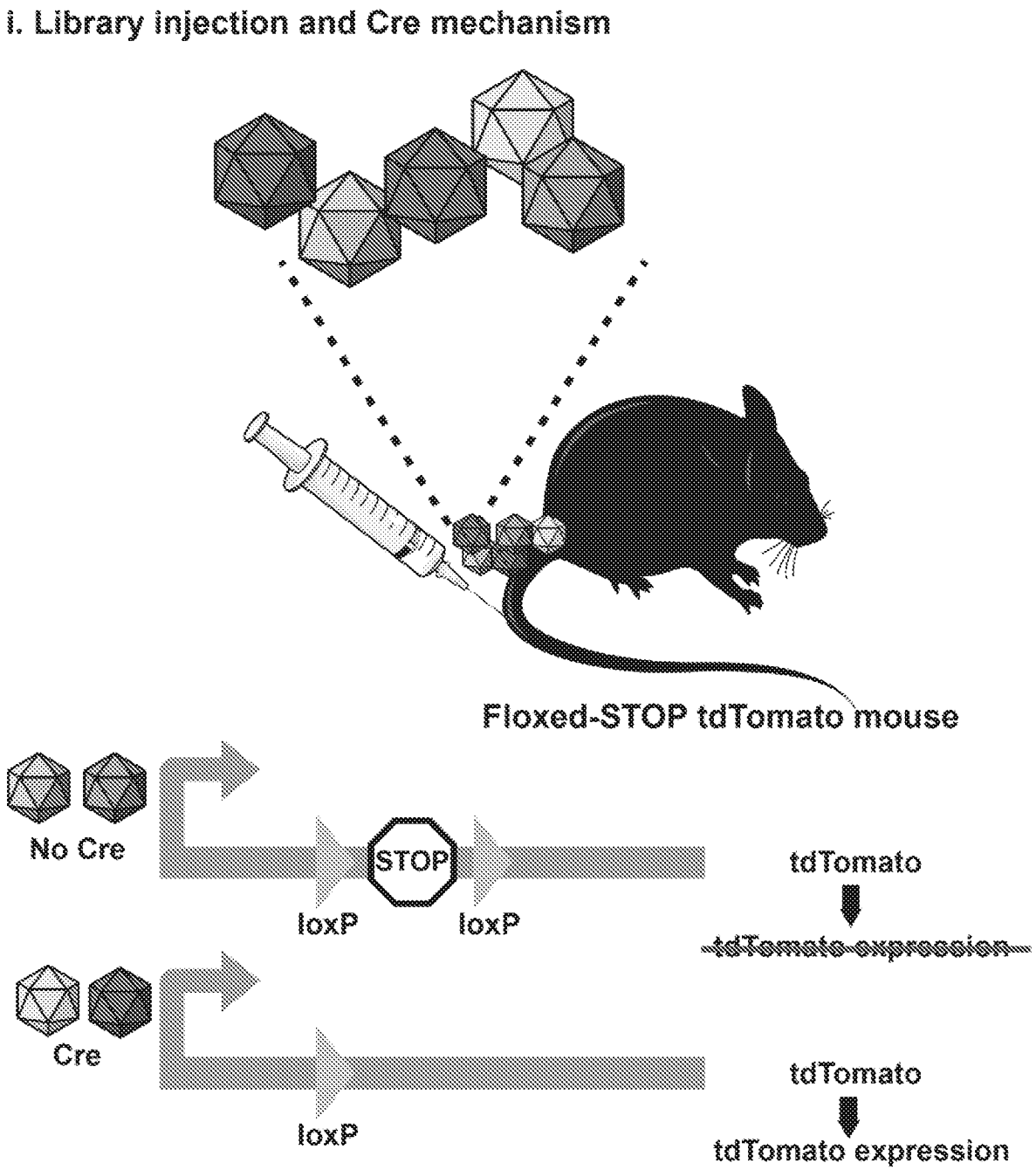


*FIG. 1B*

ii. Cell isolation and tdTomato-positive cell sorting

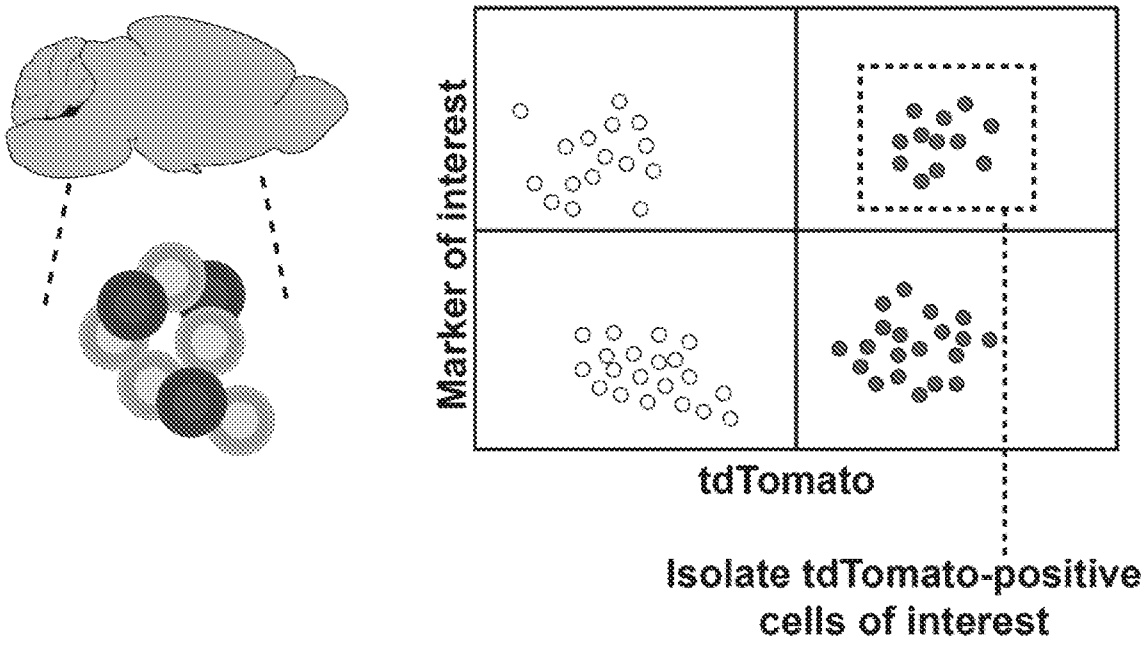


iii. Transduction-comptetent vectors

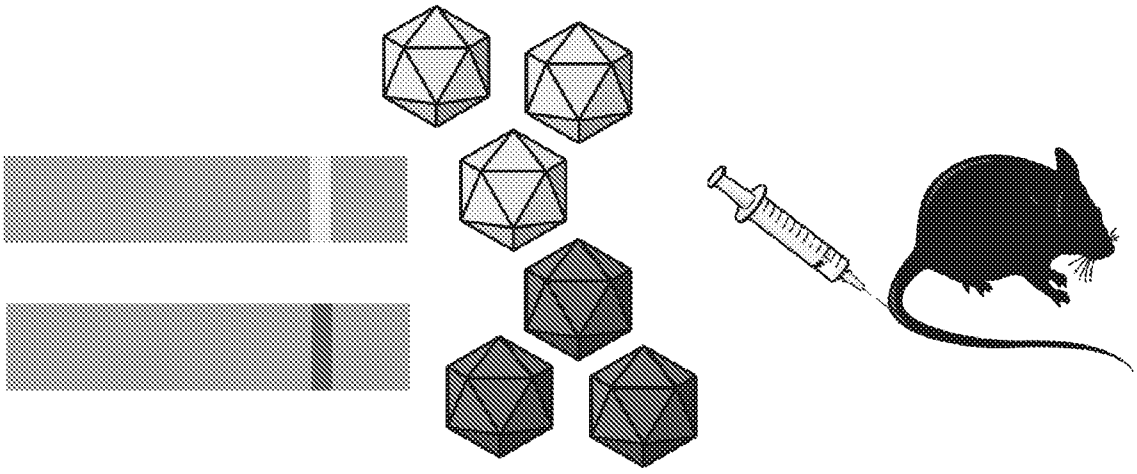

*FIG. 1B, continued*

| Nucleotide Sequence | SEQ ID NO: | Peptide Sequence | SEQ ID NO: | % of pool |
|---|---|---|---|---|
| CAGCCTCGTCTTACTGAGCTT | 17. | QPRLTEL | 18. | 0.05572947 |
| AGTCATTTTAGTAATTCTATG | 19. | SHFSNSM | 20. | 0.02365472 |
| CCGCCTTCTACGGGGAATCCT | 21. | PPSTGNP | 22. | 0.02328549 |
| AATAGTCTTGGGGTGATGGAT | 23. | NSLGVMD | 24. | 0.02276376 |
| CCTCCTATGGCTACGCCTCAG | 25. | PPMATPQ | 26. | 0.02126276 |
| CCGCATACTCGGGCTGAGCCT | 27. | PHTRAEP | 28. | 0.01834104 |
| GTGAATCAGACTAATTATTCT | 29. | VNQTNYS | 30. | 0.01784338 |
| CATGCGCCGAGGCTGGTTCAG | 31. | HAPRLVQ | 32. | 0.01539524 |
| TGGAGTAAGGAGTCGAATCAT | 33. | WSKESNH | 34. | 0.01529892 |
| ACTACTGCTGGTCCGACTGAG | 35. | TTAGPTE | 36. | 0.01419123 |
| TCGTGGCCGCAGTCGCCTTCG | 37. | SWPQSPS | 38. | 0.0139424 |
| ACTTGTGCTGTTCCGGATCGG | 39. | TCAVPDR | 40. | 0.01326816 |
| CCTCGTGCGGAGCCTCGGACG | 41. | PRAEPRT | 42. | 0.01314776 |
| CCTACTGCGGGTGTGTATCTG | 43. | PTAGVYL | 44. | 0.01308354 |
| CAGTTGAGTAATACGACGTTG | 45. | QLSNTTL | 46. | 0.01285077 |
| CGGATGGATATGGCTGTGAGG | 47. | RMDMAVR | 48. | 0.01261799 |
| CGGCCGCCGCCTGCGACTCCT | 49. | RPPPATP | 50. | 0.01257786 |
| CAGTATCTGTTTCATATTTTT | 51. | QYLFHIF | 52. | 0.01226482 |
| GGTGCTGGGACTCTTACTTCT | 53. | GAGTLTS | 54. | 0.01223271 |
| CCTCTTTCGCGTGTTGCTTTG | 55. | PLSRVAL | 56. | 0.0119277 |
| ACTACTGCTAAGACGACTGGG | 57. | TTAKTTG | 58. | 0.01187954 |
| TCGCTGCCGGCTACTCATGTG | 59. | SLPATHV | 60. | 0.01170295 |
| AGTGAGAAGGTGATTCGGAGT | 61. | SEKVIRS | 62. | 0.01136583 |
| AAGTCGACTATGCGGAAGCCG | 63. | KSTMRKP | 64. | 0.01134977 |
| GTGTCGAAGCAGAATACGACT | 65. | VSKQNTT | 66. | 0.01106081 |
| GCTGATATGACGGGGCCTACT | 67. | ADMTGPT | 68. | 0.01080396 |
| CCTACTCGTGCGACTCCTATT | 69. | PTRATPI | 70. | 0.01057921 |
| TCTTGGCCTGGGCTGTTGCTG | 71. | SWPGLLL | 72. | 0.01055513 |
| TGGAGGCTGGAGCAGTTGAAG | 73. | WRLEQLK | 74. | 0.01037051 |
| CTTCCGAGTTCTCCGGTTTTT | 75. | LPSSPVF | 76. | 0.31919829 |
| CCTCAGCGGCATCAGAATGAT | 77. | PQRHQND | 78. | 0.00414981 |
| TCGATTCCGTTTCGGTATCCG | 79. | SIPFRYP | 80. | 0.03205067 |
| CCTGATGGTCCGCAGGCTCTG | 81. | PDGPQAL | 82. | 0.00370834 |
| TCGACTACGTGGAAGTCTGAT | 83. | STTWKSD | 84. | 0.05475021 |
| TTGCAGAAGATGGCTGTTCCG | 85. | LQKMAVP | 86. | 0.00273711 |
| N/A | | Others | | 0.13220799 |

*FIG. 2A*

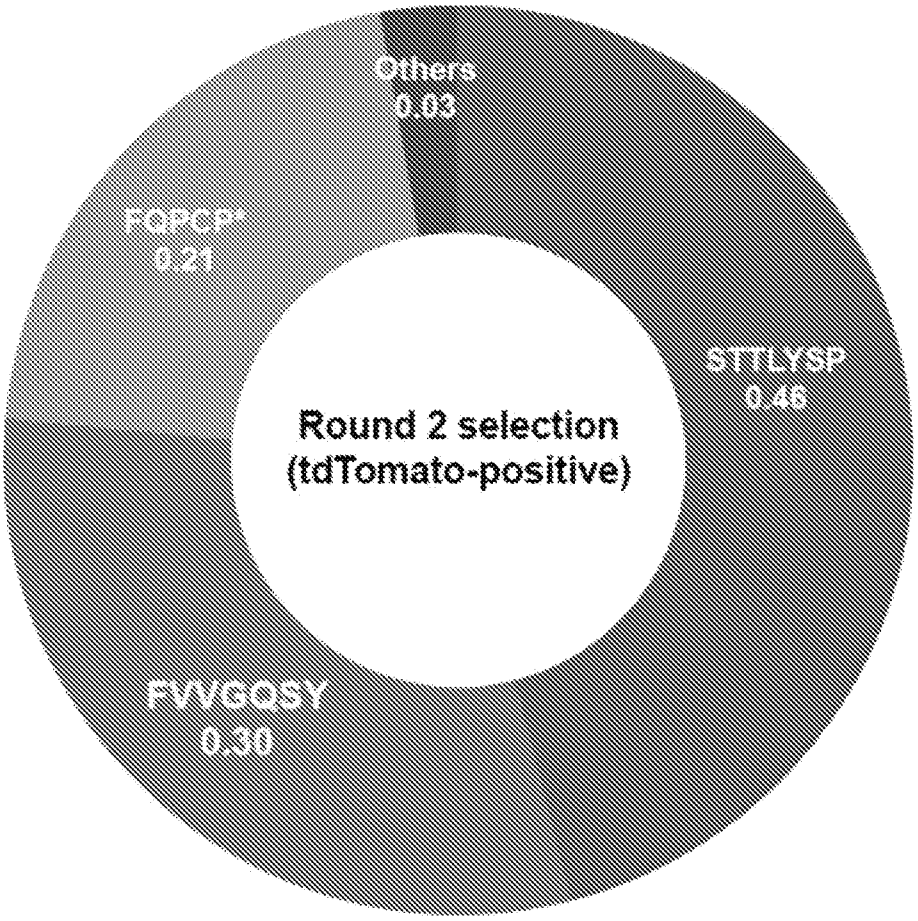


*FIG. 2B*


*FIG. 3A*

2026201434 26 Feb 2026

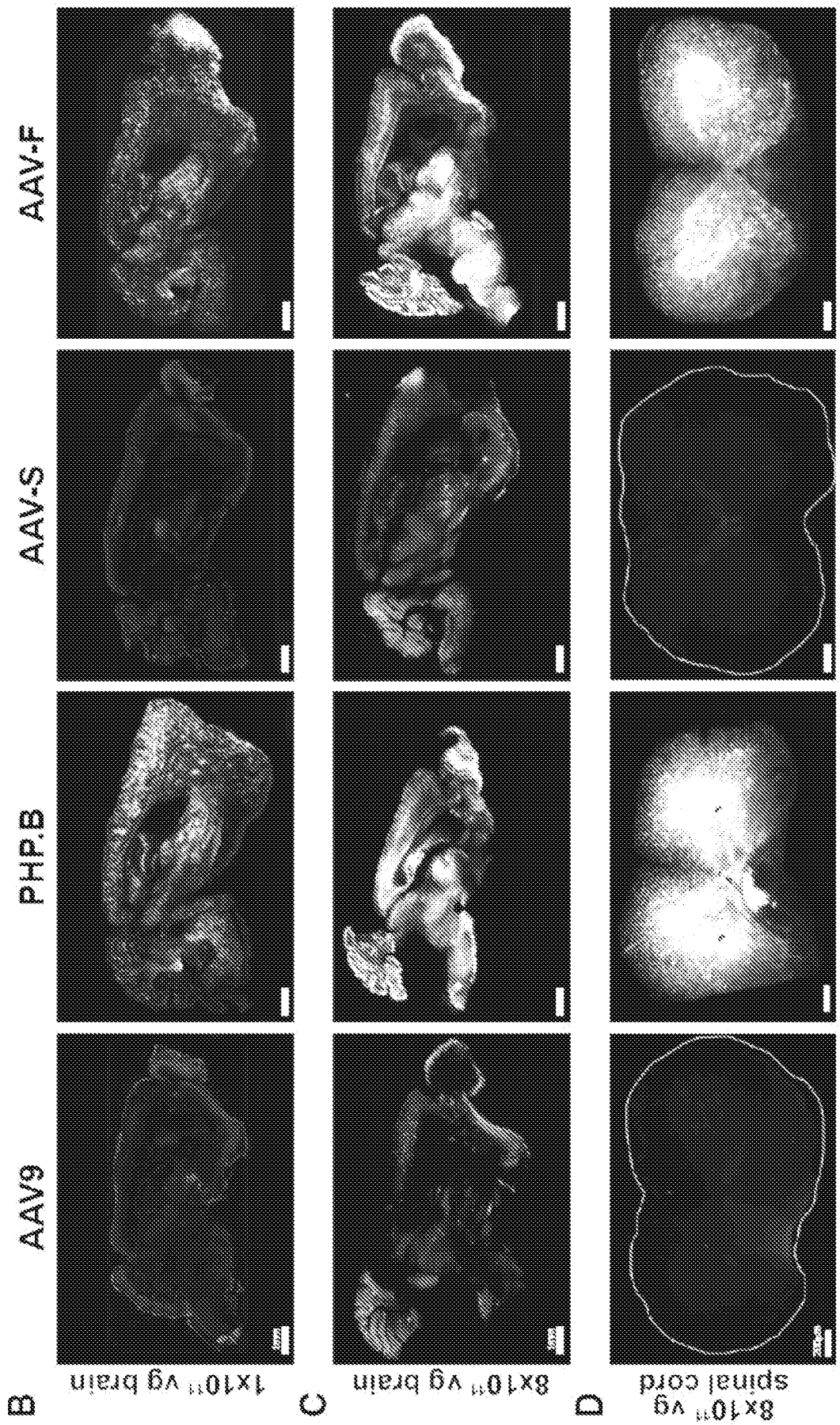


*FIGs. 3B-D*

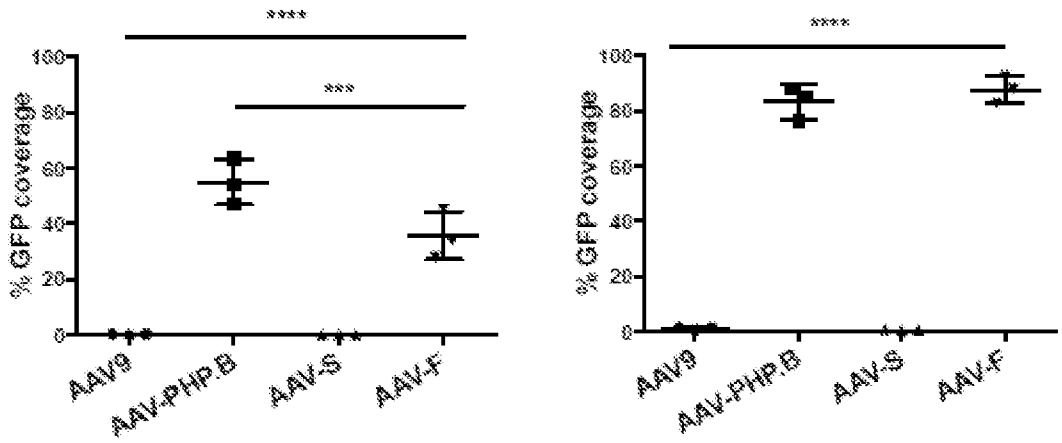


*FIG. 3E*

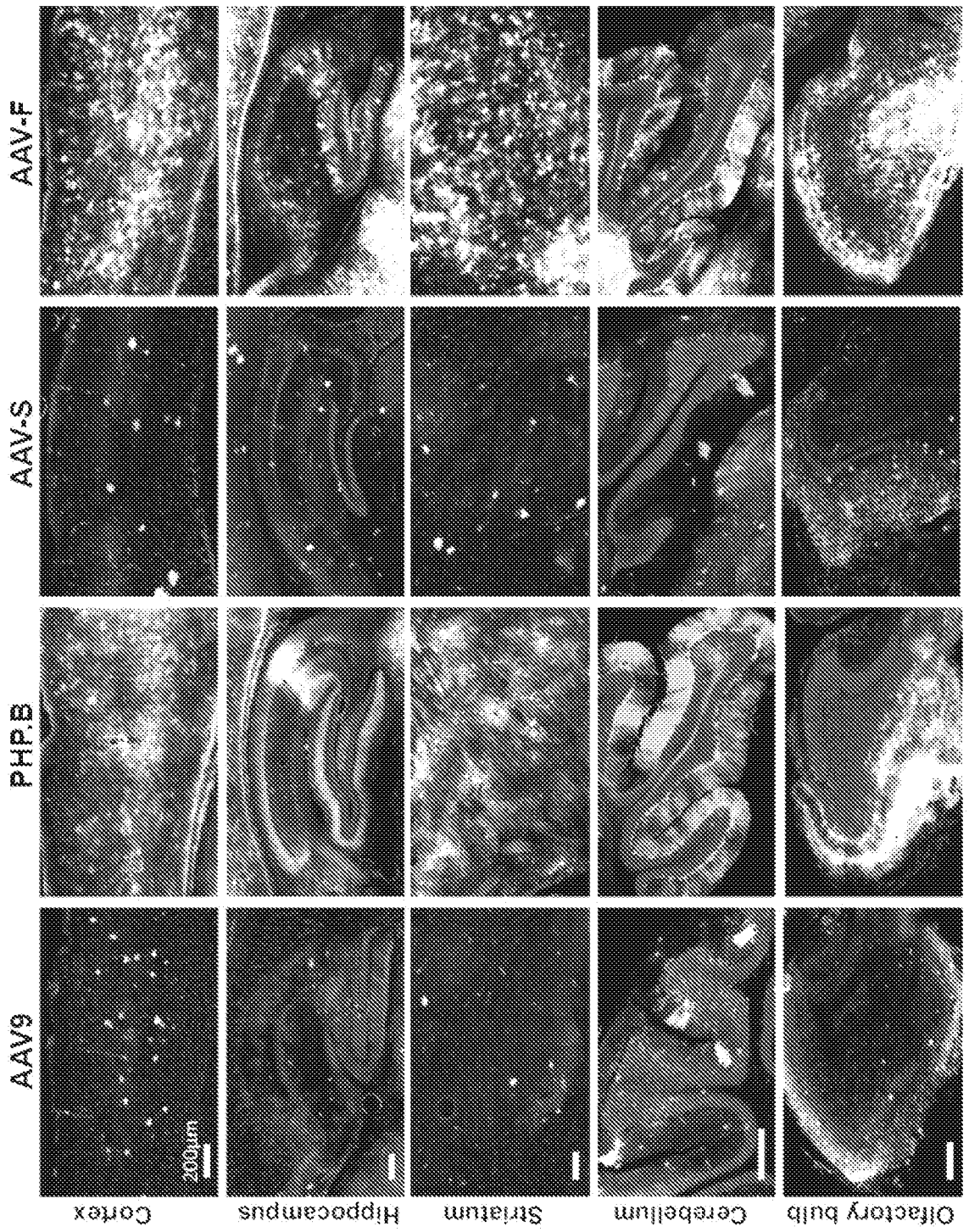


FIG. 3F

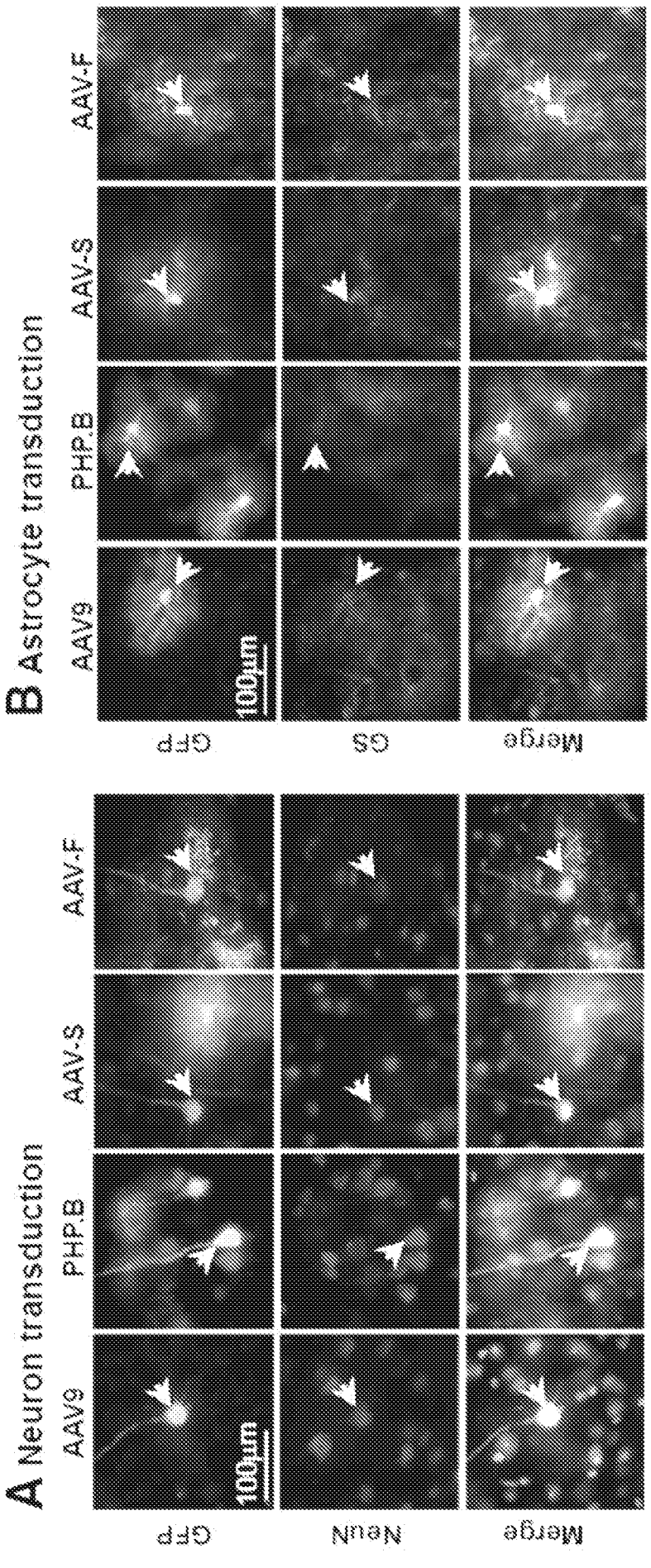


*FIGs. 4A-B*

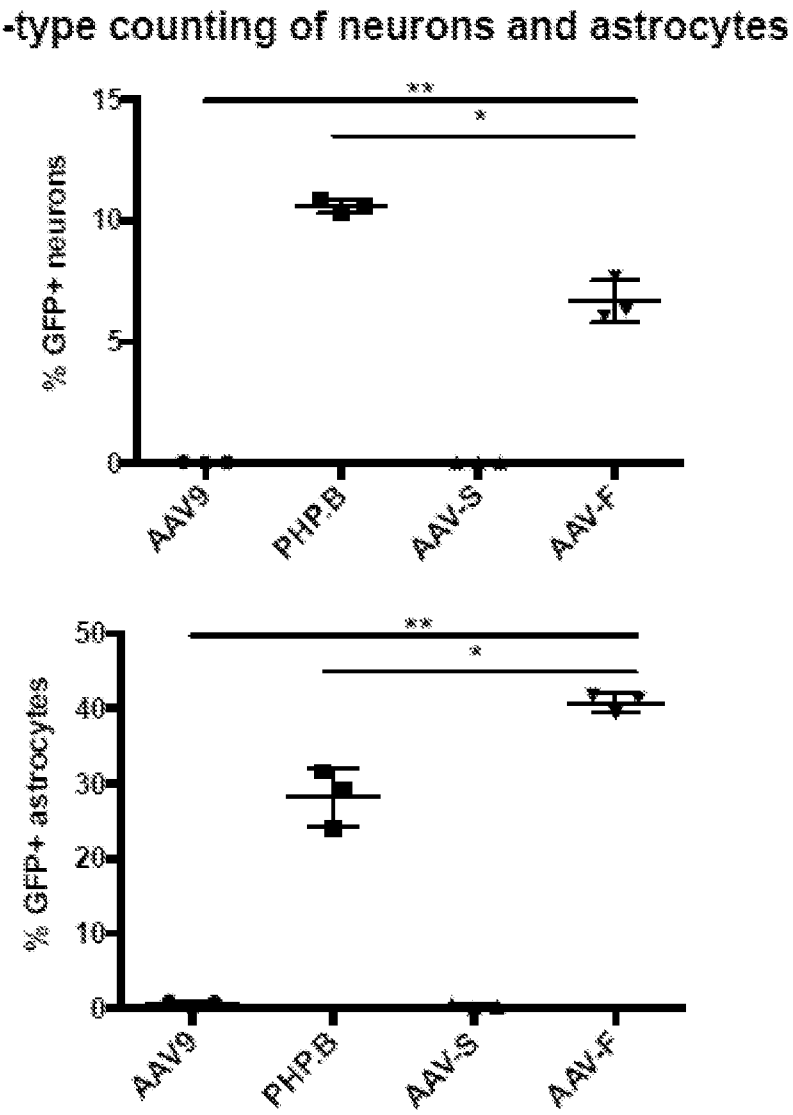


*FIG. 4C*

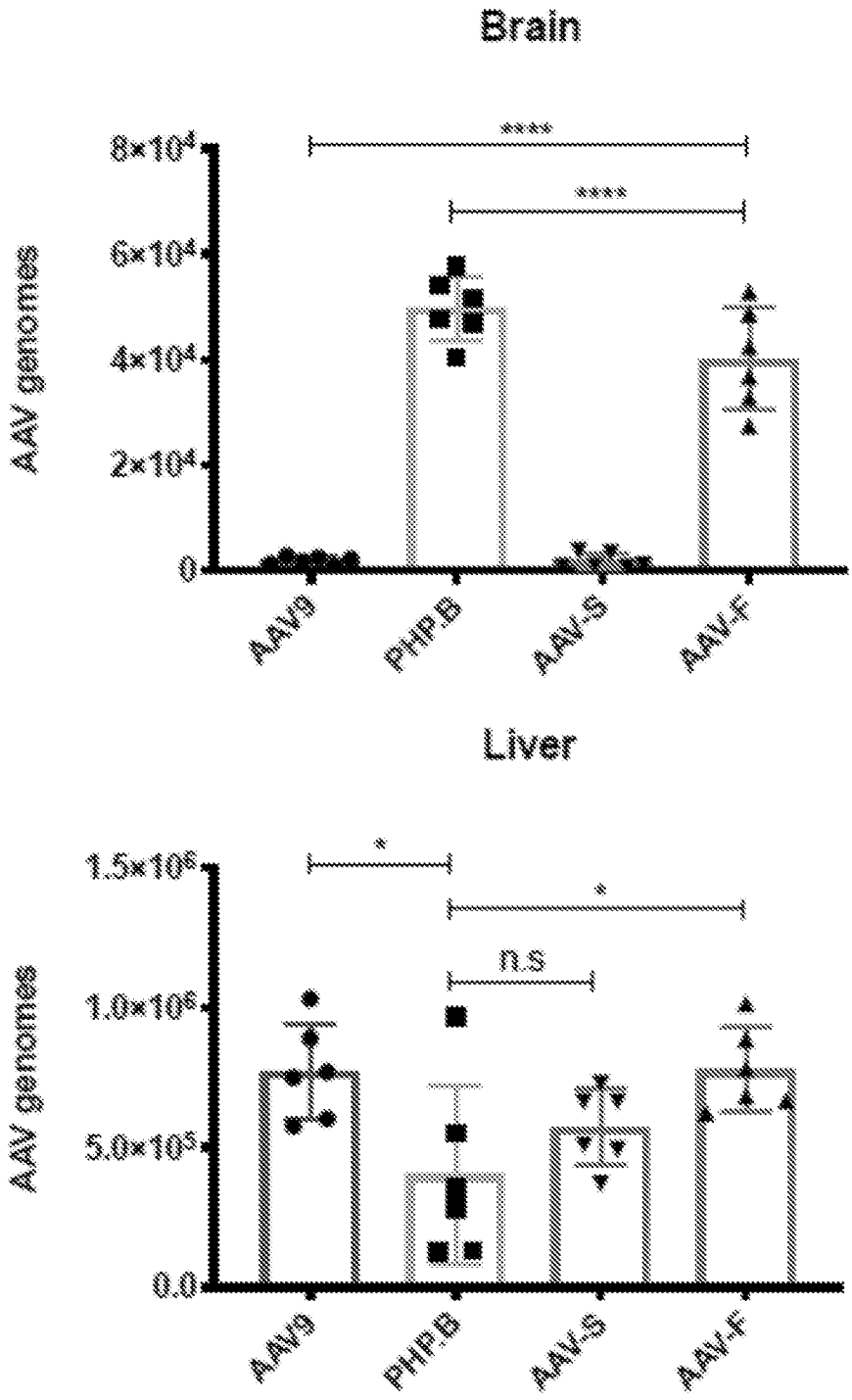


*FIG. 4D*

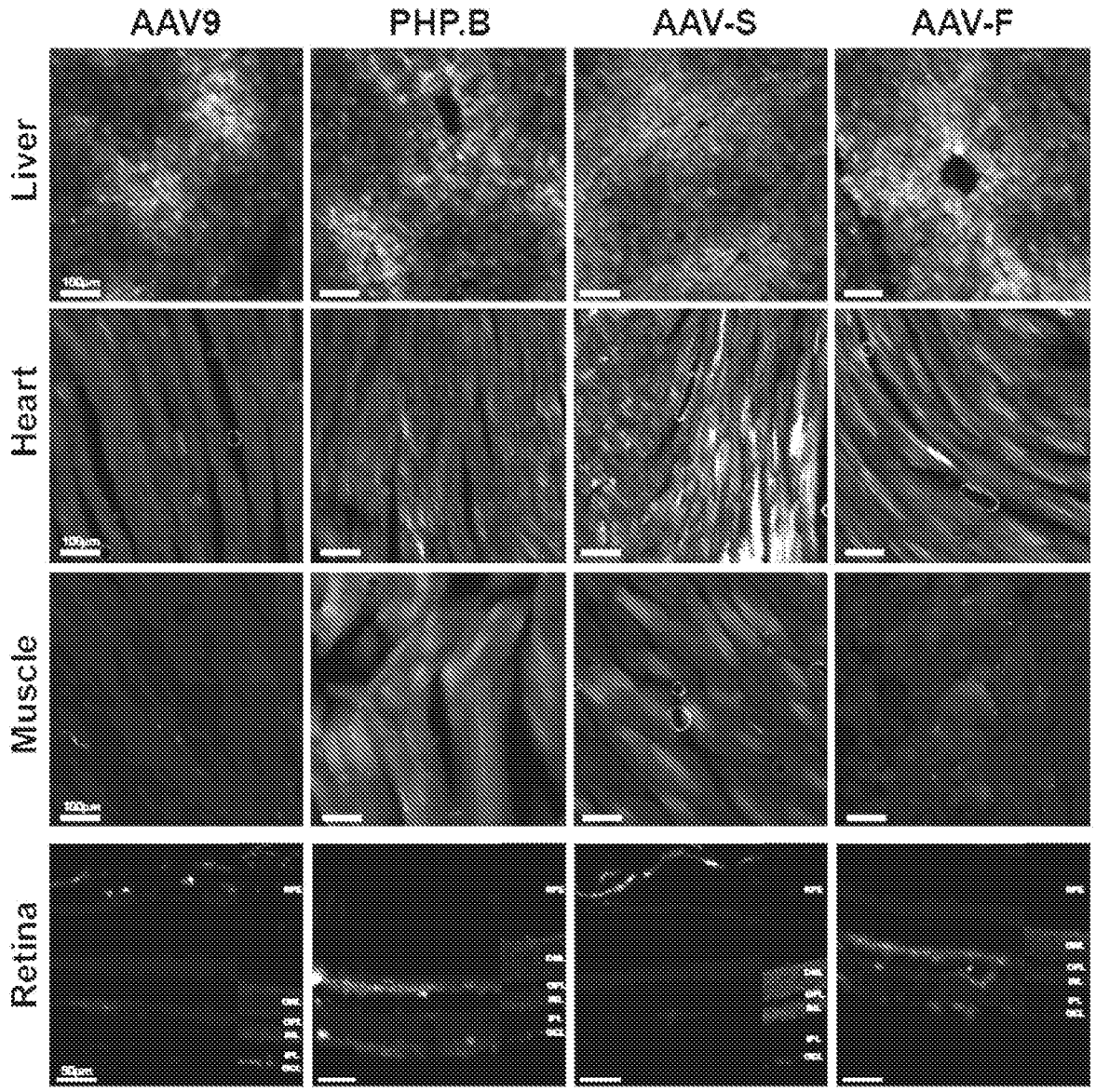


*FIG. 4E*

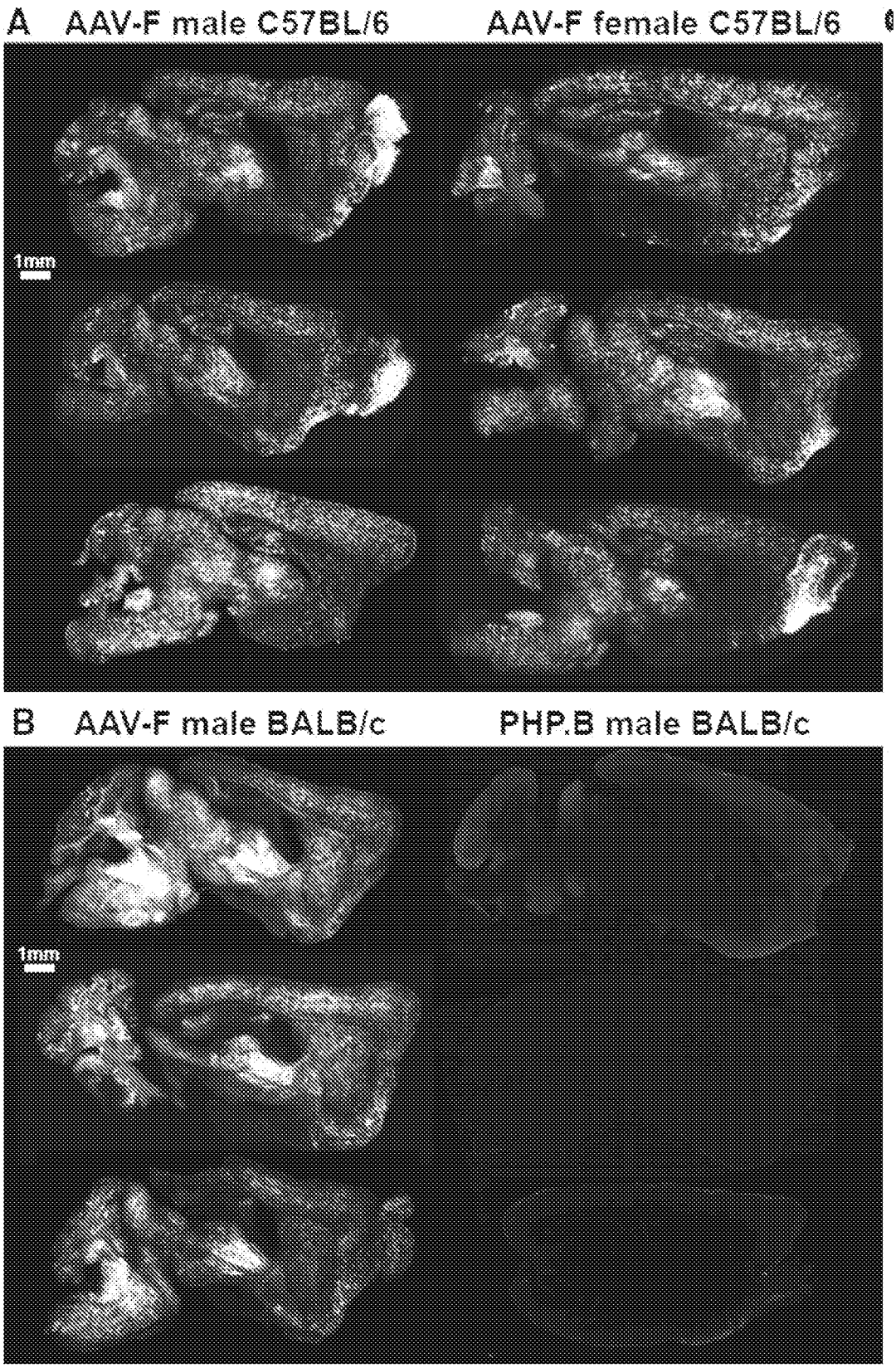


*FIGs. 5A-B*

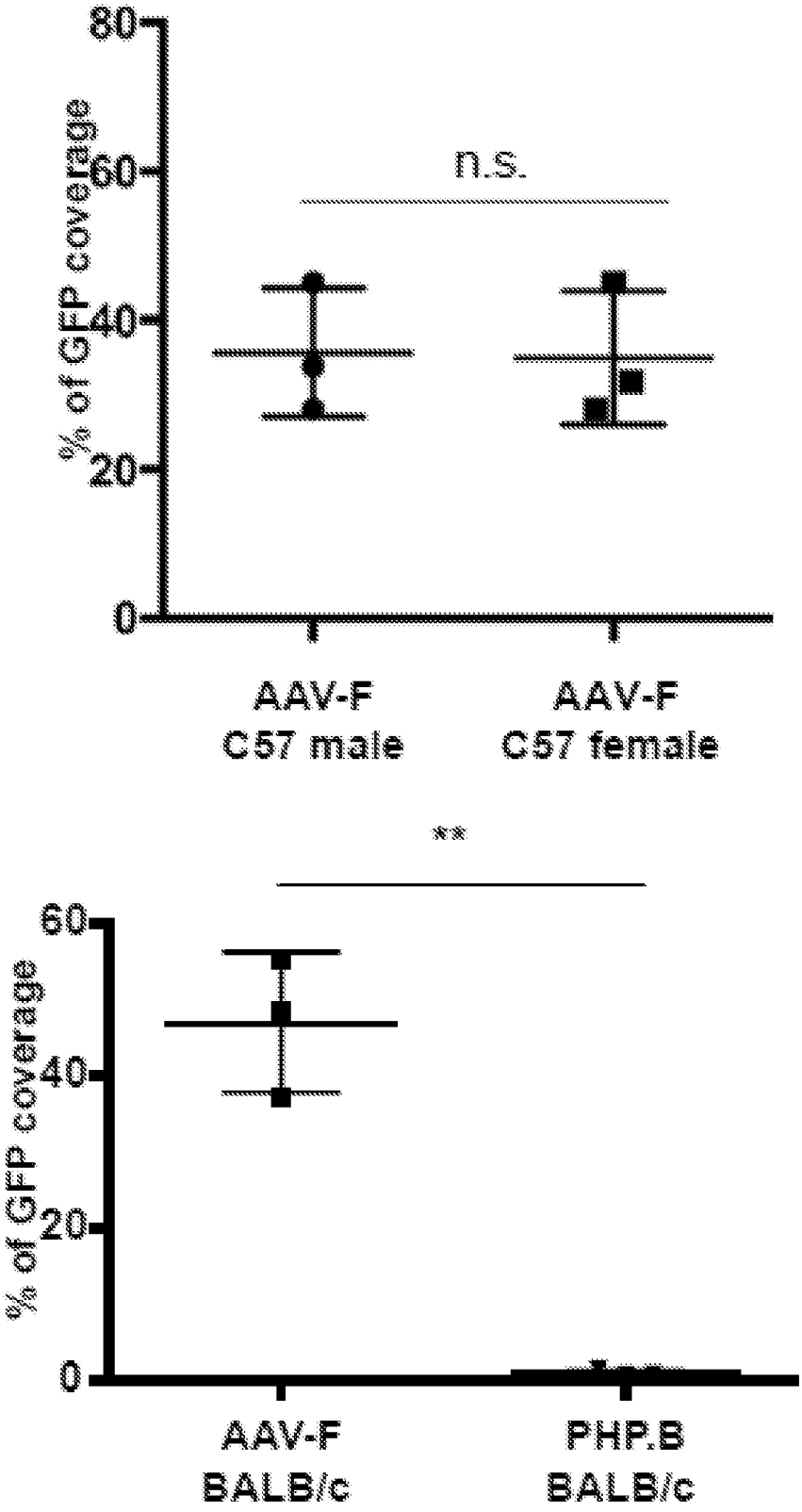


*FIG. 5C*

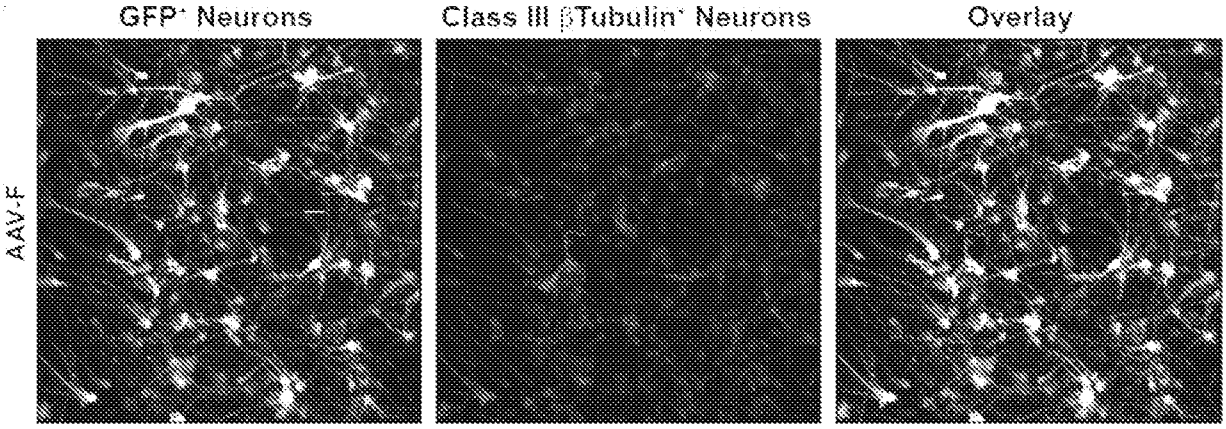


FIG. 6A

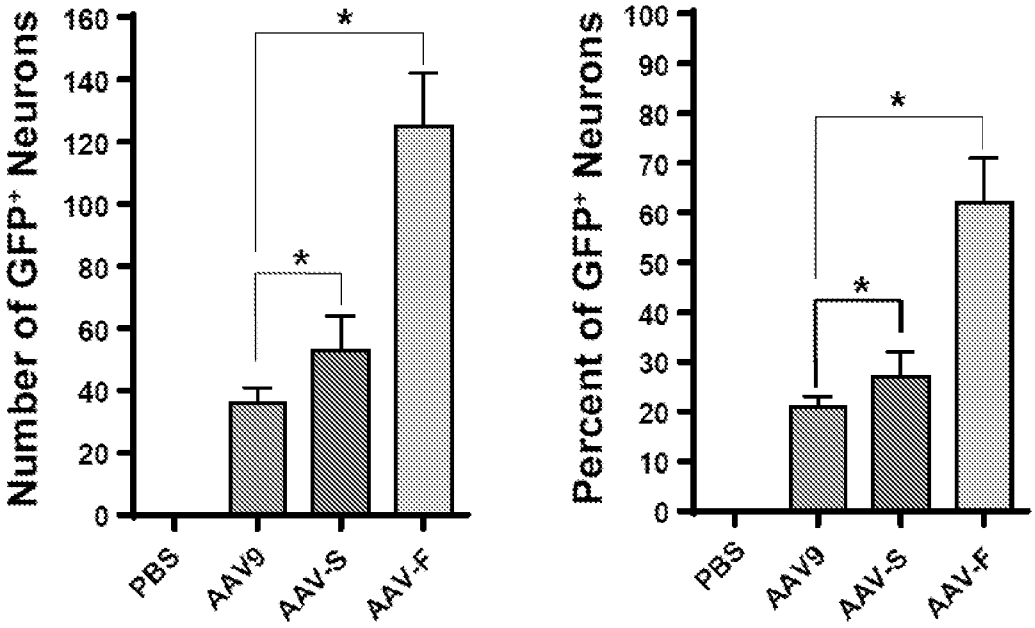


FIG. 6B

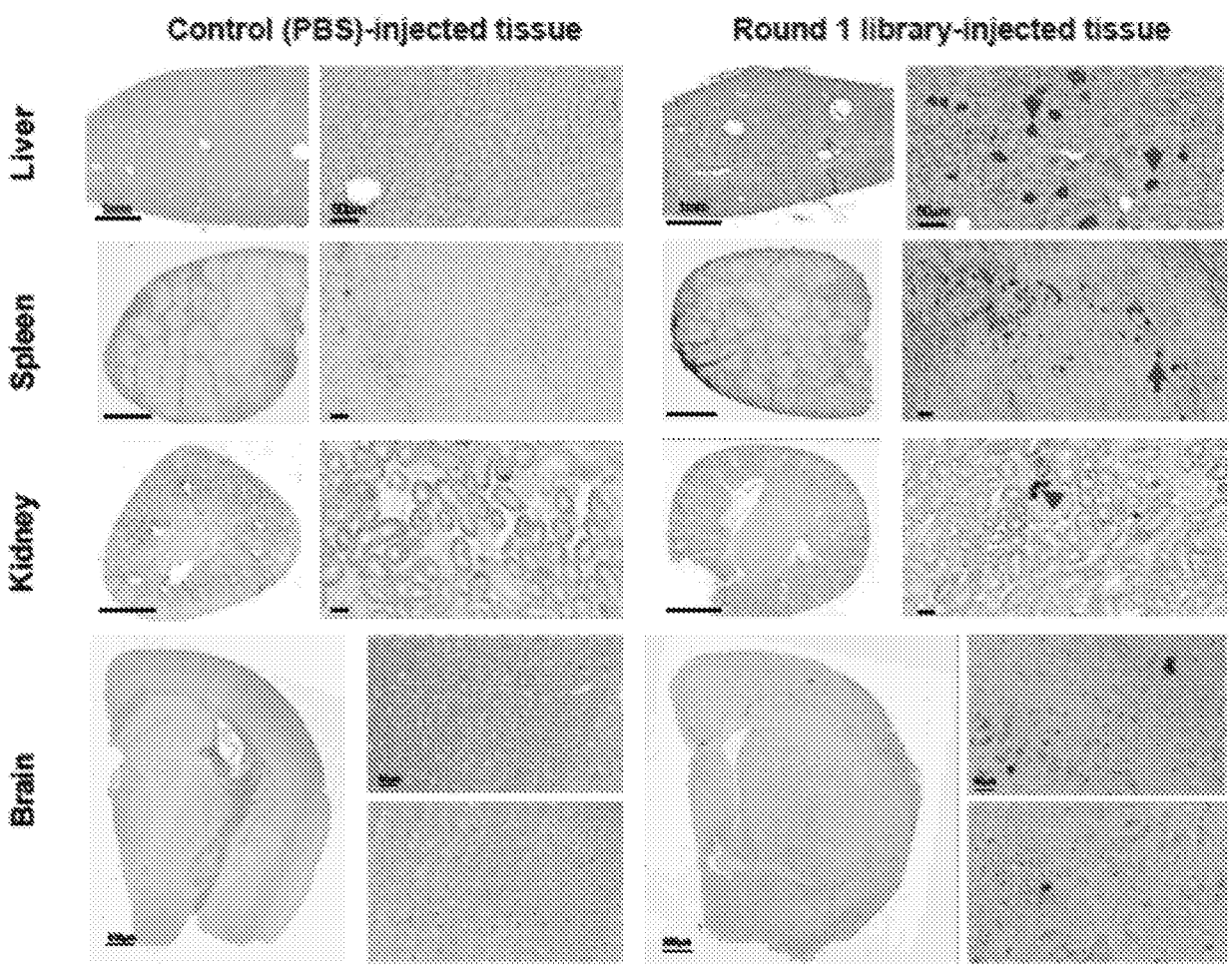


*FIG. 7A*

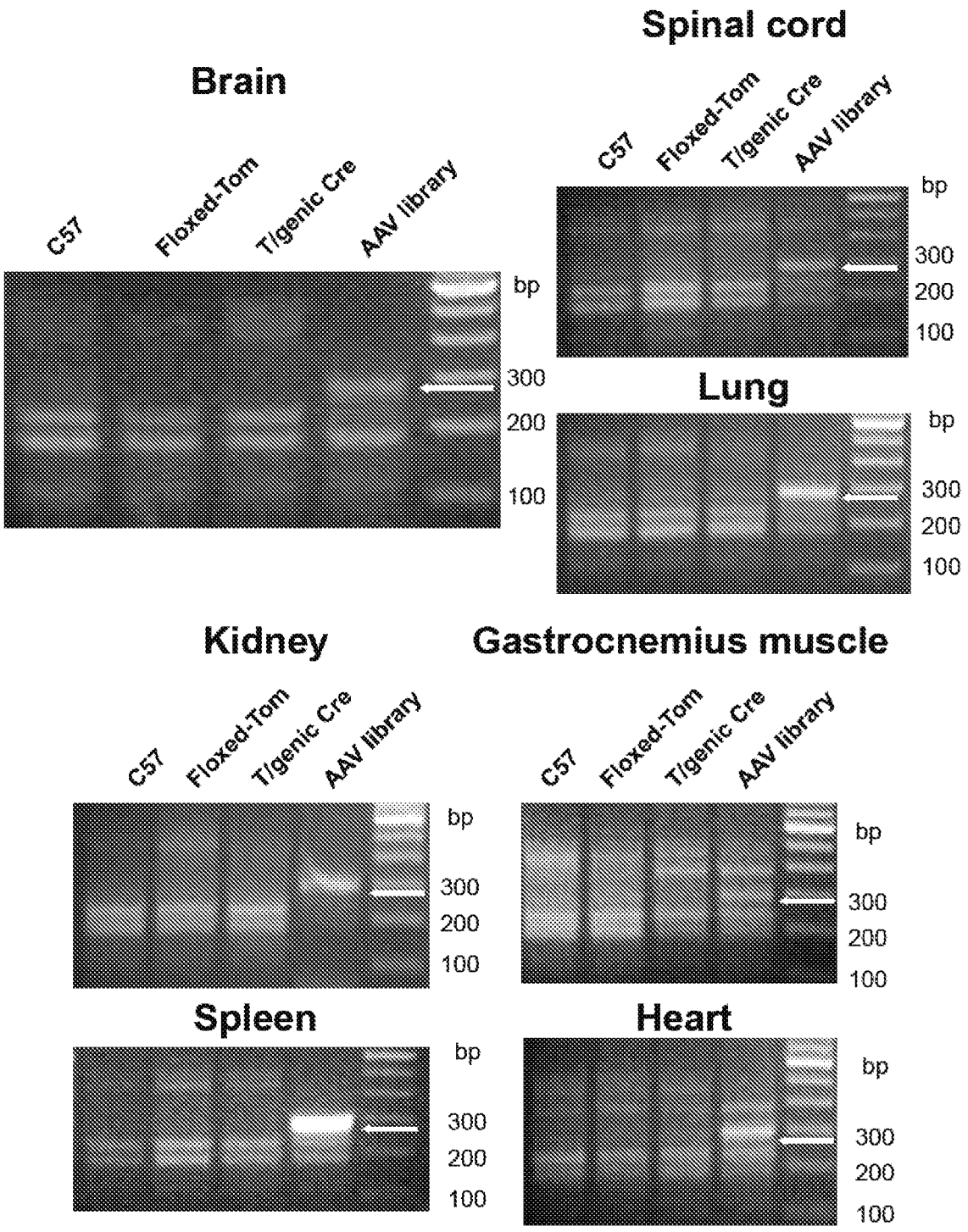


*FIG. 7B*

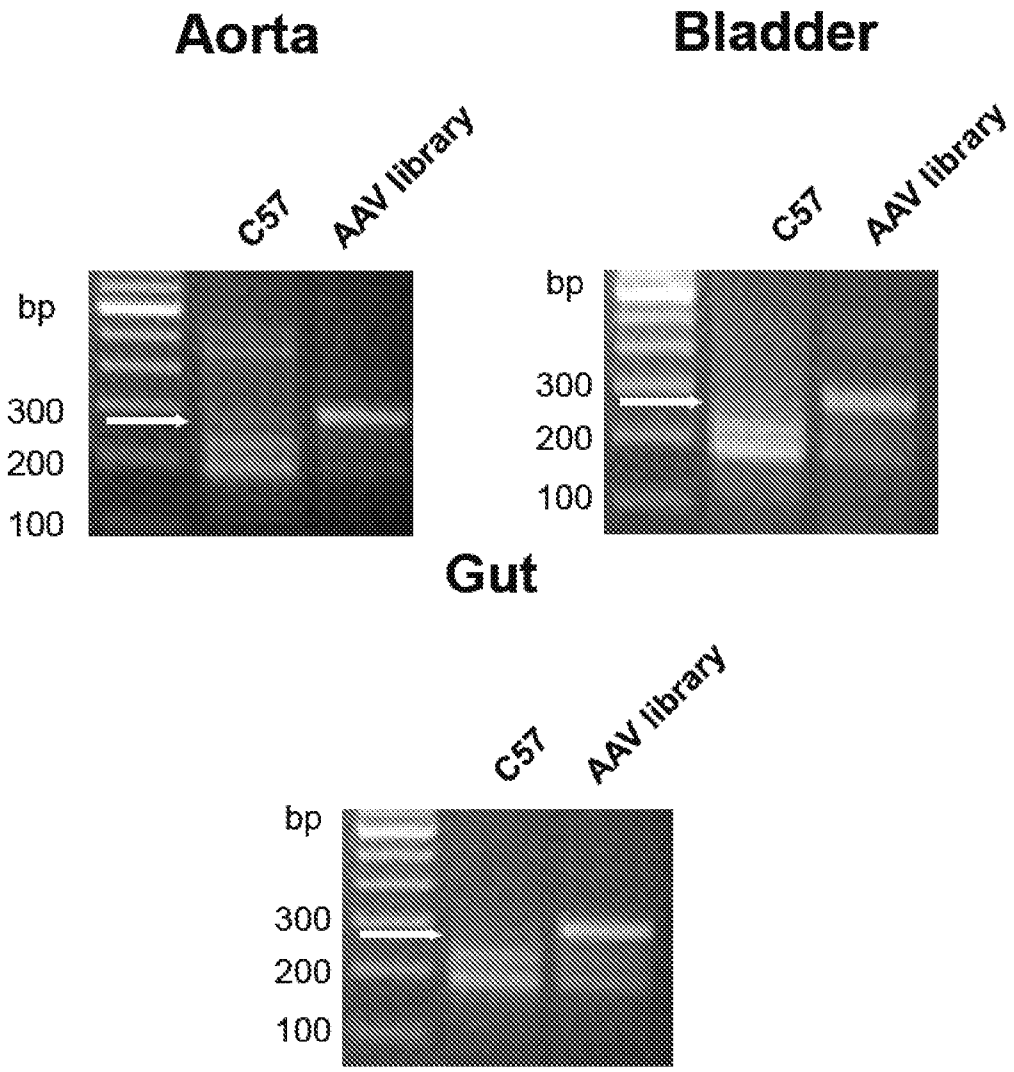


*FIG. 7B, Continued*

| DNA sequence | SEQ ID NO: | Peptide sequence | SEQ ID NO: | Frequency |
|---|---|---|---|---|
| ACGGGGTGTAAGTGTTCGCAG | 87. | TGCKCSQ | 88. | 0.05897 |
| CATCTGCCTGTTATGAATGAG | 89. | HLPVMNE | 90. | 0.055593 |
| GTTTCGTTGAATTATACTGCT | 91. | VSLNYTA | 92. | 0.052346 |
| CCTCCTCCTCCTCCGCCTGTG | 93. | PPPPPPV | 94. | 0.0498 |
| AGTTCTACTGCTAGTCGTCGT | 95. | SSTASRR | 96. | 0.048579 |
| CTGCTTGTGACGTGTCCGGAT | 97. | LLVTCPD | 98. | 0.039487 |
| TCGTTGCTGCGTTATGCTCCG | 99. | SLLRYAP | 100. | 0.039149 |
| CAGCCGCTGCGTCCGAATCTG | 101. | QPLRPNL | 102. | 0.037876 |
| GCTTTGGATACTCATCATTGG | 103. | ALDTHHW | 104. | 0.036811 |
| CGGCCTACTCGTCTTTCTCCG | 105. | RPTRLSP | 106. | 0.036811 |
| GATGCTTGGTCGGCTTCTATT | 107. | DAWSASI | 108. | 0.036213 |
| TATAAGTGTTGGCCGAGGAGT | 109. | YKCWPRS | 110. | 0.03585 |
| AAGTATCTGACTAATCTTTCT | 111. | KYLTNLS | 112. | 0.034941 |
| TCGCGGCCTCCGCCGTCTCTG | 113. | SRPPPSL | 114. | 0.030083 |
| TAGGCGCCGATTCTTTAGTTG | 115. | | | 0.029433 |
| ATGCCTCCTTCTCCTCCGGGT | 116. | MPPSPPG | 117. | 0.029069 |
| CCGTTTCCTCAGATGCTTTTT | 118. | PFPQMLF | 119. | 0.028108 |
| CCTCAGGCGTCTCATGTTAAT | 120. | PQASHVN | 121. | 0.027199 |
| GAGTATTGTTCTTAGATTCCT | 122. | EYCS | 123. | 0.026887 |
| TCGTAGAATTTGCGGGTGTTG | 124. | S | 125. | 0.025588 |
| TATTATCATTCGCTGTCGTCG | 126. | YYHSLSS | 127. | 0.024809 |
| AAGCATTCTCAGCGGCGGAAT | 128. | KHSQRRN | 129. | 0.024004 |
| TAGACTAATGTGTGGATTAAT | 130. | | | 0.023484 |
| ACTAAGACGCCTGAGCATTAG | 131. | TKTPEH | 132. | 0.019977 |
| GGGCCGGAGGGGCCGCGTCTG | 133. | GPEGPRL | 134. | 0.019536 |
| TGTACTTCTAATCTGCATGGG | 135. | CTSNLHG | 136. | 0.018263 |
| GTTATTACTCATCTGACTGAT | 137. | VITHLTD | 138. | 0.018133 |
| GATTCTAATCATTTTGGTCCG | 139. | DSNHFGP | 140. | 0.017899 |
| CCGAGTCAGCAGACTTAGATG | 141. | PSQQT | 142. | 0.014652 |
| TTTGTTGCTGATTGGGAGCCT | 143. | FVADWEP | 144. | 0.014262 |
| CTGATGCAGACTAATATTACG | 145. | LMQTNIT | 146. | 0.011742 |
| CTGGTGGTTCCTAATCGTGAT | 147. | LVVPNRD | 148. | 0.011586 |
| N/A | 149. | Others | 150. | 0.022861 |

*FIG. 7C*

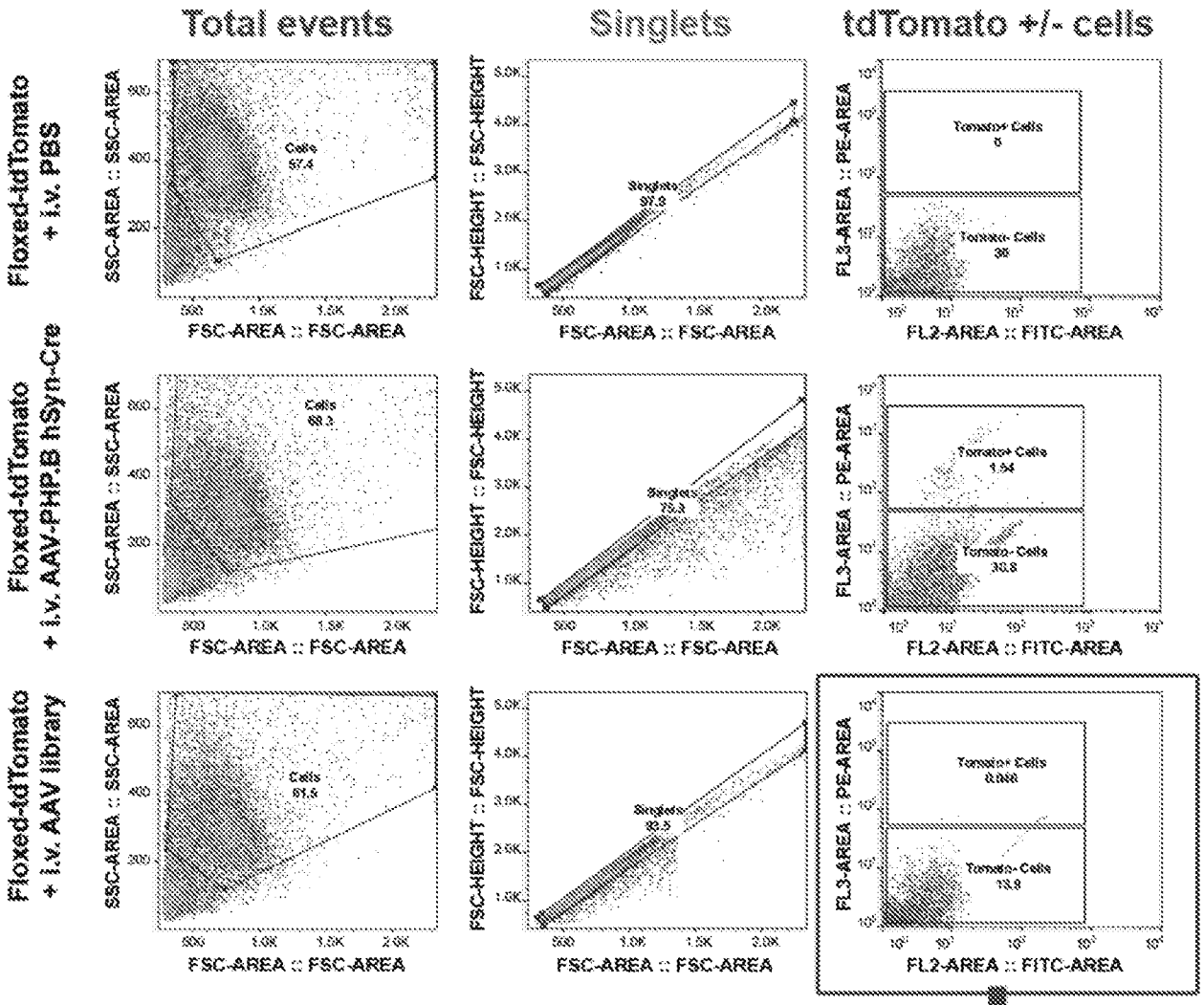


| Total events | tdTomato+ sort count | % of tdTomato+ cells |
|---|---|---|
| 8,850,410 | 3,834 | 0.0433 |

*FIG. 8A*

2026201434 26 Feb 2026

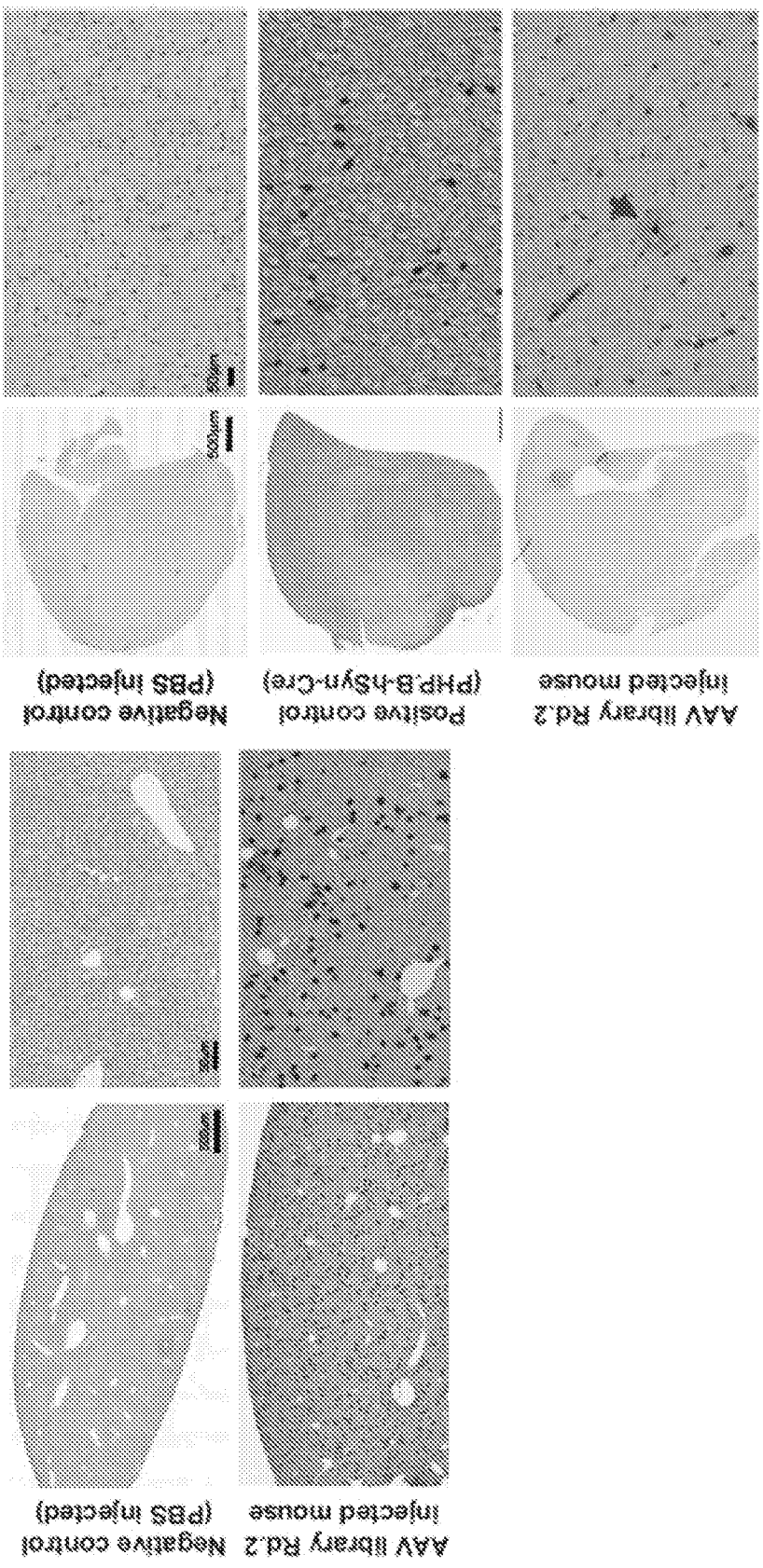


FIG. 8B

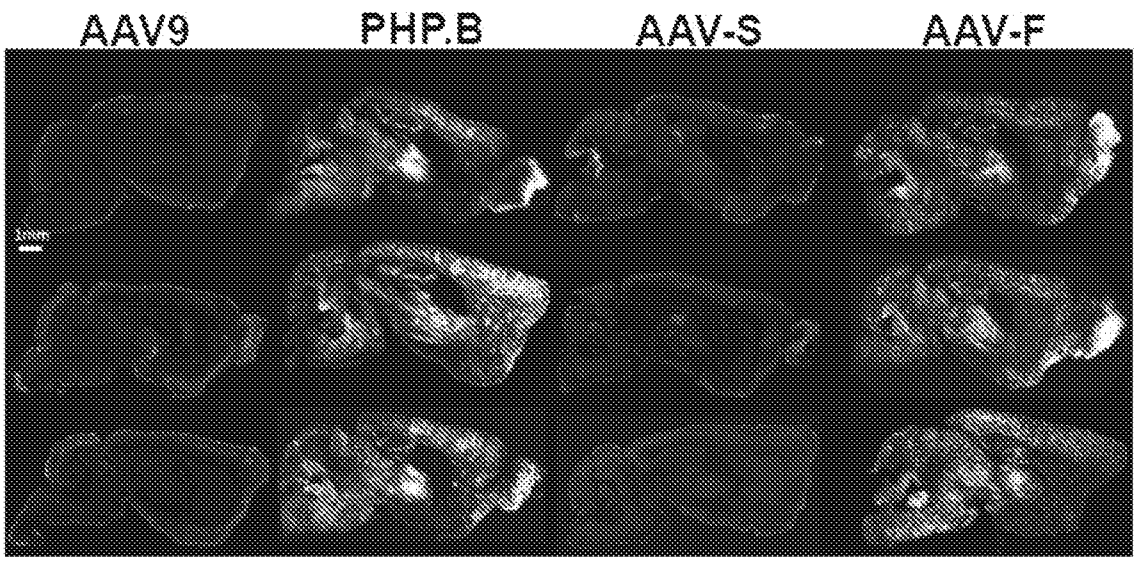


FIG. 9A

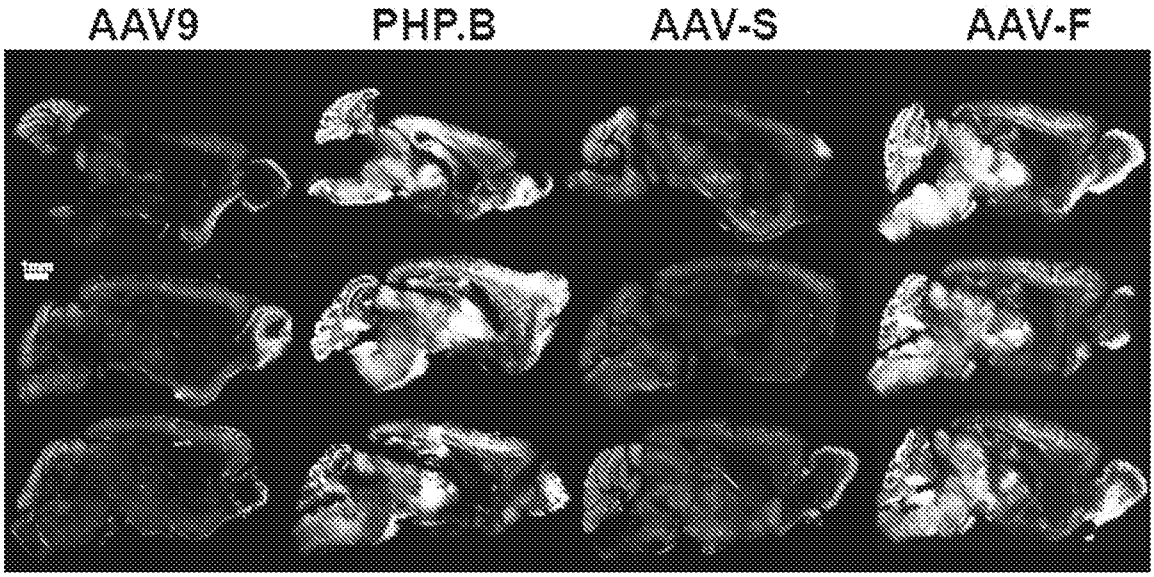


FIG. 9B

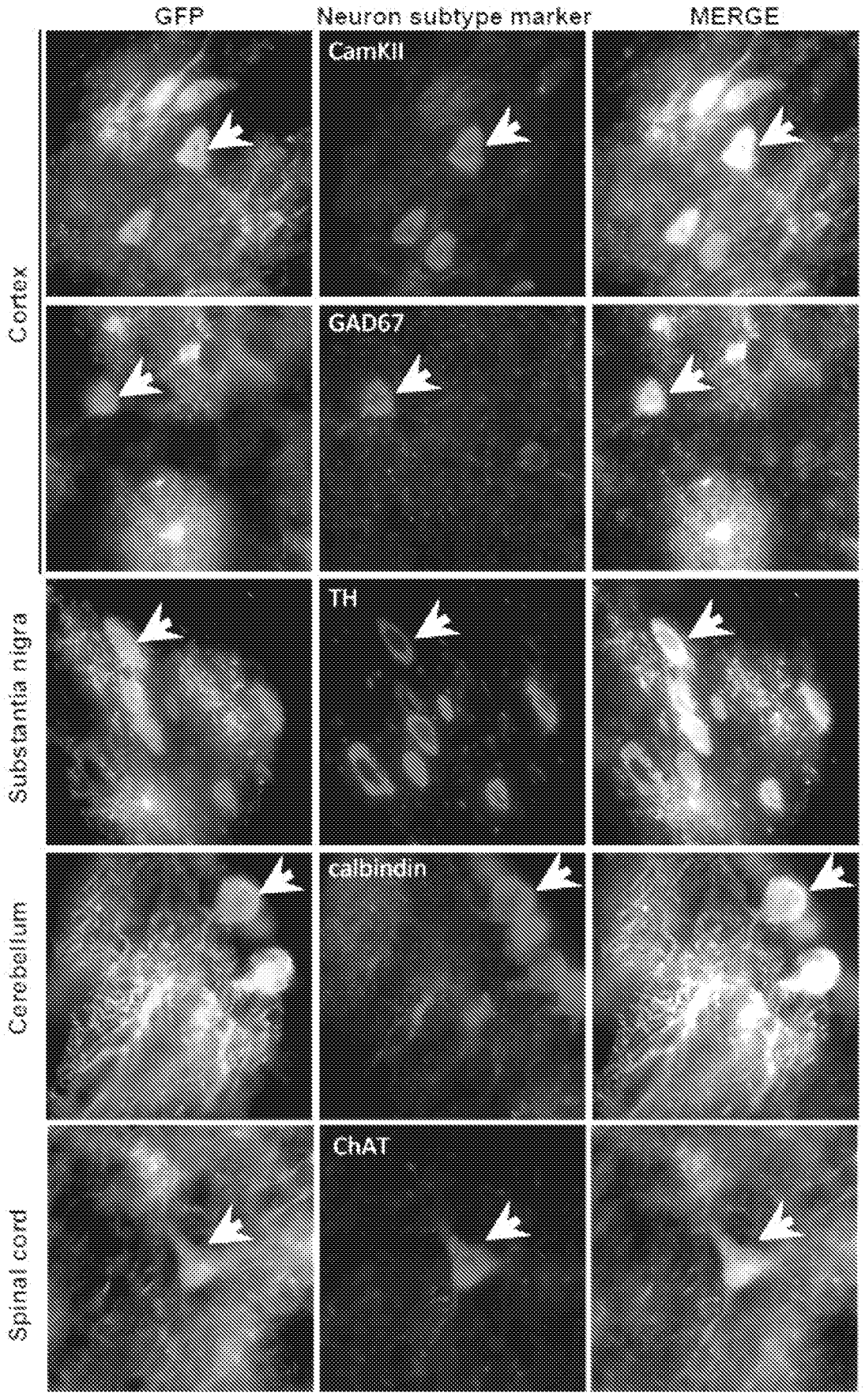


FIG. 10A

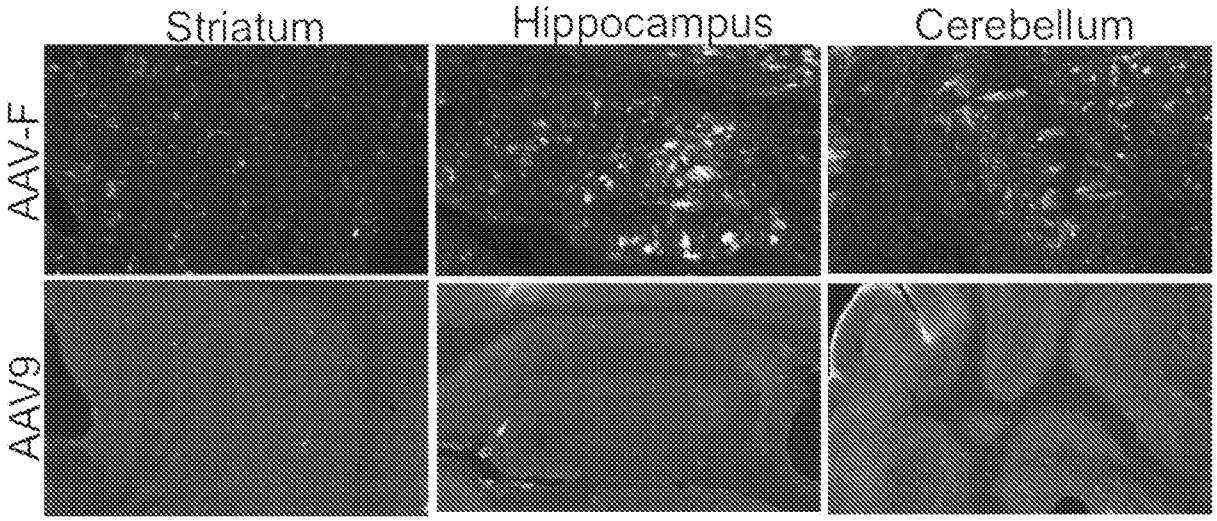


FIG. 10B

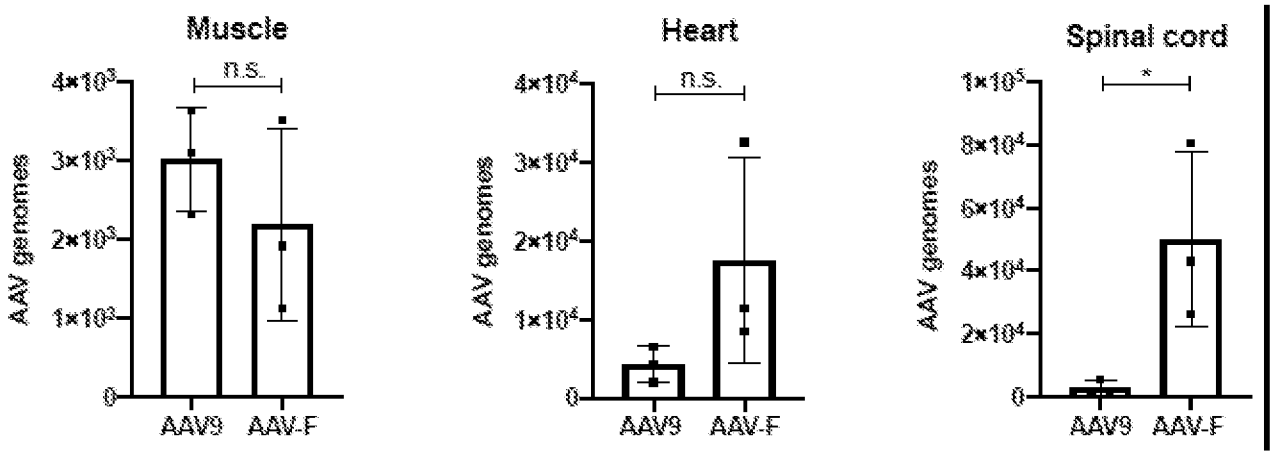


FIG. 11

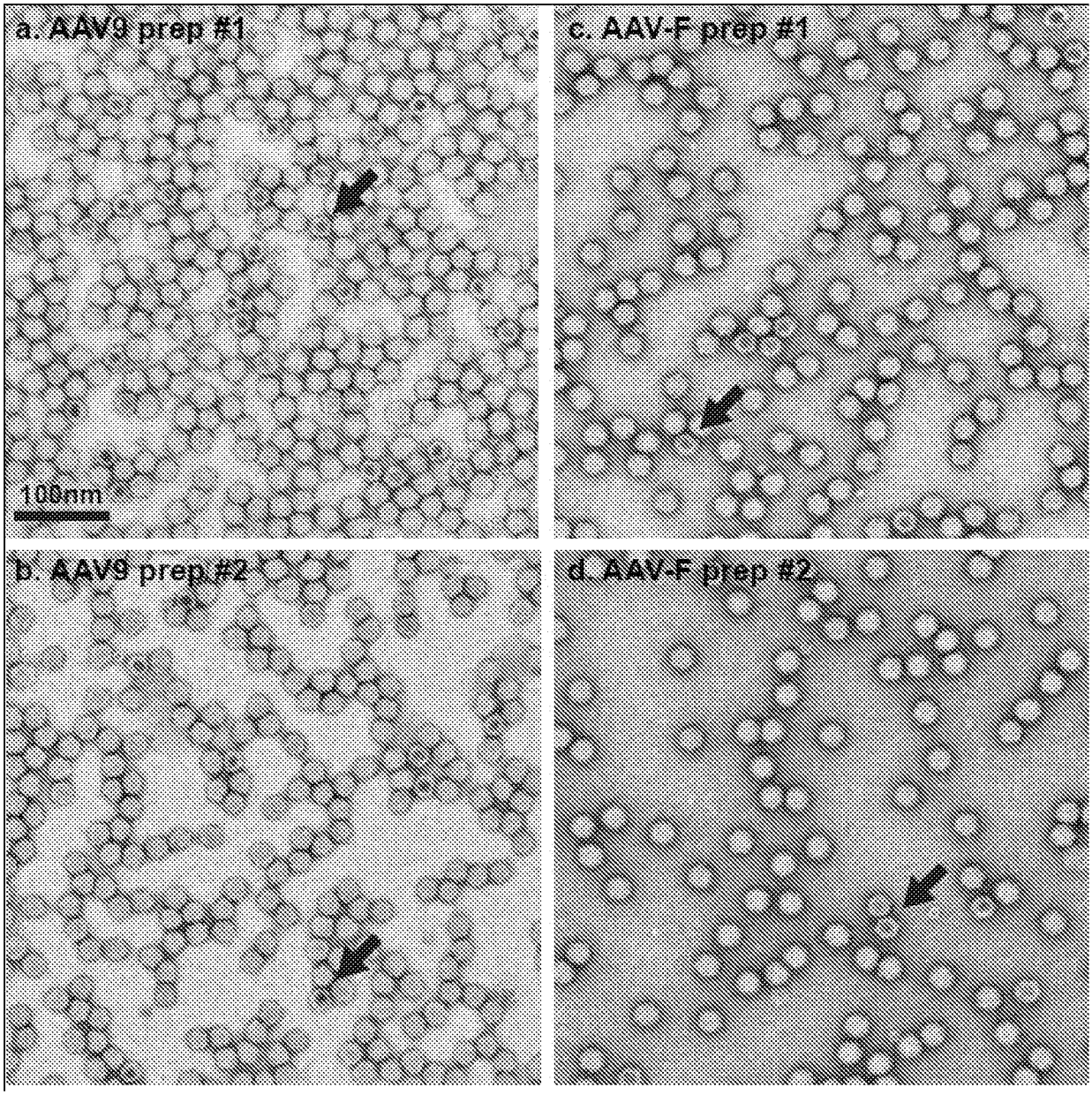


*FIGs. 12A-D*

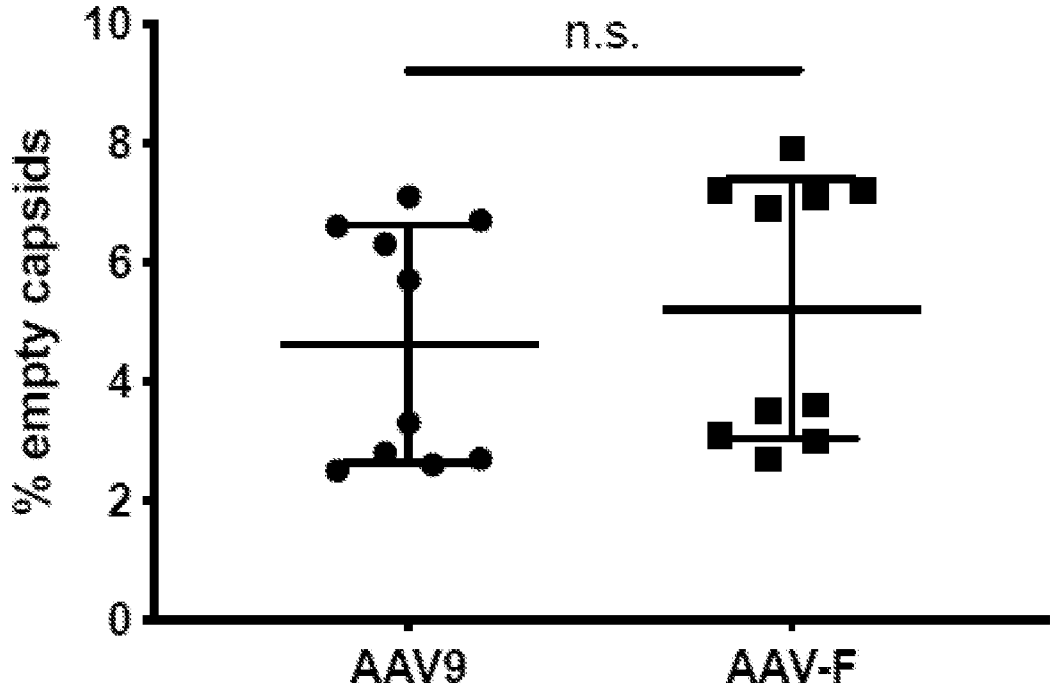


*FIG. 12E*

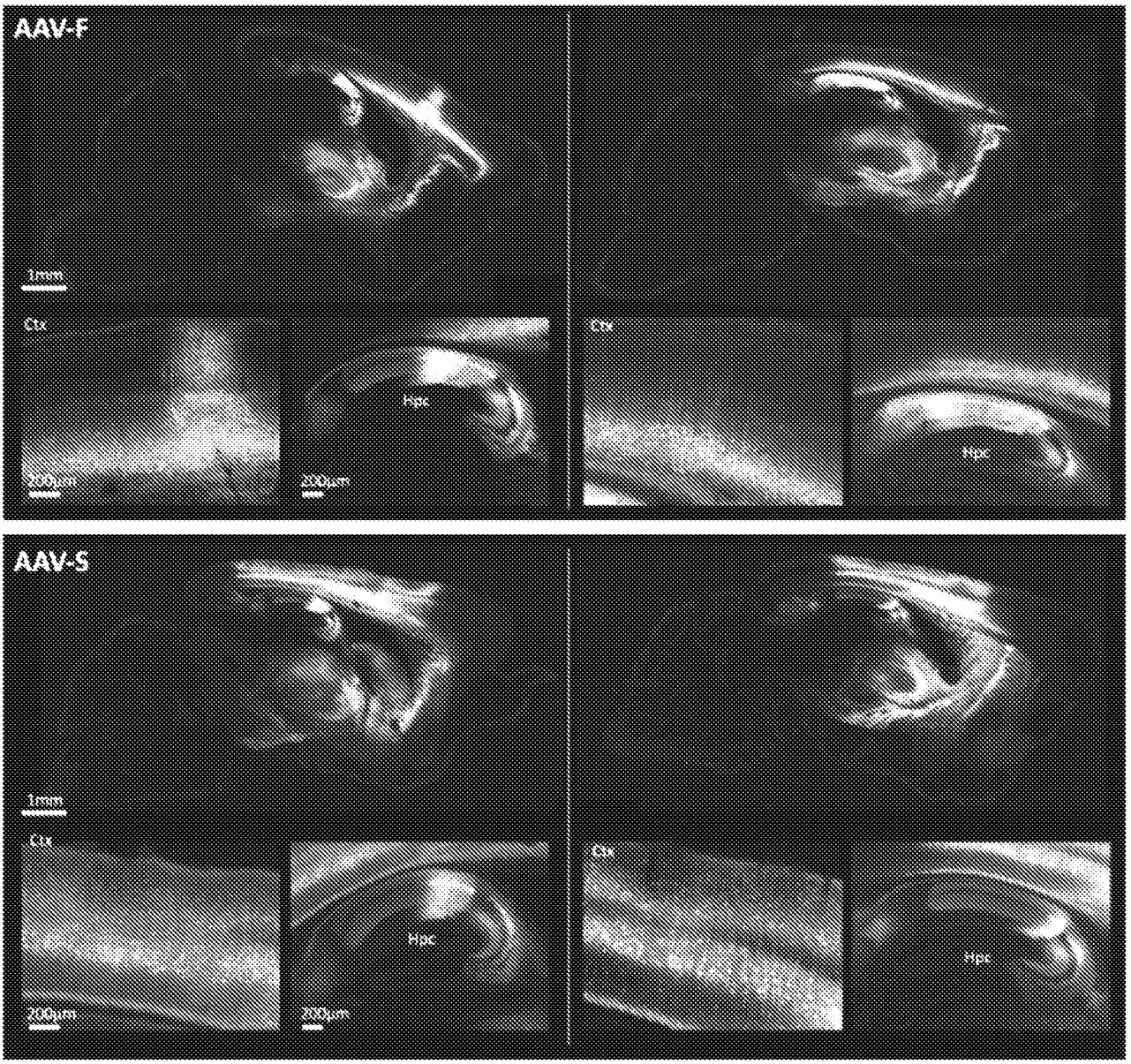


*FIG. 13*

Brain transduction after intrathecal injection

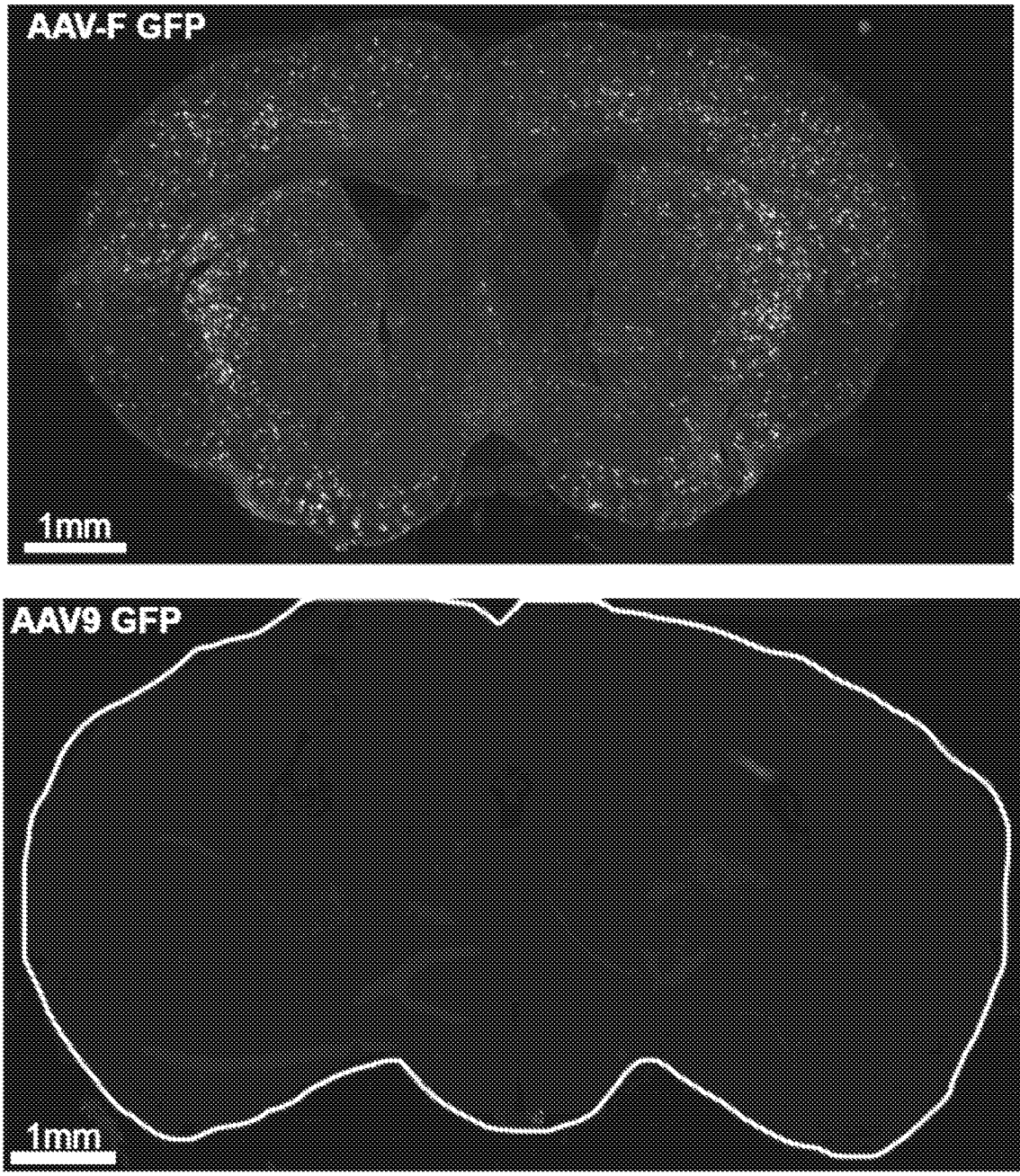


*FIG. 14A*

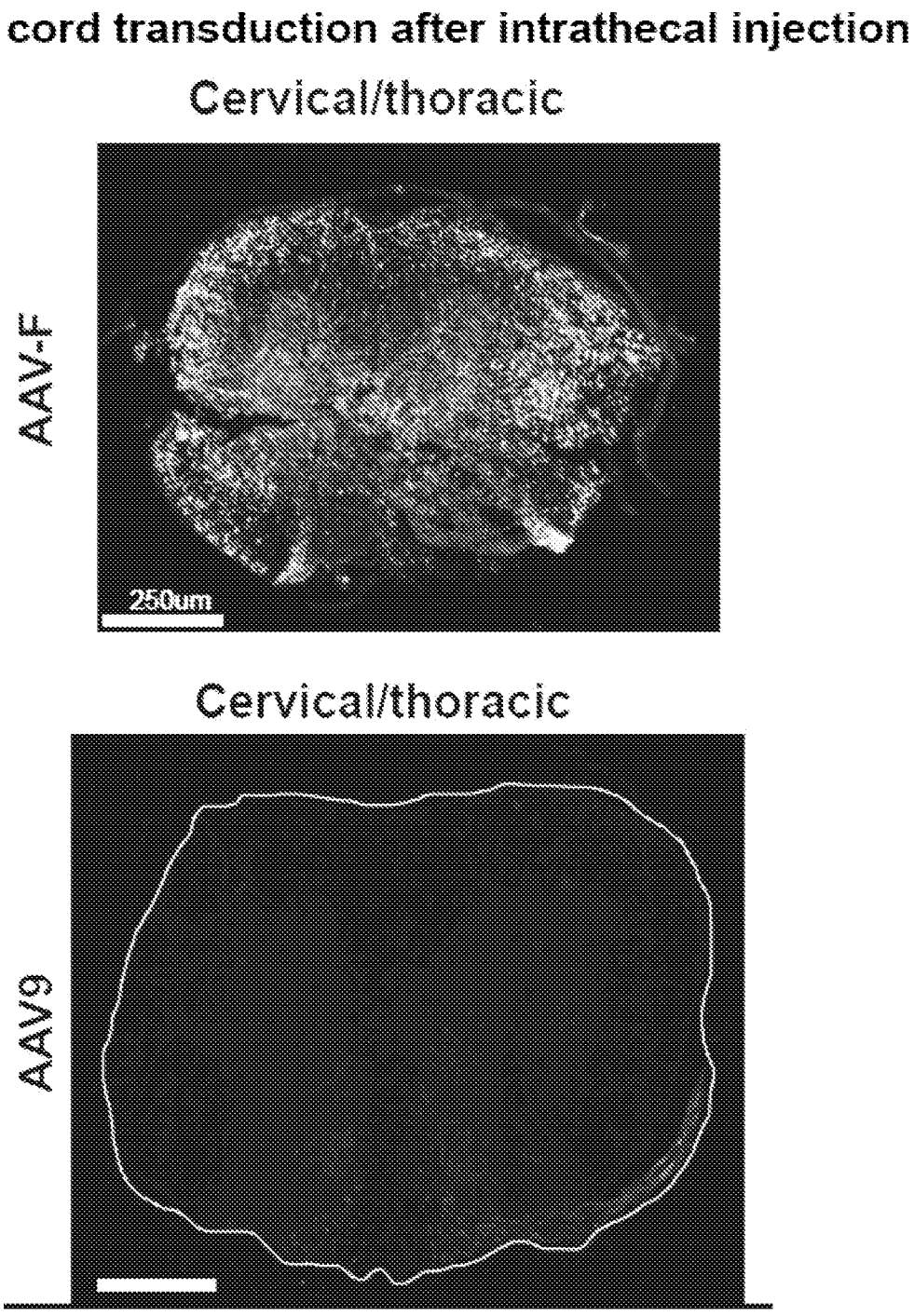


*FIG. 14A, continued*

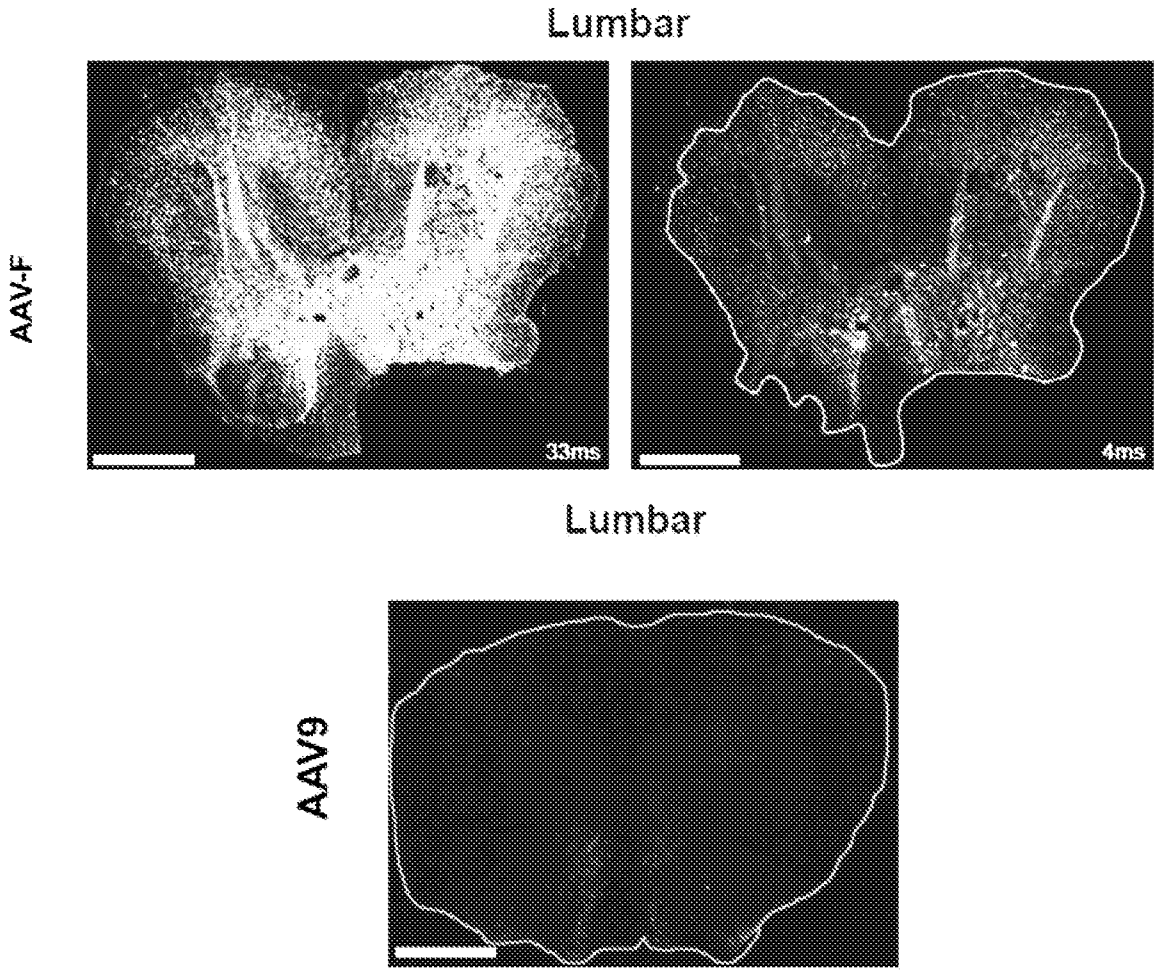


*FIG. 14A, continued*

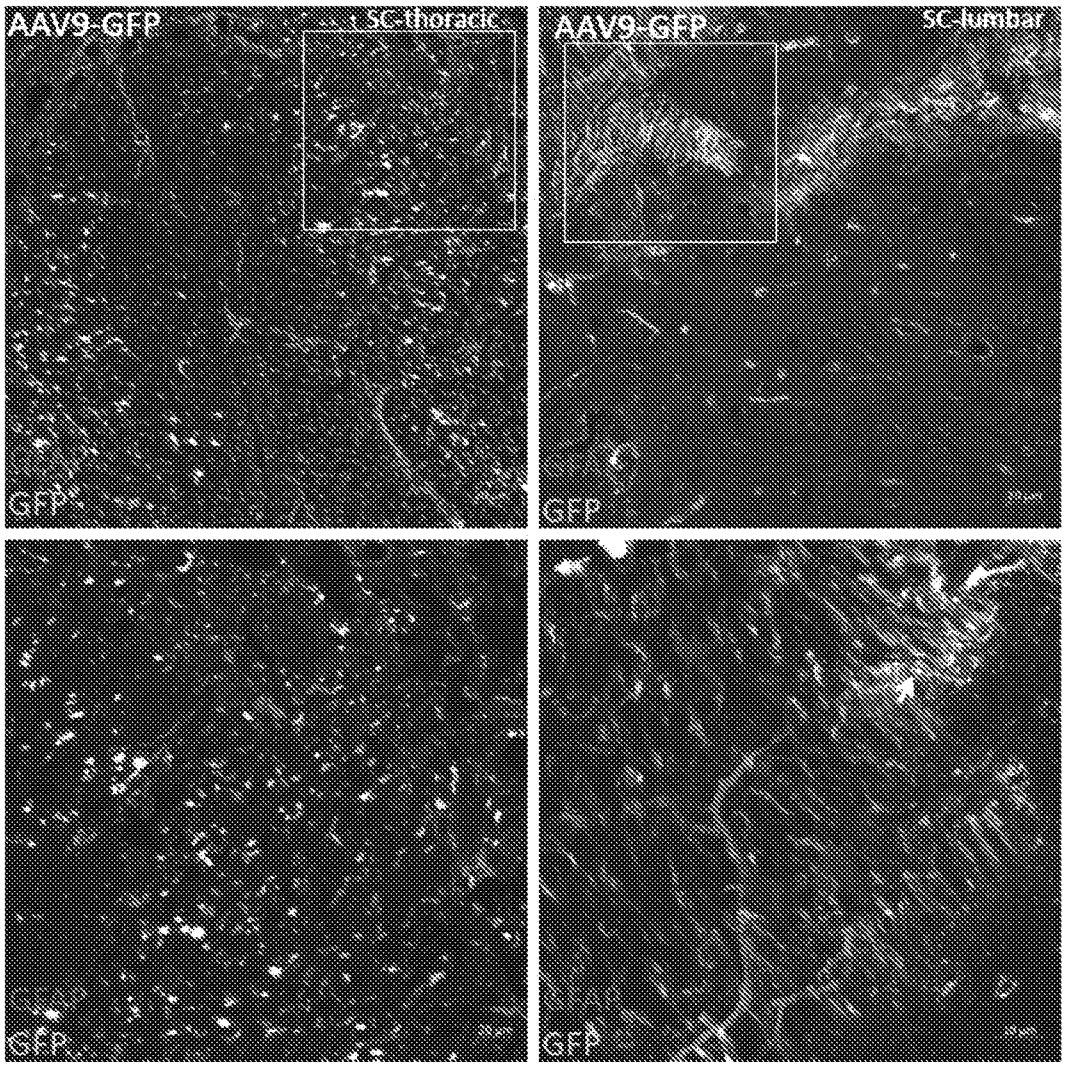


FIG. 14B

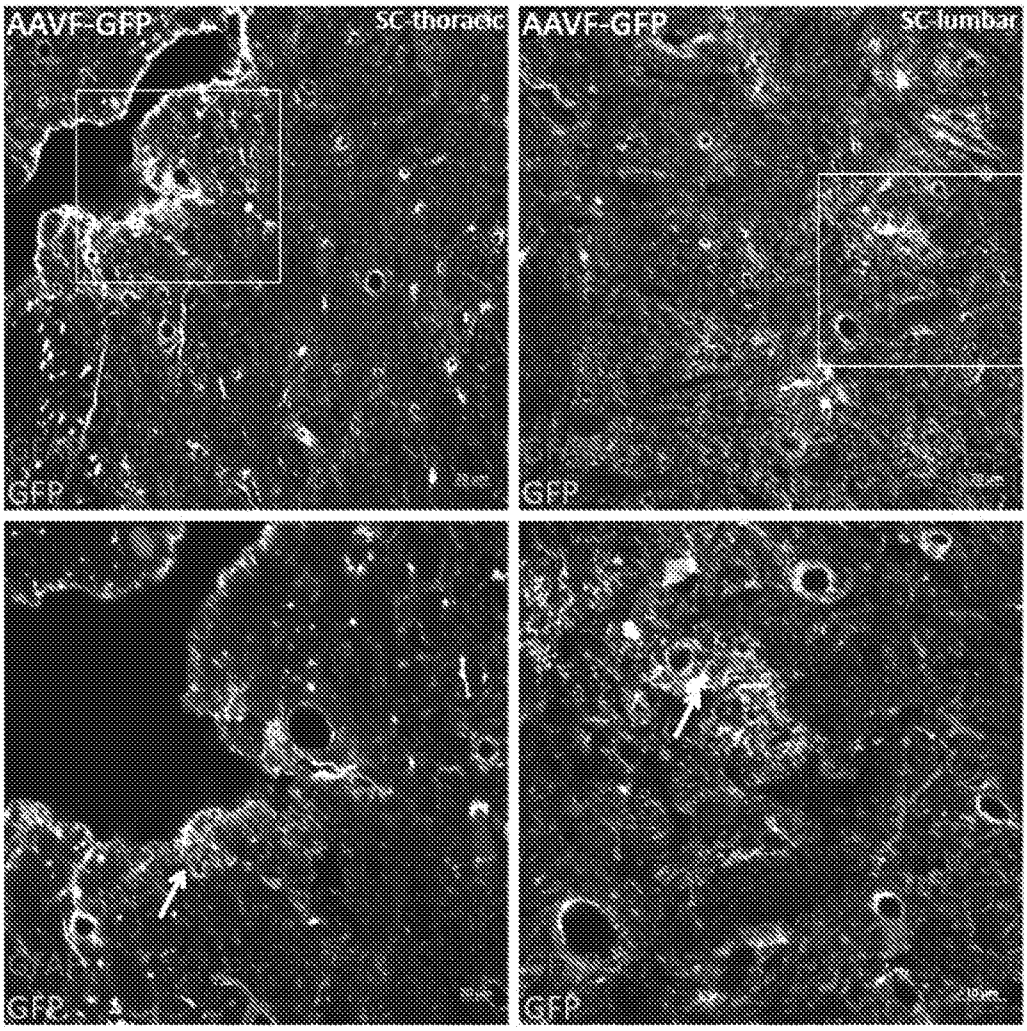


FIG. 14C

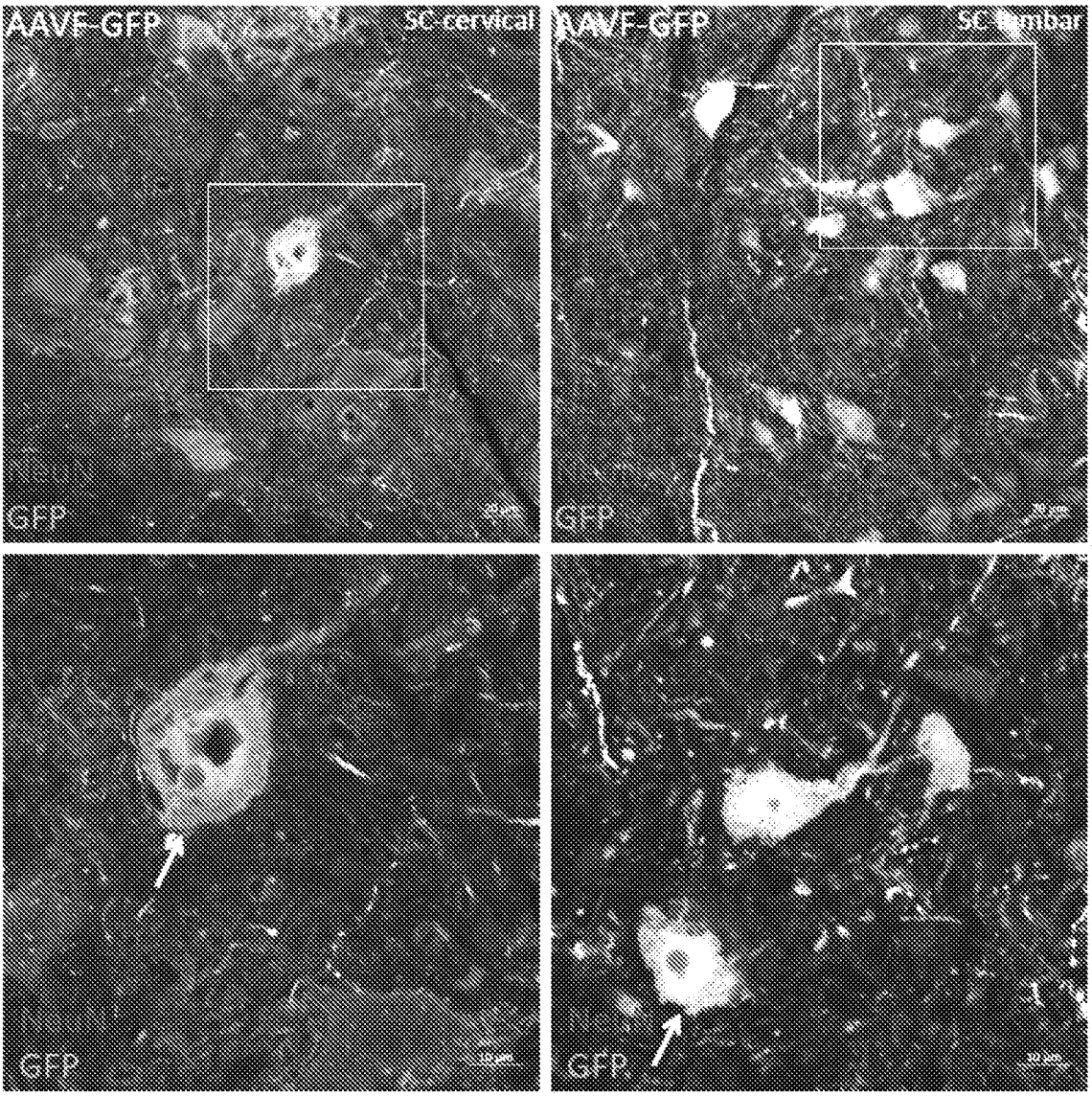


FIG. 14D

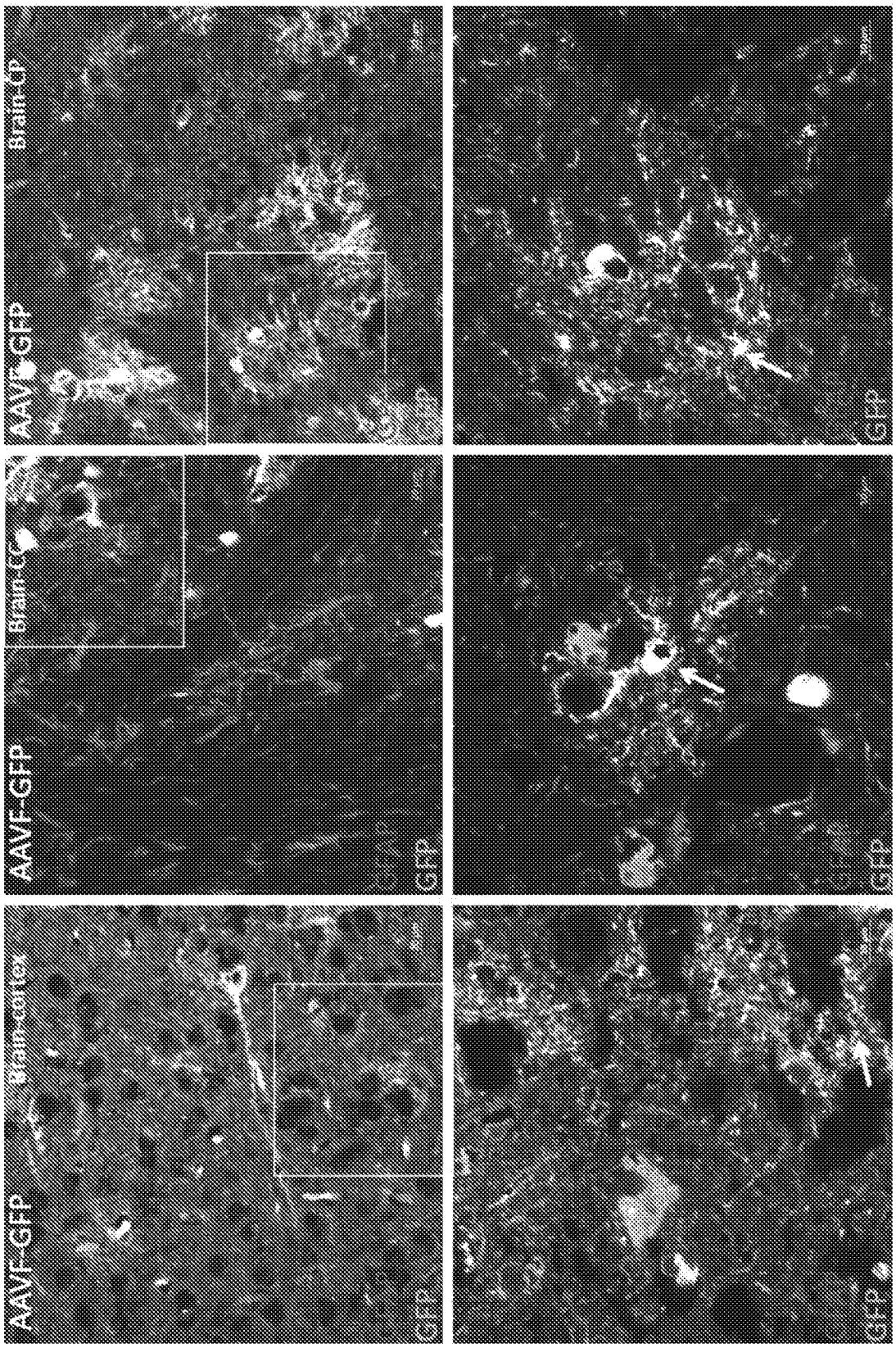


FIG. 14E

2026201434 26 Feb 2026

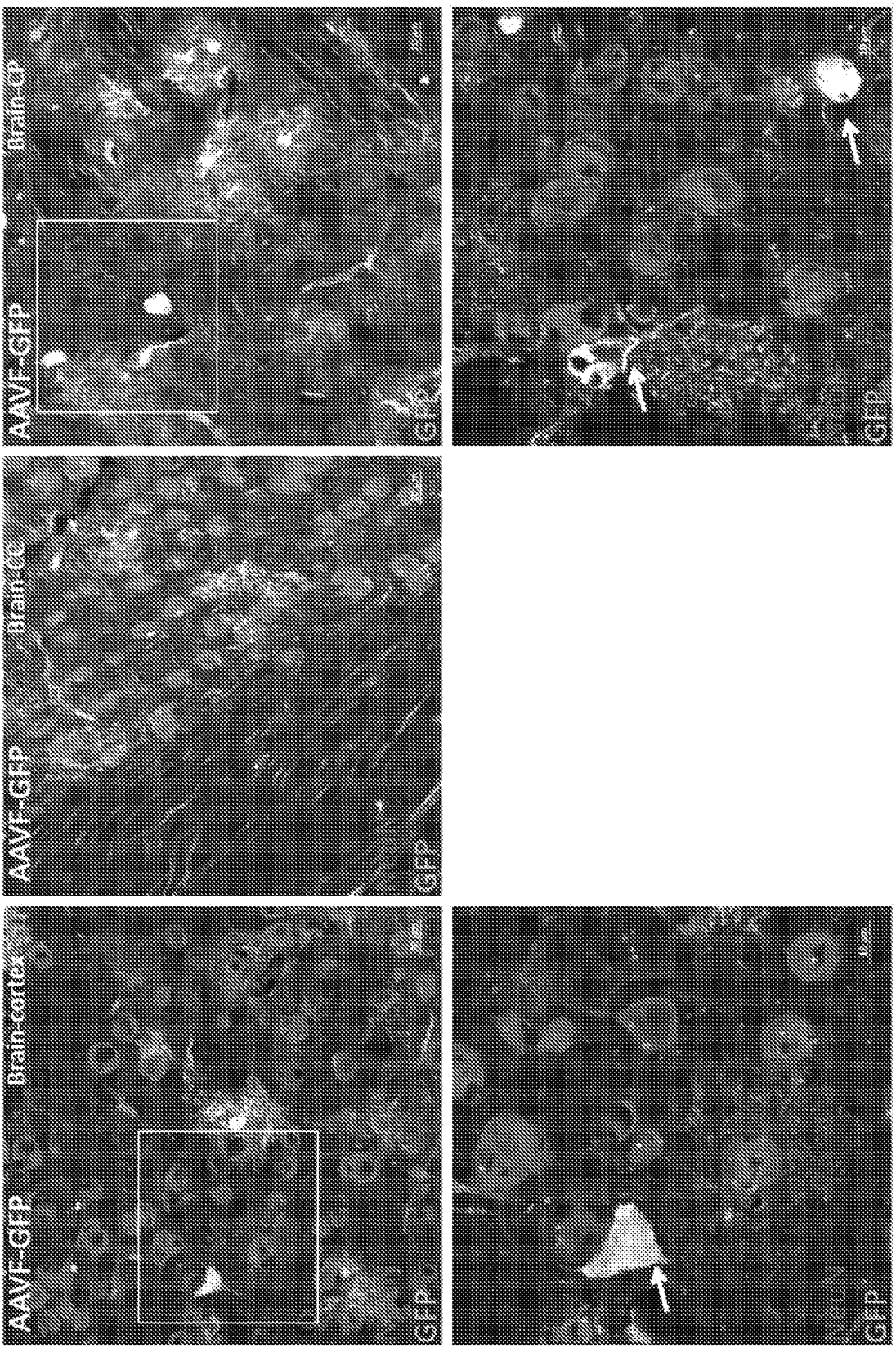


FIG. 14F

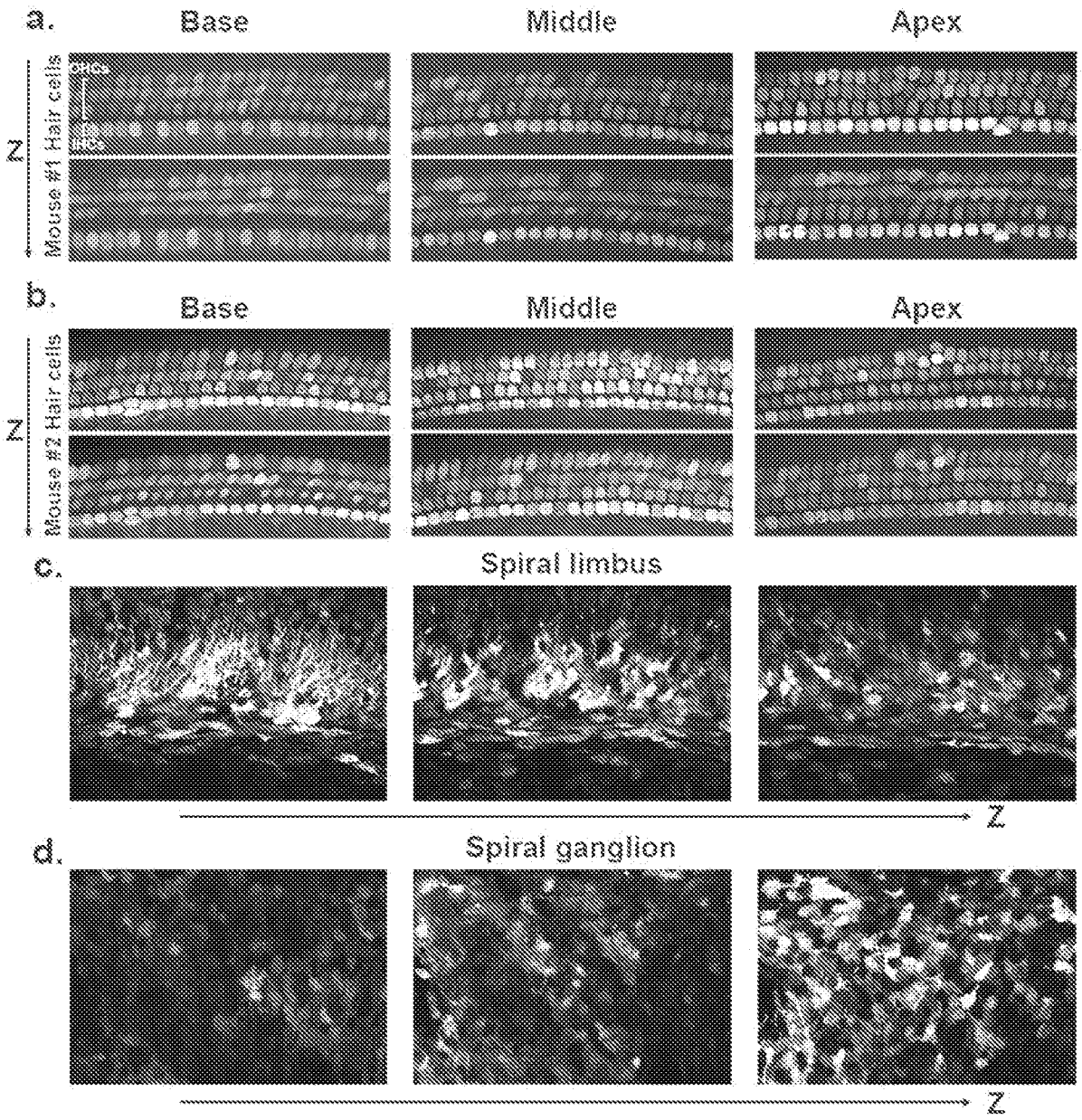


*FIGs. 15A-D*

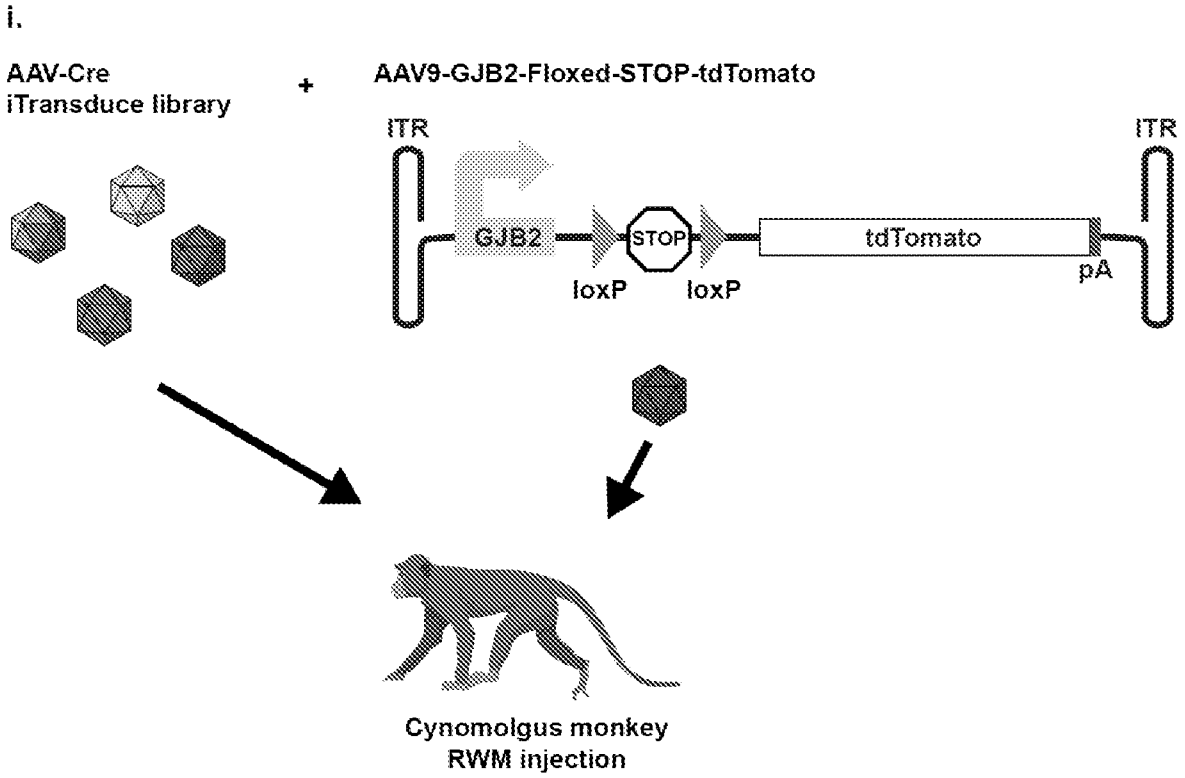


ii.

Cochlear area of interest

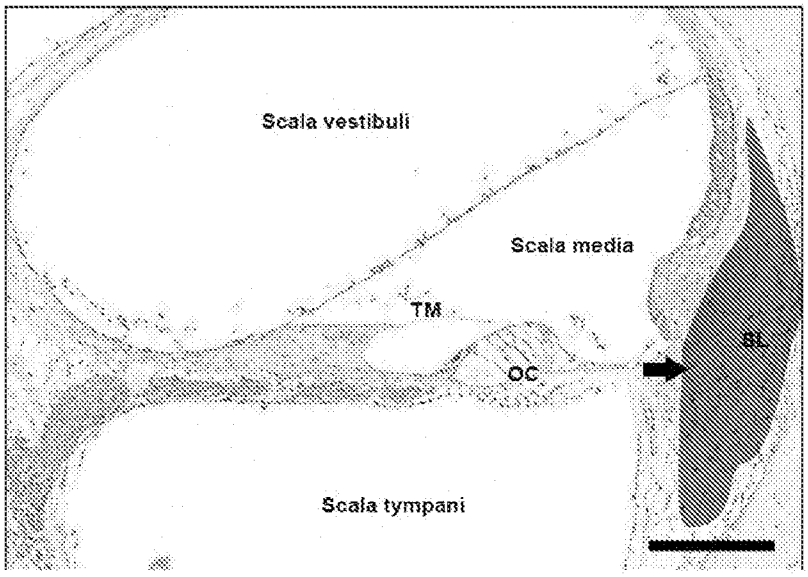


FIG. 16A

iii. Dissociate cochlea

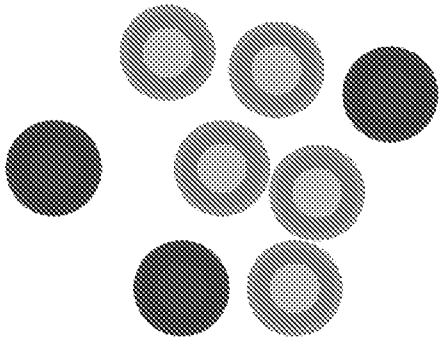

iv. Flow sort tdTomato+ fibrocytes

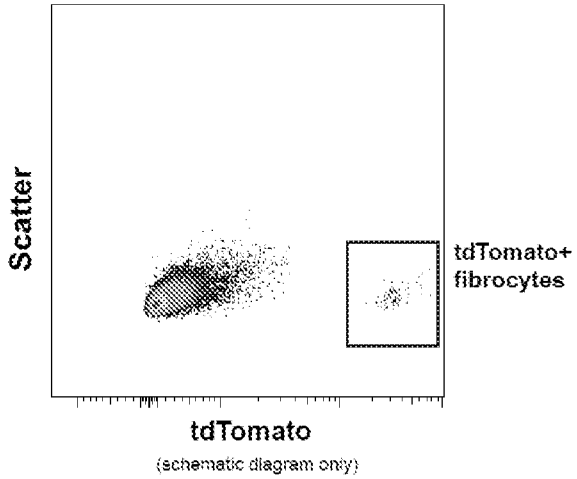


v. NGS candidate peptides

*FIG. 16A, continued*

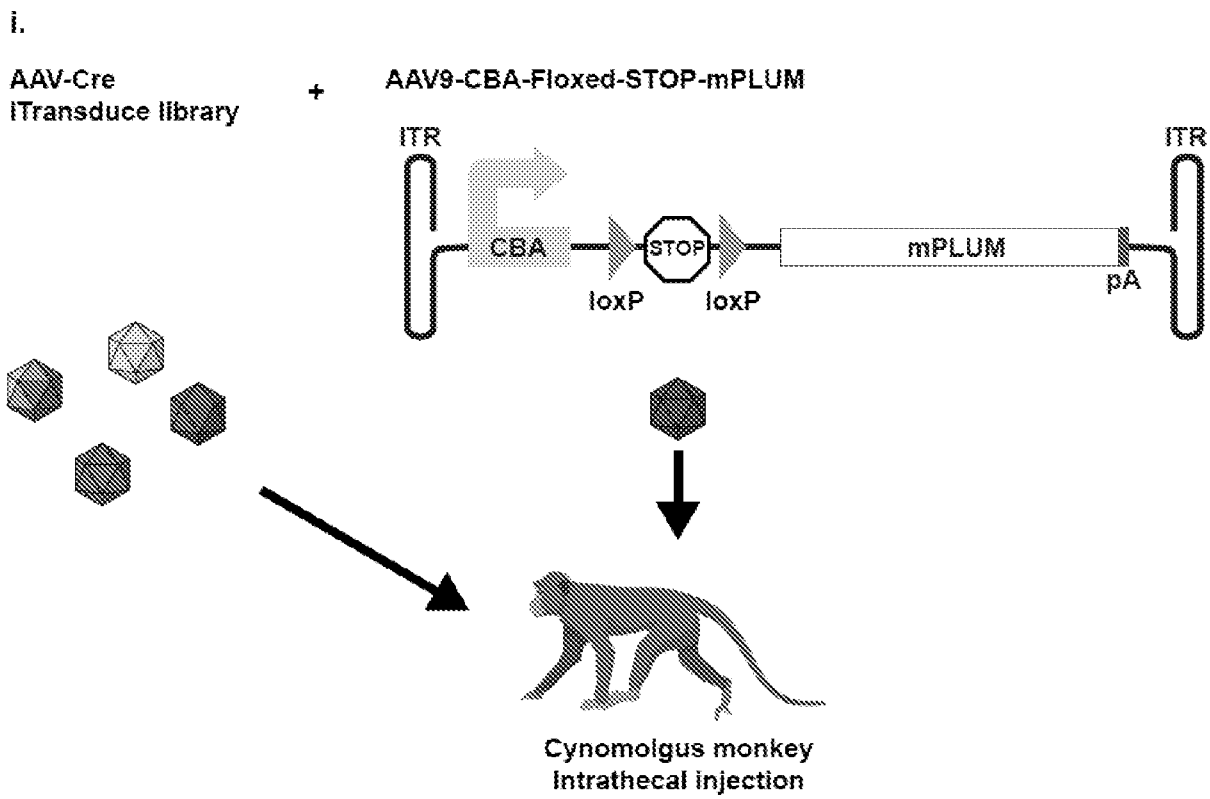


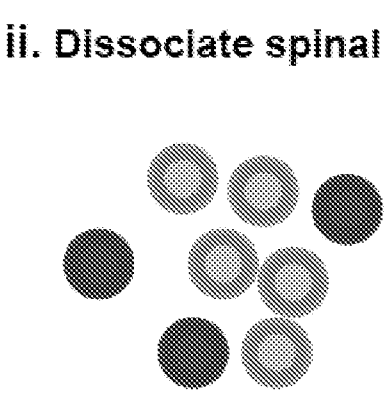


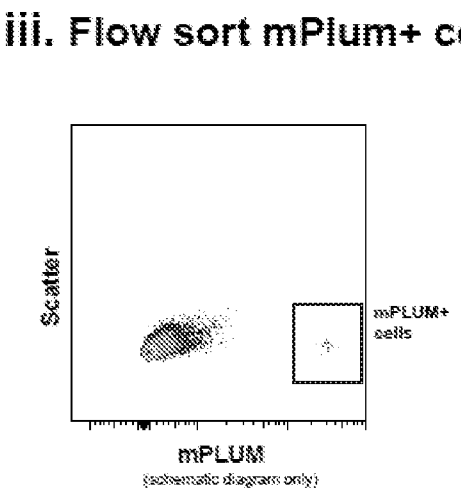


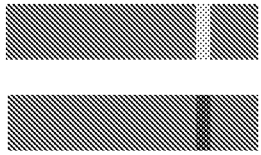


FIG. 16B